

NORWEGIAN UNIVERSITY OF LIFE SCIENCES



ACKNOWLEDGEMENTS

This work has been performed part time at the Department of Anatomy, Center for Molecular Biology and Neuroscience, University of Oslo in the period September 2008 to May 2010.

The thesis is a part of a master degree in Molecular Biology, The Norwegian University of Life Sciences (UMB). Torgeir Holen has been my supervisor and Vincent Eijsink my internal supervisor.

- I would like to express my gratitude to all those who gave me the possibility to complete this thesis.
- First, I would like to thank Ole Petter Ottersen for giving me the opportunity to perform this work at the Department of Anatomy, UiO.
- Torgeir Holen, for improving my skills in the lab and for guidance and help during these two years.
- Line Strand, for always smiling and being positive and helping me out with “everything” when problems occurred.
- Tom Tallak Solbu, Svein Erik Moe and Jan Gunnar Sørbo for good advice and answering all my questions.
- The technical staff, and especially Bjørg Riber, Karen Marie Gujord and Jorunn Knutsen for their caring and helpful attitude.
- All members in the group for the encouragement.
- Mari Kaarbø for great help with the last finish.
- The Central Laboratory, Norwegian School of Veterinary Science for willingness and help so I could manage to complete this thesis and still be an employee in the lab
- To friend and family for patience and support.
- Finally, I would like to thank my dear Jens, for always believing in me and for providing me care and comfort during this hectic phase in my life.

Oslo, May 2010

Marianne Vaadal

TABLE OF CONTENTS

ACKNOWLEDGEMENTS	1
TABLE OF CONTENTS	2
ABBREVIATION AND GLOSSARY	5
ABSTRACT	6
SAMMENDRAG	8
1 INTRODUCTION	10
1.1 THE ORIGIN OF AQUAPORINS	10
1.1.1 Aquaporins	10
1.1.2 Evolution and function of aquaporins	11
1.1.3 Structure of the aquaporin family	12
1.2 AQUAPORIN 4 (AQP4)	12
1.2.1 Secondary structure of AQP4	13
1.2.2 Tertiary- and quaternary structure of AQP4	15
1.2.3 AQP4 and square array formation	15
1.3 INWARDLY RECTIFYING POTASSIUM CHANNEL NR 4 (Kir 4.1)	17
1.3.1 Potassium spatial buffering	17
1.3.2 Localization of AQP4 and Kir4.1	18
1.4 ALPHA SYNTROPHIN	18
1.5 PDZ DOMAINS	19
1.6 PATJ	20
1.7 STATEMENTS OF PROTEIN-PROTEIN INTERACTION WITH AQP4	21
1.7.1 Statement 1: Arginines, R8 and R9 in N-terminal of AQP4a, block tetramer-tetramer binding sites	21
1.7.2 Statement 2: Palmitoylation of C13 and C17 inhibit square array formation	22
1.7.3 Statement 3: N-terminal residues of AQP4c (V24, A25 F26) is responsible for determination of square array formation	23
1.8 AIMS OF THIS STUDY	24
2 MATERIALS	26
2.1 REAGENTS USED IN DIFFERENT SECTIONS	26
2.2 BUFFERS AND GELS	28
2.3 LADDERS AND PRIMERS	30
2.4 ANTIBODIES, PROTEINS AND ENZYMES	32
2.5 BACTERIAL STRAINS, TOOLS AND INSTRUMENTS	33
3 METHODS	35
3.1 PREPARATION OF CDNA FOR Kir.4.1 ANALYSES	35
3.1.1 Total RNA-isolation and purification	35
3.1.2 cDNA synthesis by reverse transcription	36
3.2 PCR (POLYMERASE CHAIN REACTION)	37
3.3 AGAROSE GEL ELECTROPHORESIS	38
3.3.1 Purification of PCR products	39
3.4 PREPARATION OF PCR2.1-TOPO PLASMID	40
3.4.1 Sticky end ligation into plasmid by using TOPO TA cloning-kit	40
3.4.2 Growth of Escherichia coli strain	42
3.4.3 Bacterial strains	42
3.5 OVERNIGHT (ON) CULTURES	43
3.6 PLASMID PURIFICATION FROM ON CULTURES	43
3.6.1 Miniprep protocol	43
3.6.2 Endotoxin-free Maxiprep	44
3.7 RESTRICTION ENZYME DIGESTION OF DNA, PCR 2.1-TOPO PLASMID AND EXPRESSION PLASMID pCDNA 3.1/ZEO(+)	46

3.8 DNA CONCENTRATION MEASUREMENTS.....	47
3.9 STICKY END LIGATION OF KIR4.1 INTO EXPRESSION PLASMID pCDNA3.1/ZEO(+)	47
3.10 SEQUENCING.....	48
3.11 THE CELLULAR MODEL SYSTEM.....	49
3.11.1 HeLa -cells.....	49
3.11.2 Human Embryonic Kidney (HEK) 293-cells.....	49
3.12 CULTURE AND MAINTENANCE OF CELL CULTURES	50
3.12.1 HeLa cells and HEK 293 cells	50
3.12.2 Splitting cell lines	50
3.12.3 Cell thawing	51
3.12.4 Cell freezing.....	52
3.12.5 Counting cells	52
3.13 TRANSFECTION OF PLASMIDS INTO CULTURED CELLS	53
3.13.1 Transfection with Fugene 6	53
3.13.2 Harvesting of DNA from 75cm ² cell-culture containers	54
3.14 PREPARING PROTEIN HOMOGENATE FROM CULTURED CELLS.....	55
3.15 PREPARING OF SAMPLES FOR SDS-PAGE AND WESTERN BLOT	56
3.15.1 Total protein concentration determination	56
3.15.2 Preparation of lysate from cultured cells	57
3.15.3 Making SDS-PAGE gels	57
3.16 WESTERN BLOTS AND SDS POLYACRYLAMIDE GEL ELECTROPHORESIS (SDS-PAGE)	58
3.16.1 Electrophoresis on SDS-PAGE gels.....	59
3.16.2 Western Blotting	60
3.16.3 Immunolabelling and detection of proteins in SDS-PAGE	61
3.16.4 Membrane stripping.....	62
3.17 BLUE NATIVE PAGE (BN-PAGE) GEL ELECTROPHORESIS	63
3.17.1 Collection of samples for BN-PAGE	63
3.17.2 Sample preparation for BN-PAGE.....	64
3.17.3 Electrophoresis on BN-PAGE assay	64
3.18 PROTEIN TRANSFER (BLOTTING) AND IMMUNOLABELLING IN BN-PAGE.....	65
3.18.1 Blotting.....	65
3.18.2 Immunolabelling and detection for BN-PAGE	65
4 RESULTS	67
4.1 CONSTRUCTION OF KIR4.1 EXPRESSION PLASMID.....	67
4.1.1 Designing primers and PCR amplification of the Kir4.1 gene	67
4.1.2 Cloning of Kir4.1 PCR-products into a pCR2.1TOPO plasmid.....	69
4.1.3 Purifying and analyzing the pCR2.1-TOPO-Kir4.1 plasmids.....	70
4.1.5 Sequencing results from cloning of Kir4.1 into TOPO plasmid	71
4.1.6 Sub-cloning Kir4.1 insert from pCR2.1-TOPO to pcDNA3.1/Zeo(+)	73
4.1.7 Digest of the expression plasmid pcDNA3.1/Zeo(+) with EcoRI and XhoI.....	74
4.1.8 Ligation of Kir4.1-insert and expression plasmid pcDNA3.1/Zeo(+)	75
4.1.9 Sequence analysis and Maxiprep purification of pcDNA3.1/Zeo(+)-Kir4.1	76
4.1.10 Yield and quality of Endotoxin-Free MaxiPrep	77
4.1.11 Transfection of Kir4.1- pcDNA3.1/Zeo(+)- plasmid into HeLa cells.....	78
4.2 TESTING ANTIBODIES AGAINST KIR4.1 AND AQP4 IN SDS- PAGE AND BN-PAGE ASSAY	79
4.2.1 Kir4.1 labelling in SDS-PAGE.....	79
4.2.2 AQP4 labelling in SDS-PAGE assay	82
4.2.3 Cotransfection of AQP4 and Kir4.1 in BN-PAGE assay	83
4.2.4 Cotransfection of AQP4c-myc and Kir4.1.....	84
4.2.5 Cotransfection of AQP4 and Kir4.1 c-myc.....	86
4.2.6 Cotransfection of Kir4.1 and α -syntrophin	86
4.2.7 Cotransfection of AQP4 and α -syntrophin	88
4.2.8 Cotransfection of Kir4.1 and PatJ c-myc	88
4.3 SQUARE ARRAYS AND PROTEIN-PROTEIN INTERACTIONS IN ISOFORMS OF AQP4	93
4.3.1 Single mutations in AQP4c.....	93
4.3.2 Double mutations in AQP4c.....	95
4.3.3 Triple mutations in AQP4c.....	96
4.3.4 AQP4c N-terminal mutations	97
5 GENERAL DISCUSSIONS AND CONCLUSION.....	99

5.1 SPECIFICITY OF ANTIBODIES AGAINST KIR4.1 PROTEIN.....	99
5.2 POSSIBLE PROTEIN-PROTEIN INTERACTION BETWEEN AQP4 AND KIR4.1	102
5.3 POSSIBLE PROTEIN-PROTEIN INTERACTION BETWEEN A-SYNTROPHIN AND KIR4.1 AND A-SYNTROPHIN AND AQP4	105
5.4 POSSIBLE PROTEIN-PROTEIN INTERACTION BETWEEN KIR4.1 AND PATJ.....	107
5.5 TRIPLE MUTATIONS IN AQP4C	109
5.6 N-TERMINAL MUTATIONS IN AQP4C	110
5.7 SOME POSSIBLE METHODOLOGICAL LIMITATIONS OF BN-PAGE	112
REFERENCE LIST	115
APPENDIX	121

ABBREVIATION AND GLOSSARY

AA	Amino acid
Amp	Ampicillin
APS	Ammonium persulfate
AQP4	Aquaporin-4
BN-PAGE	Blue-Native Polyacrylamide gel electrophoresis
CNS	Central Nervous system
CSF	Cerebrospinal fluid
DDM	Dodecyl- β -D-maltoside
DMEM	Dulbecco's Modified Eagle Medium
DMEM(++-)	Dodecyl- β -D-maltoside with BSA and glutamine and without antibiotics
DNA	Deoxyribonucleic acid
ds RNA	Double- stranded RNA
E.coli	Escherichia coli
EDTA	Ethylene-diamine-tetra-acetic acid
EM	Electron microscopy
FCS	Fetal calf serum
FFEM	Freeze-fracture electron microscopy
G250	Commassie G-250
GAPDH	Glyceraldehyde-3-phosphate dehydrogenase
HeLa	Cervical cancer cells from Henrietta Lacks
HEPES	(4-(2-hydroxyethyl)-1-piperazineethanesulfonic acid
kDa	Kilodalton
KIR4.1	Inwardly rectifying potassium channel 4.1
LB	Luria Bertani medium
mRNA	Messenger RNA
MUPP-1	Multi-PDZ Domain Protein 1
OAP	Orthogonal arrays of particles
OD	Optical density
ON	Over night
PBS	Phosphate-buffered-saline
PCR	Polymerase chain reaction
RE	Restriction enzyme
RNA	Ribonucleic acid
RPM	Revolutions per minute
RT	Room temperature
RT-PCR	Reverse transcriptase-PCR
SDS-PAGE	Sodium dodecyl-sulfate-polyacrylamide gel electrophoresis
TAE	(Trisbase, acetic acid, EDTA)-buffer
TEMED	N,N,N',N'-Tetramethylenediamine

ABSTRACT

Aquaporin 4 (AQP4) is a membrane protein, and also the main water channel in the brain. AQP4 is distributed with highest density in the perivascular end-feet domain of astrocytes, the supporting cells of the neurons in the central nervous system. This protein has been involved in water and potassium homeostasis, and in several neurologic conditions, such as e.g brain edema.

Square arrays are large scale structures which are present in high concentrations in the same locations as AQP4, and it has been shown that AQP4 is a main contributor in the assembly of square arrays. It has been hypothesized that the ratio of different AQP4 isoforms regulates the size, structure and numerical distribution of square arrays. While square arrays so far has been studied exclusively by freeze-fracture electron microscopy, our group recently demonstrated a biochemical technique that can be used to analyze square arrays. This technique, BN-PAGE, has been used in this thesis, to test several hypotheses about how to destabilize square array assembly. This technique has also been used in order to test protein-protein interactions between AQP4 isoforms and hypothetical binding partners, e.g the inwardly rectifying potassium channel 4.1 (Kir4.1), α -syntrophin and the tight junction protein, PatJ.

There has recently been uncertainty about the specificity of immunolabelling using commercially available anti Kir4.1 antibodies in detection of Kir4.1 proteins. In the BN-PAGE assay, the use of antibodies is crucial for the detection of protein presence. To investigate a hypothetical protein interaction of any protein, a possible cross reaction of antibodies has to be controlled for. In order to test the specificity and crosslabelling of antibodies, a Kir4.1 expression construct was made. The plasmid was later expressed in two different cell lines, HeLa and HEK 293, alone or together with AQP4 isoforms, α -syntrophin or PatJ. In addition, a mutation study of the isoform AQP4c was tested in the same BN-PAGE assay to investigate the possible protein-protein binding residues between adjacent AQP4-tetramers.

The plasmid made was verified by sequencing and restriction enzyme analysis, and the HeLa expressed construct was also tested with different antibodies against Kir4.1. Since labelling was obtained, we concluded that the construction of Kir4.1 plasmid was successful. In the cross-labelling tests, different antibodies against AQP4 and Kir 4.1 were used. In conclusion, no crosslabelling between AQP4 and Kir4.1 was seen in the assay tested. In the coexpression

studies of AQP4 and its potential binding partner, we were not able to detect any interaction between these proteins using the BN-PAGE assay.

As part of a larger study, single, double and triple mutations of AQP4 were tested in the BN-PAGE assay to test if the mutations could destroy square array assembly of AQP4 (Strand, Moe, Solbu, Vaadal and Holen, *Biochemistry*, 2009). In addition, five N-terminal mutations of AQP4c were tested. We were not able to reveal any loss of square array assembly in any of these mutations in the BN-PAGE assay.

How the structure of square arrays relates to the isoforms of AQP4, or even what purpose the organization of water channels into these structures serves, is still not understood.

SAMMENDRAG

Aquaporin 4 (AQP4) er et membranprotein som danner vannkanaler i hjernen. AQP4-kanaler er normalt konsentrert i perivaskulære membraner i endeføtter til astrocytter, som er støtteceller for nevroner i det sentrale nervesystemet. AQP4 har også en viktig rolle i vann og kalium homeostase, og det er vist at vannkanalen AQP4 spiller en sentral rolle i utviklingen av hjerneødem etter for eksempel hjerneslag.

”Square arrays” er store, regulære strukturer som finnes i høye konsentrasjoner i astrocyttenes endeføtter og som kolokaliserer med AQP4. Det har vist seg at flere AQP4 isoformer er byggesteiner i disse strukturene. Det er gjort spekulasjoner rundt hvorvidt mengden av de ulike AQP4 isoformene bestemmer hvor store strukturene skal bli og hvordan de blir organisert. Elektronmikroskopi av frysesnitt har i mange år vært den eneste tilgjengelige metoden for å analysere ”square-array” strukturene. I 2008 publiserte vår gruppe en artikkel hvor et nytt molekylær-biologisk verktøy (BN-PAGE) ble verifisert for bruk i forskningen rund oppbygningen av ”square arrays. BN-PAGE metoden har også blitt brukt i denne masteroppgaven, men da for å teste ulike hypoteser som er publisert rundt oppbygningen av disse strukturene. Metoden har også blitt brukt til å undersøke protein-protein interaksjoner mellom AQP4 isoformer, og mellom AQP4 og andre potensielle bindings partnere, for eksempel en kalium kanal (Kir4.1), α -syntrophin og det cytosolisk proteinet, PatJ.

I det siste har det hersket tvil om hvorvidt enkelte Kir4.1 antistoffer er spesifikke nok for å kunne brukes i kolokalisasjons studier med blant annet AQP4. Antistoff spesifisitet er grunnleggende viktig for å kunne verifisere tilstedeværelse av et bestemt protein i flere analytiske metoder, deriblandt BN-PAGE. Derfor var det viktig å kunne verifisere antistoffene som skulle brukes i oppgaven. Det ble derfor laget et Kir4.1 konstrukt, som ble uttrykt i ulike cellelinjer, og deretter testet med antistoffene som skulle brukes videre. Etter verifiseringen av antistoffene ble det gjort ekspresjonsforsøk hvor Kir4.1 konstruktet ble uttrykt alene eller sammen med en AQP4 isoform, eller en av de andre potensielle bindings proteinene som allerede er nevnt. Det ble ikke gjort resultater som kan bekrefte interaksjoner mellom noen av disse proteinene.

Som en del av en større studie, ble single, doble og triple mutasjoner testet i BN-PAGE systemet i håp om å bryte ned de allerede påviste ”square arrays” av AQP4 (Strand, Moe,

Solbu, Vaadal and Holen, *Biochemistry*, 2009). Det ble i tillegg gjort en mutasjonstudie hvor isoformen AQP4c ble undersøkt ved hjelp av den samme metoden for å se om det var mulig å påvise protein interaksjoner mellom bestemte aminosyrer i to AQP4 tetramer komplekser. Heller ikke her ble det vist noen nedbrytning av square array strukturene.

Det er fortsatt uklart hvordan de ulike isoformene av AQP4 bidrar til oppbyggingen av square array strukturene, og man har heller ikke forstått hensikten med å organisere AQP4 vannkanalene på en slik måte.

1 INTRODUCTION

1.1 The origin of Aquaporins

A long standing question in medical physiology is how water is transported over the cell membrane. This lipid bilayer separates the interior of the cell from the world outside and maintains gradients of ions and nutrition. For a long time simple diffusion across the membrane was the only known mechanism for water transport. However, this mechanism could not explain how large amounts of water could cross membranes in for example kidneys. To account for this water transport, there were suggestions about the existents of channels or pores that allowed fast and selective passage of water (Orci et al., 1977).

Peter Agre and co-workers (1987) discovered another water-transport system. In the study by Agre and co-workers, they describe what happened when they tried to isolate an Rh- antigen from erythrocytes (Agre et al., 1987). Their samples were contaminated with a very hydrophobic protein. In their experiment, cDNA from this protein was isolated and injected into *Xenopus laevis* oocytes. An interesting observation was made; the oocytes injected with cDNA started to swell and burst when placed in distilled water. The hydrophobic protein they had discovered was named CHIP 28 (channel-like integral protein of 28 kDa), and renamed later as Aquaporin nr 1 (AQP1). The first aquaporin was found. For the discovery of aquaporins, Peter Agre received the Nobel Prize in chemistry in 2003.

1.1.1 Aquaporins

A general BLAST search on “Aquaporin-1” show that all aquaporins are members of the “Major intrinsic protein” (MIP) superfamily. Proteins in this family function as membrane channels and are able to selectively transport water and small neutral molecules in and out of the cell. These proteins have a tree-dimensional structure building a pore and they also share a common fold: the N-terminal cytosolic part of the protein is followed by three transmembrane helices, and a semi-helix, a pattern that is repeated, which thus most probably have arisen through gene duplication (Murata et al., 2000).

The aquaporin family can be divided into two major sub-groups according to their permeability characteristics and sequence similarity. The “Aquaporins” are water-selective

channels and can only transport water-molecules. The “Aquaporin” group includes AQP0, AQP1, AQP2, **AQP4**, AQP5, AQP6 and AQP8. AQP6 forms an anion channel and AQP8 are permeable to urea, thus they only belong to this group based on sequence similarity and homology (Ma et al., 1997; Yasui et al., 1999).

The other sub-group is glycerol uptake facilitators (GlpFs), also called “Aquaglyceroporin”. AQP3, AQP7, AQP9 and AQP10 are members of this group, which are selective for water and small, neutral solutes like glycerol (Ishibashi et al., 1994).

AQP11 and AQP12 also belong to the aquaporin-family but no water permeability has been shown in experiments *in vitro*.

So far, 13 different aquaporins have been reported, and our own research group have identified new isoforms of AQP4 (Moe et al., 2008). The different aquaporins have distinct cellular and sub-cellular localizations, and aquaporins can be found in all kingdoms of life. However, GlpFs have only been characterized in microorganisms (Tanghe et al., 2006).

1.1.2 Evolution and function of aquaporins

The cell interior is separated from the matrix outside by a membrane consistent of two layers of phospholipids. Many proteins, vital for the cell, are embedded in the membrane. These proteins are responsible for structural integrity, maintaining electric and osmotic gradients and provide energy for physiological processes in the cell (Hibino et al., 2010). A cell's interior is mostly water, which can diffuse through the cell membrane but only at a limited rate. Now we know that cells that exhibit higher water permeability than others, most probably have proteins intergraded in the lipid bilayer, which facilitates conductance of water.

All the 13 mammalian aquaporins vary in their water permeability, where AQP0 is the poorest conductor and AQP4 is the most efficient water pore (Yang et al., 1997). The large number of aquaporins in the genome of humans, plants and vertebrates, reflects the importance of these proteins and their regulations of the water homeostasis. The bacteria *E.coli* contains both a specific water pore (AQPZ) and a glycerol facilitator (GlpF) (Fu et al., 2000). Since bacteria contains two paralogous aquaporins, duplications appears to have occurred early in the evolution (Borgnia and Agre, 2001). Aquaporins are also found in plants, one example is a protein in

spinach, SoPIP2 belonging to the the PIP-family. Since these proteins share sequence identity, all the aquaporins also share common conserved motifs, suggested to be important for the function of the protein (Frayse et al., 2005). When comparing all the aquaporin proteins, the similarity varies from 25 % - 40 % between the different aquaporins (Pao et al., 1991).

1.1.3 Structure of the aquaporin family

Some of the aquaporins have got their structure determined, by using electron crystallography on double-layered, two-dimensional crystals. Other structural information has been obtained from the amino acid sequence alone. By using hydropathy plots to localize α -helical membrane-spanning segments in the amino acid sequence, some of the 2D-structure can be predicted. The first structure of a water-channel (for AQP1), was made using this last mentioned method, and revealed an AQP-fold that now is known to be common for all aquaporins (Murata et al., 2000). AQP4 is described in detail below as one example, as all aquaporins share a common secondary, tertiary and to some degree also the quaternary structure.

1.2 Aquaporin 4 (AQP4)

AQP4 is the predominant water channel in the mammalian brain (Jung et al., 1994). The proteins are found in high concentrations around blood vessels, and are mainly localized around astrocyte endfeet and in retinal Müller cells (Nielsen et al., 1997) (see appendix 1) Astrocytes surround neurons and support them by suppling nutrition and oxygen. They insulate one neuron from the other as well as destroying pathogens and removing dead neurons when necessary.

AQP4 is expressed as two major isoforms of 32 kDa and 30 kDa (Jung et al., 1994). AQP4a (M1) and AQP4c (M23) differ in length of the primary sequence and their capacity of transporting water (Jung et al., 1994; Hasegawa et al., 1994). These are splice variants resulting from different translational initiation points. Translation initiation at the amino acid methionin in position one produces the longest isoform M1 (323aa), while initiation at position 23 produces the shortest isoform M23 (Jung et al., 1994; Lu et al., 1996). Both isoforms are present in the brain but it seems that M 23 is at least three-fold more commonly expressed (Neely et al., 1999). Neely and collaborators claimed in 1999 that M1 and M23 had

the same ability to transport water. In 2004 Silberstein and co-workers demonstrated an eight-fold higher water permeability for the isoform M23 compared to M1 (Silberstein et al., 2004). This statement has not yet been fully explored, and at present time no different functions of the two isoforms have been found.

Our group has recently demonstrated that AQP4 has at least four other isoforms than AQP4a and AQP4c (Moe et al., 2008). The new isoforms, AQP4b, AQP4d, AQP4e and f, were found in rat brain and kidney tissue and show different ability to transport water (Fig.1). One of the new isoforms (AQP4e) was shown to transport water like M1 and M23 while the other isoforms did not. In addition, AQP4e was transported to the plasma membrane, while AQP4b, -d and -f were retained in intracellular areas when transfected into HeLa cells and CRL 2006 astrocytes. It was also found that AQP4d was concentrated in the cis-Golgi area. AQP4b, d, and f only have four- and five-transmembrane α -helices, and this can be of importance for the lack of water transport ability. AQP4e (Mz) is most probably also part of the assembly of square arrays (Sorbo et al., 2008).

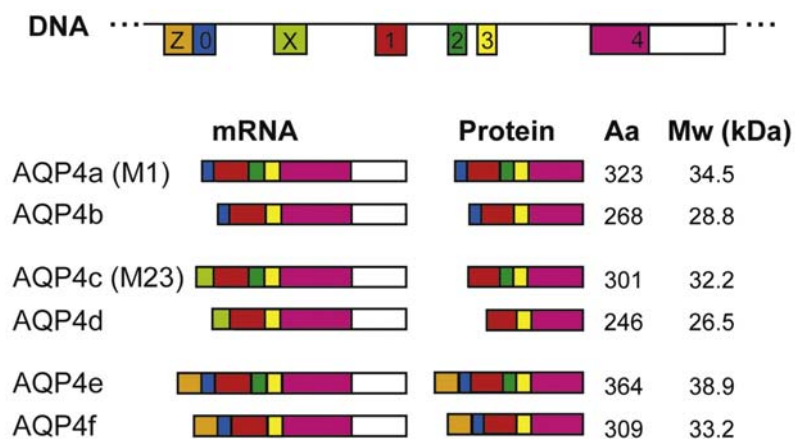


Figure 1. Model of six AQP4-isoforms. Different start codons have different colours. A new codon was found in the new exon Z, giving rise to AQP4e, later called Mz. This protein has the longest mRNA and the largest protein size, with a novel N-terminal (Reprinted from Moe *et al* 2008).

1.2.1 Secondary structure of AQP4

Early in this century, the resolution of the electron crystallographic analyses was improved, and a new density map could be used for modelling a new atomic structure of AQP4. Fujiyoshi and collaborators published in 2006 an atomic structure with 3.2 Ångstrom resolutions (Hiroaki et al., 2006). This is the structure we based our experimental set-up on in both the article published by Strand and coworkers and for this thesis (Strand et al., 2009).

Figure 2 is a topographic diagram of an AQP4-molecule, and shows the main element of the protein. The six α -helices (rods) are denoted H1-H6, and the loops A-E. All helices are transmembrane helices, except for two shorter, 3-10 α -helices that are responsible for building the pore. Both the C- and N-terminal of the protein is on the cytoplasmic side of the membrane. The transmembrane helix nr 1(H1) and H2 are close to the N-terminal. They are connected on the extracellular side through loop A. Loop B which connects H2 and H3, folds back into the membrane and here the first conserved NPA-motif were identified (Yong J. and TongHui M., 2007).

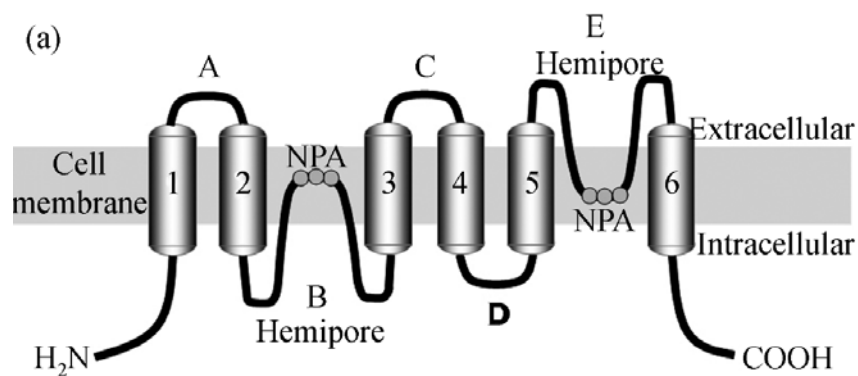


Figure 2. Secondary arrangement of AQP4 with six helices (rods), loops (black) and the NPA motif. See text for details. (Reprinted from Ma TongHui *et al.* 2007).

One hallmark of the structure of the aquaporin family is the conserved, three amino acid sequence NPA (asparagine-proline-alanine), which is quite common in proteins. The first NPA-motif is placed midway through the membrane in loop B. The second one is located in the extracellular loop E but the motif itself is located in the membrane. The two highly conserved NPAs are structural domains that play an important role for the water-selectivity. In the secondary structure the motifs are far apart, but when the protein coil into its tertiary structure, asparagine residues in the motif come close to each other making a hydrophobic environment in the pore. Inside the pore, a constriction site is located right under the NPA-motif. The channel is narrowed and only one water molecule can pass through this slit at one time, helped by the bonding with one of the Asparagine residues. This area is called the ar/R constriction site because of a conserved aromatic/arginine residue found at the same site in AQP1. The channel is narrowed because of sterical hindrance from an aromatic histidine residue, and will limit the permeation of molecules bigger than water, including hydrated ions (Gonen and Walz, 2006; Tani *et al.*, 2009). In addition, other functions of NPA motifs in AQP4 have been suggested. It has been shown by mutating different amino acids in the NPA

motif, that AQP4's expression pattern on the plasma membrane can change, indicating an important role of NPA motifs in AQP4 plasma membrane targeting (Guan et al., 2010).

1.2.2 Tertiary- and quaternary structure of AQP4

Most proteins are made of more than one polypeptide chain. According to the nomenclature of Schellman and Lindström-Lang, all proteins have a quaternary structure (Linderstrøm-Lang KU, 1952). Primary structure and the amino acid sequence means the same, secondary structure correspond to the α -helices and β -sheets, and tertiary structure the chain fold.

AQP4's tertiary structure corresponds to a monomeric subunit, where each subunit consist of the six α -helices described previously which together make up the pore (see appendix 2). In the native state the AQP4 protein consists of four monomers together forming a tetramer (the quaternary structure). It is not clear how the interactions between the monomers in the tetramer are formed but the subunit in the tetramer is believed to interact with each other through the cytoplasmic loop D, connecting helices four and five involved in tetramer-interaction (Hiroaki et al., 2006). In the literature one can find more than one suggestion about which residues are important for the stabilization of the tetramer complex of AQP4, and there are different research-groups testing out series of current hypotheses in this field (see section 1.7).

1.2.3 AQP4 and square array formation

Perivascular membranes of astrocyte end-feet contain regular arrays of intramembrane particles (IMPs). The intramembrane particles are visible on EM in FFEM preparation images. In freeze fracture electron micrographs, Wolburg and coworkers showed that >50% of the total surface of end-feet could be covered by these structures (Wolburg, 1995). These structures have been referred to as square arrays or orthogonal arranged particles (OAP's) (Landis and Reese, 1981) Many IMP's together corresponds to one tetramer, and four tetramers together correspond to one square array (Fig.3).

Square arrays are large protein complexes, and AQP4 is a main component of these arrays (Furman et al., 2003). They also demonstrated that both isoforms (M1 and M23) contributed to the assembly of the square arrays but with different fractions. By transfecting Chinese hamster ovary (CHO) cells with the two AQP4 isoforms confocal immunofluorescence indicated that transfection with M23 alone or together with M1 gave arose to square array

assemblies. Cells transfected with the isoform M1 alone exhibited none or few detectable assemblies. In addition, CHO cells transfected with M23 had large, raft-like square arrays with uniform lattice pattern. These arrays varied in size, but generally contained >100 IMPs. However, the average square array seen in astrocytes, contains 17 IMP (Furman et al., 2003). Many of these rafts appeared to be formed from side-to-side associations of smaller square arrays. By labelling of the rafts with immunogold particles they observed that M23 isoform predominantly existed within square arrays, and was rarely observed in other areas of the plasma membrane, indicating this isoform as important for the organizing of the square arrays. They concluded that the isoform M23 is the only one able to form square arrays alone, and attendance of isoform M1 destabilized the assembly to some degree. In addition, Yang and coworkers showed that square arrays disappeared in AQP4 knock-out mice (Ma et al., 1997).

Our group has discovered that the internal composition of square arrays contains not only M1 and M23 but also one novel AQP4 isoform, Mz (Sorbo et al., 2008). M1 and Mz can interact with M23 and be incorporated into higher order structures. Higher order structures are AQP4-complexes containing 4 X, 12 X, 16 X, 20 X and so on tetramers. By using two-dimensional blue native polyacrylamide gel electrophoresis (BN-PAGE) (section 3.17), we have managed to visualize these higher order structures isolated from transfected HeLa cells and CLR 2006 cells (Strand et al., 2009). The function of these square arrays is still not known.

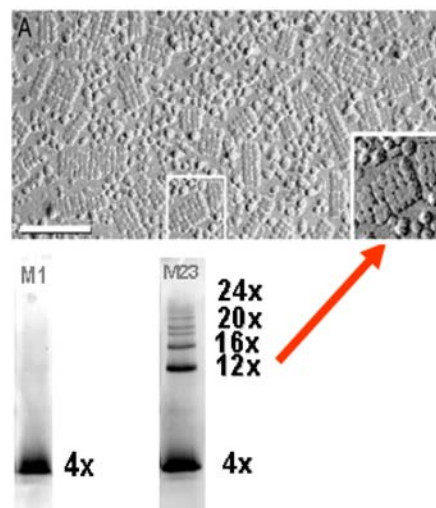


Figure 3. Panel A shows the pattern of square arrays *in vivo* by a electron micrograph. Under left, the tetramer band from AQP4a (M1) is shown. No higher order band visible. On the left, the pattern of AQP4c with higher order bands is shown. A hypothetical “ladder” of complexes is shown. The higher order bands *in vitro* indicate the square arrays *in vivo* (red arrow) (Fig. 3A is from Furman, Rash *et al* 2003. M1 and M23 are from Sorbo *et al* 2008).

Aquaporin 4 is not the only membrane protein expressed in the endfeet of astrocytes. The potassium channel Kir4.1 has shown to colocalize with AQP4, in different membrane domains (Nagelhus et al., 1999), giving rise to speculations of a possible collaboration between these two proteins.

1.3 Inwardly rectifying potassium channel nr 4 (Kir 4.1)

The inwardly rectifying potassium channel nr 4 (Kir4.1) is like AQP4, a transmembrane protein expressed in astrocytes facing blood vessels, in the central nervous system (CNS), and in the retinal Müller cells (Kofuji et al., 2000). The Kir4.1 protein has also been demonstrated in oligodendrocytes, which is another kind of glia cells (Butt and Kalsi, 2006). There have been contradictory reports concerning Kir4.1 in oligodendrocytes, since some research groups have not been able to detect Kir4.1 in these cells (Higashi et al., 2001). There are four main groups of Kir channels: 1) The classical Kir channels (Kir2) contribute to set the resting membrane potential (RMP) and to repolarise the cell after a nerve impulse; 2) G protein-gated Kir channels (Kir3) which are regulated by G protein-coupled receptors and 3) ATP-sensitive Kir channels (Kir6) which play an important role in cellular metabolism. The last member is 4) Kir transport channels (Kir1, Kir4, Kir5, Kir7) which is coupled to the process potassium spatial buffering (1.3.1).

The Kir channels can be activated by phospholipids, ions and through binding proteins. The Kir channel is made up of two transmembrane α -helices, with both the NH₂ and COOH-terminals at the cytoplasmic side of the membrane. In addition, an extracellular loop folds back outside the membrane and contributes in creating the selectivity filter in the pore. The Kir channels are tetrameric structures and can be formed by coassembly of homomeric or heteromeric sub-structures. The different assembly of structures gives them characteristic properties (Hibino et al., 2010). It has been shown that the heteromeric co-assembly of Kir4.1 and Kir5.1 generates channels with strong rectifying capacity. In contrast with a homomeric Kir5.1 protein not being functional and a homomeric Kir4.1 protein being just weakly rectifying (Casamassima et al., 2003).

1.3.1 Potassium spatial buffering

Inwardly rectifying K⁺ channels allow potassium to move more easily into the cell than out. These channels are involved in the process of spatial buffering. This process helps to regulate

the extracellular K⁺ concentration. During action potential in the axons of neurons, potassium is released into the extracellular space. Astrocytes will absorb potassium from the surroundings via strongly rectifying Kir channels, in order to reset the membranes potential. Potassium is extruded from glia cells where the concentration of potassium is high and redistributed through the astroglia network to areas with low potassium concentration (Connors et al., 2004).

1.3.2 Localization of AQP4 and Kir4.1

AQP4 has been shown, by postembedding immunogold labeling, to colocalize with Kir4.1 in retinal Müller cells (Nagelhus et al., 1999). Both proteins are enriched in plasma membrane domains facing the blood vessel. Astrocytic uptake of potassium after neural activity causes the osmolarity in the extracellular space to change (Dietzel et al., 1980). This change facilitates shrinkage of the intermolecular space indicating removal of water (Sykova, 1991). Nagelhus and collaborators (1999) suggested that removal of water is mediated by AQP4 to specific extracellular compartments, indicating AQP4 and Kir4.1 to have a functional interaction.

The subcellular distribution of Kir4.1 and AQP4 in glia cells gave rise to a theory of extracellular proteins contributing to the organization of Kir4.1 proteins in the membrane. Both AQP4 and Kir4.1 contains the PDZ binding motifs SXV (Jung et al., 1994; Takumi et al., 1998) (section 1.5). These domains are responsible for protein-protein interactions between many molecules within the CNS (Hung and Sheng, 2002). Kir4.1 contains, as already mentioned, a PDZ domain-binding region at its C terminus, and *in vitro* studies have shown that Kir4.1 can connect by interactions with proteins that possess these domains. One specific group of proteins shown to include this motif are the syntrophins, which are found as part of a multiprotein complex known as the dystrophin-glycoprotein complex (DGC) (Adams et al., 1993).

1.4 Alpha syntrophin

The dystrophine associated protein complex (DAPC) is a huge assembly of proteins expressed in several organs, e.g. brain and muscle tissue (Adams et al., 1993). The dystrophine gene is the biggest in the genome and localized on the X-chromosome. Mutations in the dystrophine

gene can lead to muscular dystrophies in male offspring. In this complex, another membrane associated protein is found: α -syntrophin is a scaffolding protein expressed in astrocytes and skeletal muscle, and an important contributor to the formation of the DAPC complex. α -syntrophin has a PDZ domain (section 1.5) on its C-terminal end. It has been suggested that the C-terminus of the α -syntrophin binds to dystrophin via the PDZ domain, while the PDZ domain also can recruit other proteins to the dystrophin complex, like e.g. Kir4.1 (Neely et al., 2001; Amiry-Moghaddam et al., 2004).

AQP4 has a SSV (serine-serine-valine) sequence thought to bind to the PDZ domain of α -syntrophin, however this has not been shown experimentally.

1.5 PDZ domains

The *Postsynaptic density protein-95 (PSD-95)*, *Discs large protein*, *Zonula occludens -1 (ZO-1)* (PDZ), domain is a conserved domain with ability to bind other proteins by recognizing and binding short peptide sequences situated at the C-terminal of the ligand protein (Ranganathan and Ross, 1997). This sequence differ in different PDZ domains but for syntrophin and some types of K^+ channels, PDZ binds to the short T / S-X-V (T is threonine, S is serine, X is any amino acid, V is valine) sequence. The ligand binds to an extended groove formed by six β -strand and two α -helixes. The strands form an open barrel structure with one α -helix in each end forming a lid. Proteins can have multiple PDZ domains, varying from two to ten in certain proteins, thus the binding affinity can vary from weak to strong (cooperative binding) (Grootjans et al., 1997).

PDZ domains are often associated with other interactions domains, which can hold receptors and signalling proteins together, forming big scaffold proteins. In the CNS, at the postsynaptic density, a PDZ scaffold protein (PSD-95) is located near the postsynaptic membrane. It has been demonstrated that PSD-95 (which contain three PDZ domains) can be labelled with antibodies from both the extracellular and the cytoplasmic side of the protein (Petersen et al., 2003). It is therefore likely that the protein is associated with the membrane and is in a good position to interact with both receptors, membrane ion channels and cytoplasmic proteins.

PDZ domains do more than connecting different proteins together. They can direct molecular complexes to specific sites, thereby contributing to e.g. synaptic plasticity. This is often done by indirect interaction via another protein, recruited to the membrane by the PDZ domain (Kang et al., 2000). This can indicate that binding to lipid membranes is another general property of PDZ domains (Wu et al., 2007a; Wu et al., 2007b), which is also found in the protein PatJ.

1.6 PatJ

Tight junctions are the areas where two cell membranes join together. The junctions make a barrier and regulate the passage of ions and molecules between cells, forcing them to enter the cell, in order to move in the tissue. Another function of the junctions is physical support to the cell and preventing lateral diffusion of integral proteins in the membrane. Tight junctions also form channels and pores and can consist of different combinations of proteins according to the tissue or organ where the junctions are situated (Gonzalez-Mariscal and Nava, 2005).

In epithelial cells, the tight junctions are composed of three main types of transmembrane proteins: occludin, claudin and junctional adhesion molecules (JAM). In addition, large protein complexes are associated with the junctions, consisting of different proteins. One of the complexes contains the tight junction protein, PatJ. PatJ is an evolutionarily conserved protein that regulates tight junction formation and epithelial polarity (Shin et al., 2005).

PatJ also contains ten PDZ domains. A study from Shin *et al* , shown that by mutating PDZ domains of PatJ, loss of interaction with a wound healing protein, Par 3, was observed (Shin et al., 2007). With ten PDZ domains, PatJ has the possibility to organize multimeric protein complexes at the plasma membrane, where it is located (Storrs and Silverstein, 2007) (Fig.4).

PatJ have highly homologues molecular structures, as the paralog protein Multi-PDZ Domain Protein 1 (MUPP-1). They also co-express in many tissues, e.g. kindeys .Both have the ability to interact with other junction associated protein and their share a common expression rate (Adachi et al., 2009). Sindic and group showed in 2008, that the rectifying potassium channel Kir4.2 co-expressed with the tight junction protein MUPP-1. A Kir4.2 construct lacking the SSV domain on its N-terminal, showed no co-immunoprecipitation with MUPP-1. They also saw that MUPP-1 reduced Kir4.2 expression on the cell surface, and they concluded that

MUPP-1 and Kir4.2 participated in a protein complex regulating transport of potassium (Sindic et al., 2009). This is the background for our hypothesis of a possible protein interaction between PatJ and Kir4.1

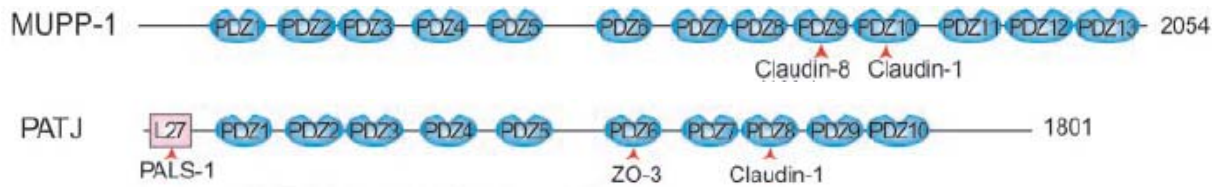


Figure 4. Diagrammatic representation of protein similarities between MUPP-1 and PatJ. Their binding partners, where known, are indicated with arrow-head. The number of amino acids is indicated at the right. (Reprinted from Adachi *et al* 2009).

1.7 Statements of protein-protein interaction with AQP4

The study of square arrays started in the early 1970s and the link between AQP4 and square arrays was established by Rash and co-workers in 2003, (Furman et al., 2003). No physiological reason is known for the precursors of the square arrays, but it is no doubt that this massive structure plays an important role, thus many research groups are interested in these issues. The main statements used as background information for square array assembly in this study are summarized below.

1.7.1 Statement 1: Arginines, R8 and R9 in N-terminal of AQP4a, block tetramer-tetramer binding sites

As mentioned above, Hiroaki and collaborators demonstrated that the crystal structure of rat AQP4c isoform was reconstituted into lipid bilayers (Hiroaki et al., 2006). Furman and group suggested that the N-terminal of AQP4a interfered with the array formation (Furman et al., 2003). Hiroaki and co-workers generated a peptide corresponding to a native N-terminal of AQP4 (Hiroaki et al., 2006). All the Arginine residues in the peptide were mutated into Lysine residues. While native AQP4 N-terminal destroyed the formation of arrays, their mutated N-terminal showed no sign of influence on the formed square arrays. They therefore proposed that the conserved, positively charged residues R8 and R9 in the N-terminal of AQP4a, blocked the formation of square arrays by interacting with the tetramer-tetramer

binding site seen in the crystal, and special the residues Arginine (R)108, Glycine (G)157, Tryptophan (W)231 and Tyrosine (Y) 250 (Fig.5).

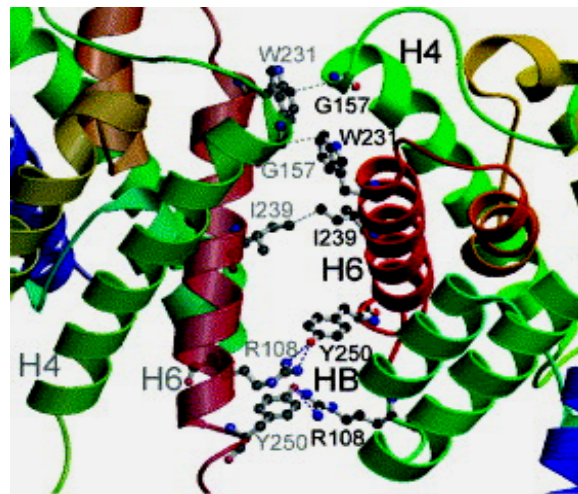


Figure 5. This figure shows the hypothetical bindingsites between two adjacent AQP4 tetramers. The target aminoacids are shown in ball-and stick model. (Figure from Hiroaki *et al* 2006).

In the study by Strand and coworkers (Strand *et al.*, 2009) this hypothesis was tested by mutating arginine residues (R8K and R9K), and the effect of these mutations were evaluated in a BN-PAGE assay. No effect was found when mutating R8 and R9, indicating that these residues, included another mutation (W10K), was not the sites blocking the tetramer-tetramer formation of AQP4.

1.7.2 Statement 2: Palmitoylation of C13 and C17 inhibit square array formation

Suzuki and collaborators constructed a series of N-terminal deletion mutants in order to investigate why the N-terminus of AQP4a interfered with the formation of square arrays (Suzuki *et al.*, 2008). Nine different mutant deletions were made, including two cysteins at residue no. 13 and 17 of the N-terminal of AQP4a. The mutants were expressed in CHO cells, and transfectants were confirmed by immunoblotting. It was shown that the cysteine (C) mutants interrupted the formation of square arrays, and two palmitylated N-terminal cysteins were revealed by biochemical analysis. These cysteines have been posttranslational modified through a thioester bond.

These findings were then tested in Strand and coworkers (Strand *et al.*, 2009) by the use of BN-PAGE assay. The results indicated that if one cystein was mutated, no destabilized effect on square array assembly was detected. However, with a C13A/C17A double mutation

introduced, a clear change occurred in the pattern of bands, and a the higher order band disappeared, indicating no formation of square arrays. These results supported the Suzuki model and validated the use of BN-PAGE as an assay suitable for protein-protein interactions.

1.7.3 Statement 3: N-terminal residues of AQP4c (V24, A25 F26) is responsible for determination of square array formation

Verkman and coworkers used single molecular tracking to follow movement induced by fluorescently labelled AQP4 mutants in cell membranes *in vivo*, establishing the molecular determinants of square arrays assembly (Crane et al., 2008). They observed that unmutated M1(AQP4a) moved freely, while unmutated M23(AQP4c) was immobile indicating square arrays presence. Cotransfection of myc-tagged M1 and M23 were performed in different cell line (COS-7, MDCK and CHO-cells), but no slowing of diffusion where observed.

To isolate the role of specific domains within the AQP4 isoforms, N-terminal mutants of AQP4c were made and transfected into COS7-cells. The diffusion patterns by the single molecular tracking system were then observed. It was found that square arrays disappeared by downstream deletions of specific residues of M23, Valine24, Alanine25 and Phenylalanine26. The formation of square arrays was also prevented by introducing Proline residues at specific sites downstream from the N-terminus of M23. It was concluded that M23 assembly of square arrays is stabilized by hydrophobic interactions involving some of these residues tested, and that M1 destabilization of square arrays resulted from blocking of this interaction by seven residues upstreams from Methylene 23.

The same mutations of AQP4c have been tested in the BN PAGE assay described in this study.

1.8 Aims of this study

The aim of this study was to investigate protein-protein interactions of AQP4 and AQP4 isoforms using a biochemical assay (BN-PAGE) developed by our group for the purpose of visualizing square arrays. Other biology, biochemistry and anatomical tools, have also been used.

Since it already exist preliminary data showing interactions between the best known isoforms of AQP4a and AQP4c, we hypothesized possible interactions between other AQP4 isoforms visualized by the BN- PAGE system.

There have been several reports, based on indirect data, that AQP4 might be a molecular binding partner for several other proteins (Amiry-Moghaddam and Ottersen, 2003). In additions to testing AQP4 isoform protein-protein interactions, the hypothesis of AQP4 binding to α -syntrophin, Kir4.1 and PatJ were tested using the same BN-PAGE assay developed to investigate AQP4 isoforms. In this section, the PDZ binding motif is common in both AQP4, syntrophin and PatJ. PDZ domain is interesting in this thesis for three reasons:

- AQP4 is thought to be interacting with α -syntrophin via a PDZ domain located at C-terminal of syntrophin (Amiry-Moghaddam et al., 2004).
- AQP4 and Kir4.1 colocalize in glia cells, and the subcellular distribution of Kir4.1 is thought to be influenced by a possible anchoring complex, suggesting PDZ containing protein (Leonoudakis et al., 2004).
- PatJ, which is a paralog to another protein containing PDZ domain, Multi-PDZ domain protein-1 (MUPP-1), have demonstrated interaction with the inwardly rectifying potassium channel Kir4.2 (Sindic et al., 2009).

The work in this thesis was divided into three parts, where each part to a certain degree depended on successful results from the preceding part:

1. Initially, as an introduction to learn and use the BN-PAGE-system, different AQP4-single, double and –triple mutations already made for an ongoing project in the laboratory, were

analyzed using this system. Later N-terminal mutations of AQP4c was analysed in purpose of testing the hypothesis in section 1.7.3

2a. Next step was to review and test antibodies against the potential AQP4 partners, Kir4.1, syntrophin and PatJ. This included cloning a Kir4.1 construct, used for investigating antibody specificity.

2b. In addition myc-tagged versions of interesting AQP4- interactions candidates were made, since there are not specific antibodies available for all candidates.

3. If successful detection of all the interesting AQP4-interaction partners could be obtained by the use of antibodies, the next step would be to co-express Kir4.1, α -syntrophin and Pat-J with AQP4 isoforms in a HeLa cell and HEK 293 cell system, to investigate potential protein interactions between these candidates by the use of the BN-PAGE system.

2 MATERIALS

2.1 Reagents used in different sections

Table 1. Reagents and equipment used in section 3.1

Items	Specification	Manufacturers
Dissection tool	*****	American Tools
High capacity cDNA Reverse Transcription Kit	7368813	Applied Biosystem
Kontes® Microtube Pellet Pestle®	Size 16	Sc-Ed Warehouse USA
RNAlater RNA Stabilization Reagent	76106	Qbiogene
RNeasy-kit	75114	Qiagen

Table 2 . Reagents used in section 3.1.2

Items	Specification	Manufacturers
10 X RT buffer	10 µL	QBiogene
100 mM dNTP	4 µL	QBiogene
10 X Random primer	10 µL	QBiogene
Nuclease free water	up to a total volume of 50 µL	QBiogene
500 U Reverse Transcriptase	5 µL	Q-BioTag (5 U/µL)

Table 3. Reagents and equipment used in section 3.3

Items	Specification	Manufacturers
Agarose	15510-027	Invitrogen
Sybr-Green	S7585	Invitrogen
Loading dye	See table 16	Self made
TrackIt 1 Kb DNA Ladder	10488-072	Invitrogen
PCR mastermix:	Volume	Final concentration
10 X Incubation buffer	5.0 µL	1 X
MgCl ₂ (25 mM)	5.0 µL	5 mM
dNTP(2.5 mM each)	2.0 µL	200 uM
Primer F 20M each/stock	1.5 µL	1 pmol
Primer R 20M each/stock	1.5 µL	1 pmol
Templat DNA	1.0 µL	100-1000 ng
DNA polymerase	0.2 µL	5U
MQ H2O	To 50 µL	

Table 4. Reagents and equipment used in section 3.4 For bacteria strain see table 26.

Items	Specification	Manufacturers
Topo TA cloning ®- kit	10486-378	Invitrogen
S.O.C media	15544-034	Invitrogen

Table 5. Reagents and equipment used in section 3.5

Items	Specification	Manufacturers
LB-media with ampicillin	100 µg/ml	Sigma

Table 6. Reagents and equipment used in section 3.6.1

Items	Specification	Manufacturers
Qiaprep Miniprep-kit	27106	Qiagen

Table 7. Reagents and equipment used in section 3.6.2

Items	Specification	Manufacturers
Endofree plasmid Maxi-kit	12362	Qiagen

Table 8. Reagents and equipment used in section 3.7

Items	Specification	Manufacturers
Restriction buffers C and D	100 mM NaCl, 50 mM Tris-HCL, 100 mM DTT (pH=7.9)	Sigma
BSA	10 mg/mL, 10270	Gibco
Restriction enzymes	10000 units/mL	New England Biolabs

Table 9. Reagents and equipment used in section 3.15.1

Items	Specification	Manufacturers
Bio-Rad DC-kit	1479-563	Bio-Rad

Table 10. Reagents and equipment used in section 3.9

Items	Specification	Manufacturers
1X Quick ligase buffer	136-456	BioLabs
Quick ligase enzyme	10000 u/ mL	BioLabs
pcDNA/Zeo+ plasmid	*****	Invitrogen

Table 11. Reagents and equipment used in section 3.10

Items	Specification	Manufacturers
ABI PRISM® Big Dye terminator V.3.1 Sequencing kit	4336919, Big dye 3.1 enzyme, 5 X buffer	Applied Biosystems

Table 12. Reagents and equipment used in section 3.12.2

Items	Specification	Manufacturers
Biowhittaker ® EDTA trypsin	200 mg/L EDTA, 1700000 u/L trypsin	Lonza
DMEM medium	With added glucose 4.5 g/L and L-glutamin, 11960	Gibco
PBS (working solution pH=7.4)	137 mM NaCl, 2.7 mM KCl, 4.3 mM Na ₂ HPO ₄ ×7H ₂ O 1.4 mM KH ₂ PO ₄	Self made

Table 13. Reagents and equipment used in section 3.12.5

Items	Specification	Manufacturers
Biowhittaker ® EDTA trypsin	200 mg/L EDTA, 1700000 u/L trypsin	Lonza
Fuchs-rosenthal counting chamber	15170-230	VWR
Tryptophan Blue	302643	Sigma

Table 14. Reagents and equipment used in section 3.13.1

Items	Specification	Manufacturers
DMEM	With added glucose 4.5 g/L and L-glutamin, 11960	Gibco
Fugene 6 transfection Reagents	124-33	Roche
Opti-MEM®	Reduced-serum with L-glutamin, 31985-047	Invitrogen

Table 15. Equipment used for Western blot and BN-PAGE

Items	Specification	Manufacturers
SDS-PAGE	*****	*****
<ul style="list-style-type: none"> Criterion PVDF membrane 0.2µm pore size m cassette 	BR-162-0170	Bio-Rad
<ul style="list-style-type: none"> Criterion precast gels 	345-0006	Bio-Rad
<ul style="list-style-type: none"> Criterion build up system 	345-1086	Bio-Rad
<ul style="list-style-type: none"> Coomassie 	161-0787	Bio-Rad
BN-PAGE	*****	*****
Native Page™ Novex® Bis-Tris Gel system, 4-16 %	BN-1002BOX	Invitrogen
Criterion PVDF membrane 0.2µm pore size	BR-9127018	Bio-Rad
ECF Western blotting Detection Reagens	1067873	GE Healthcare

2.2 Buffers and gels

Table 16. Buffers used in section 3.3

Items	Specification	Manufacturers
0.5 X TAE	242 g TRIS base, 57.1g glacial acetic acid 100 ml 0.5 M EDTA pH=8.0	Sigma
2 % agarose	6 g Agarose in 300 mL 0.5 X TAE buffer	Invitrogen
0.6 X Loading dye	0.25 % Bromphenol blue 30 % glycerol 10 mM Tris-HCL pH 8.0	Sigma

Table 17. Buffers used in section 3.16 (Western blot). All reagents from Sigma.

Items	Specification	Method / technique
Acrylamid:bisacrylamide (40%T. 2.6%C) 100 ml	38.96 g acrylamide 1.04 g bisacrylamid	Add dH ₂ O to a final volume of 100 ml. Filter through a 0.45 µm filter
4x resolving gel buffer 200 ml	36.3 g Tris base 170 ml dH ₂ O	Adjust pH to 8.8 with 6 M HCl. Cool the solution to room temperature and

		readjust to pH 8.8 with 6 M HCl. Add dH ₂ O to a final volume of 200 ml and store at 4°C.
4x stacking gel buffer 200 ml	12.1 g Tris base 170 ml dH ₂ O	Adjust pH to 6.8 with 6 M HCl. Cool the solution to room temperature and readjust to pH 6.8 with 6 M HCl. Add dH ₂ O to a final volume of 200 ml and store at 4°C
10% SDS 100 ml	10 g. SDS	Add dH ₂ O to a final volume of 100 ml and store at RT.
10% APS	1 g. APS	Add dH ₂ O to a final volume of 10 ml and make 100 or 500 µl aliquots and store in the freezer.
Urea 9M	*****	Sigma
Loading buffer 8 ml	1.6 ml 1.5 M Tris-HCl pH 6.8 0.42 g. SDS 2.4 ml glycerol Trace amount of bromphenol blue 0.4 ml β-mercaptoethanol (if you use DTT instead, use 10% of total volume) 3.6 ml dH ₂ O	
1.5 M Tris-HCl 200 ml	36.342 g. Tris 150 ml dH ₂ O	Adjust pH with HCl and add dH ₂ O to a final volume of 200 ml.
Towbin blotting buffer 3 L	300 ml 10x Towbin blotting buffer 600 ml MetOH 2100 ml dH ₂ O	pH should be 8,3 without adjustments (pKa of Tris is 8,3). Do not adjust pH. Store at 4°C
Electrophoresis buffer (Laemmli buffer) 10X	To 800ml of dH ₂ O add 30,3g Tris (Mm=121,14g/mol) 144,1g Glycine (Mm=75,07g/mol) 10,0g SDS (Mm=288,38g/mol)	pH should be 8,3 without adjustments (pKa of Tris is 8,3). Do not adjust pH. Add dH ₂ O to 1000ml Store at 4°C
Milk solution 1 L	50 g. non-fat dried milk powder, 0.5 g. NaN ₃	Add TBST buffer to a final volume of 1 L.
TBST 8 L	400 ml 20x TBS buffer 40 ml 10% v/v Tween	*****

	7560 ml dH ₂ O	
Stripping solution	100 mM 2-Mercaptoethanol 2% SDS	*****

Table 18. Buffers used in section 3.17 (BN-PAGE). All reagents from Invitrogen.

Items	Stock solution	Volume	Total concentration
Dark catodebuffer	Running buffer (20X)	10 mL	~1X (50mM BisTris, 50mM Tricine, pH 6,8) ~1X (0.02 % Coomassie G-250) *****
	Cathode additive (20X) (0.4 % Coomassie G-250) MQ H ₂ O	10 mL Add up to total volume of 200 mL	
	Running buffer (20X)	10 mL	
Light catodebuffer	Running buffer (20X)	10 mL	~1X (50mM BisTris, 50mM Tricine, pH 6,8) ~0.1X (0.002 % Coomassie G-250)
	Cathode additive (20X) (0.4 % Coomassie G-250)	1 mL	
	MQ H ₂ O	Add up to total volume of 200mL	
Anode buffer	Running buffer (20X)	50 mL	~5X (250mM BisTris, 250mM Tricine, pH 6,8) *****
	MQ H ₂ O	Add up to a total volume of 200 mL	
Transfer / BN - blotting buffer	Transfer buffer(20 X)	50 mL	1 X ~22 %
	Methanol (96 %)	Add up to a total volume of 1000 mL	
	MQ-H ₂ O	750 mL	

2.3 Ladders and primers

Table 19. Ladders used in this thesis. Volumes correspond to ~2g protein.

Ladder	Volume used	Manufacturers
Gene Ruler™ 1 kb DNA ladder	3 µL	Fermentas
Lambda-HindIII-EcoRI	1 µL	Promega
Magic Marker	2 µL	Invitrogen
Native Marker (unstained)	3 µL	Invitrogen
Presicion Plus Protein Std.	5 µL	Bio-Rad
See Blue	5 µL	Invitrogen
TrackIt 1kb DNA ladder (0.1µg/µL)	2 µL	Invitrogen

Table 20. Primers used in this thesis

Name	Description
Fen 1-1314	Reverse primer used as control on sportP-plasmid in the amplification of Kir4.1 gene
Fen1-897	Forward primer used as control on sportP-plasmid in the amplification of Kir4.1 gene
Kir4.1-1367	Reverse primer for amplification of Kir4.1 gene
Kir4.1-KE2	Forward primer for amplification of Kir4.1 gene
Kir4.1-KE243	Forward primer for amplification of Kir4.1 gene used together with a reverse primer with myc-tag
Kir4.1-kh2	Forward primer for amplification of Kir4.1 gene
Kir4.1-Kh243	Forward primer for amplification of Kir4.1 gene
Kir4.1-myc X2	Reverse primer for amplification of Kir4.1 gene with myc-tag
Kir4.1-mycX1	Reverse primer for amplification of Kir4.1 gene with myc tag
Kir4.1-X2	Reverse primer for amplification of Kir4.1 gene
BHG reverse primer	Sequencing primer
T7 primer	Sequencing primer

Table 21. PCR primer sequences used in this thesis

Name	Sequence	Restriction site in sequence
Fen 1-897_forward	GGCTACCGAGGACATGGACT	*****
Fen1-1314_reverse	TTCGCTCCTCAGAGAACTGC	*****
Kir4.1-KE2_forward	GAATTCGCCACCATGACGTCGGTCGCTAAGGTC	*****
Kir4.1-KE243_forward	GAATTCGCCACCATGACGTCGGTCGCTAAGGT	*****
Kir4.1-kh2_forward	AGCTTGCCACCATGACGTCGGTCGCTAAGGTC	*****
Kir4.1-Kh243_forward	AAGCTTGCCACCATGACGTCGGTCGCTAAGGT	Has HindIII site and Kozak at 5' end.
Kir4.1-myc X2_reverse	5'-CTCGAGCTACAGATCCTCTTCTGAGATGAGTTTTTGTTC TCCGACGTTGCTGATGCGCACACT-3	*****
Kir4.1-mycX1_reverse	CTCGAGCTACAGATCCTCTTCTGAGATGAGTTTTTGTTC TCC GACGTTGCTGATGCGCACAC	*****
Kir4.1-X1367_reverse	CTCGAGATATCAGACGTTGCTGATG	Has XhoI site at 5' end, for pcDNA3.1/Zeo cloning

Kir4.1-X2_ reverse	CTCGAGATATCAGACGTTGCTGATGC	*****
-----------------------	----------------------------	-------

2.4 Antibodies, proteins and enzymes

Table 22. Primary antibodies used in this thesis.

Primary antibodies	Description	Manufacturers
AQP4 (C-19) sc-9888	Anti-goat, 200 µg/mL	Santa Cruz Biotechnology, Inc.
AQP4 LS-C3805	Anti-rabbit, 1 mg/ml	LifeSpan Biosciences
Kir 4.1 APC-035	Anti-rabbit, 0.8 mg/ml	Alomone labs
Kir 4.1 K1864	Anti-rabbit, 0.3 mg/ml	Nordic Biosite
Kir 4.1 ab55380	Anti-mouse monoclonal 1 mg/ml (only used for comparison)	Abcam
c-Myc (A-14) sc-789	Anti-rabbit, 200 µg/mL	Santa Cruz Biotechnology, Inc.
Syntrophin alpha 1 ab 11187	Anti-rabbit, 7.7 mg/ml	Abcam
GFP rabbit polyclonal ab6556	Anti-rabbit , 0.5 mg/ml	Abcam
GAPDH antibody ab9484	Anti-mouse, 1 mg/ml	Abcam

Table 23. Secondary antibodies used in this thesis (1:10 000 dilution).

Secondary antibodies	Description	Manufacturers
Anti-rabbit A2556 (Alkaline-phosphatase)	Produced in mouse (whole molecule), monclonal	Sigma
Anti-goat IgG A4187 Alkaline-phosphatase	Produced in rabbit (Whole molecule)	Sigma
Anti-mouse IgG A3563 (Alkaline-phosphatase)	Produced in sheep (Whole molecule)	Sigma

Table 24. Enzymes used in this thesis.

Name	Description	Manufacturers
Complete Protease Inhibitor coctail	*****	Roche
DNA ligase	Mo202L	New England BioLabs
Phusion® High-Fidelity DNA Polymerase	F53011	New England BioLabs
Taq DNA polymerase	Mo267L	New England BioLabs
Trypsin-EDTA	C ₁₀ H ₁₆ N ₂ O ₈	Lonza
Topoisomerase 1	In the TOPO-kit	Invitrogen

Table 25. Plasmids used in this thesis.

Plasmid	Description and use	Source of reference
Mx1pCI-Neo-M23-R86A-G135A-I217A	Expression plasmid used as vector for transfection of trippelmutations	Made by a group member
Mx22pCI-Neo-M23-I217-Y228	Expression plasmid used as vector for transfection of doublelmutations	Made by a group member
Mx35pCI-Neo-M23-R86A-W209A-I217A	Expression plasmid used as vector for transfection of trippelmutations	Made by a group member
Mx5pCI-Neo-M23-G135A-I217A-Y228A	Expression plasmid used as vector for transfection of trippelmutations	Made by a group member
Mx9-Kir4.1/pcDNA(Zeo)+	Expression plasmid used as vector for transfection of Kir4.1	Made by a group member
Mx9pCI-Neo-M23_W209A-I217A-Y228A	Expression plasmid used as vector for transfection of trippelmutations	Made by a group member
pcDNA3.1/Zeo(+)	Expression plasmid	Invitrogen V860-20
pCR®2.1-TOPO	Cloning plasmid	Invitrogen K4500-01
pHIV_mAQP4_shRNA_mirGFP	Lenthi construct (RNAi) with GFP (used as control in transfections assay of HeLa and HEK293 cells)	Made by a group member
pSport1	Expression plasmid used as vector for transfection of both Kir4.1 and Kir4.1-myc	Open biosystem /Image id 3088116
pXOOM-AQP4	Expression plasmid	Made by a group member

2.5 Bacterial strains, tools and instruments

Table 26. Bacterial strains used in the thesis.

Strain	Specification	Manufacturers
Library Efficiency® DH5alpha™ competent cells	18263-012	Invitrogen
Subcloning Efficiency™ DH5 alpha™ competent cells	18265-017	Invitrogen

Table 27 Analytical tools used in this thesis.

Software	Manufacturers
Chromas Lite /Share-It!	Digital River GmbH, Australia
ImageQuant Tools	UiO
Photoshop	Microsoft

Table 28. Instruments used in this thesis.

Instruments	Spesifications	Manufacturers
ABI prism 3100 DNA sequencer	Sequencing	Applied Biosystem
Bechmark Reader	Protein concentration estimation	Bio-Rad
Electrophoretic power supply	EPS 3500 xc	Bio-Rad
Gene Amp® PCR system 9700	Conventional PCR	Applied Biosystem
Magnetic stirrer	*****	Lational Labnet
Microscope light	Axiovert 25	Zeiss
ND-1000 full spectrum UV/VIS Nanodrop	Measuring of DNA concentration	Nanodrop
pH Meter With Ph And Conductivity Expansion Units	S47K	Mettler-Toledo
Table top centrifuge with cooling	Rotina 35 R	Hettich , Germany
UV transmitter	Uvitech	Bio-Rad
Cell incubation chamber	Sanyo IR Sensor	Bergman

Table 29. Other laboratory equipment.

Laboratory equipment	Manufacturers
Cell containes	Corning
Eppendorp tubes	Axygen Quality
Glass equipment	Meszansky
Pipettes (automatic and regular)	BioHit
Sterile filters; 0.22 µm pore size	Millipore
Strippettes1, 10 ml and 50 ml	Costar
Syringes 2 mL	Omniflyx, Brauns

3 METHODS

All materials used in chapter 3 are listed in chapter 2.

3.1 Preparation of cDNA for Kir.4.1 analyses

This is the first step towards making a Kir4.1 construct, which was used to test antibody specificity for Kir4. RNA and protein extracts were obtained from adult, wildtype, female C57/129/AQP4 KO-mice. The mouse was sacrificed by elevated CO₂ and decapitated. The tissue dissected was stored in chilled RNA-later to inhibit RNAases, before homogenized in a clean Kontes Homogenizer, size 16.

Protocol

- Remove the skin carefully from the skull by using forceps and scissors.
- Cut the skull mid-sagittal from behind of the brain.
- Remove the brain from the skull carefully, and put it on a clean tinfoil.
- Localize cerebral cortex and cerebellum.
- ~20 mg of tissue from cerebral cortex and from cerebellum is dissected as thin slices by using a common dissection tool-kit.
- Put the slices in 500 µL of RNAlater, and label “cortex” or “cerebellum”.
- Put one slice at a time in the Kontez Homogenizer and drain off RNAlater.
- Add 350 µl of lysis-buffer (RNeasy-kit, Qiagen) to 20 mg of tissue.
- Homogenate by 20 strokes and pipette the homogenate into a RNeasy column (RNeasy mini-kit spin columns (Qiagen)) that has been prepared according to the protocol in the kit, or a tube for storage.

The homogenate obtained was purified using RNeasy mini-kit spin columns (Qiagen) (section 3.1.1) for making cDNA (section 3.1.2). The homogenate was frozen at -20 °C until needed.

3.1.1 Total RNA-isolation and purification

When working with RNA is it very important not to contaminate the sample with any RNAses. The bench-coat was changed, as well as gloves, and the use of tips with filter when performing RNA work to prevent degradation of RNA from RNAses.

For RNA extractions the “RNeasy mini kit-spin columns” (Qiagen) was used according to the manufacturer's instruction. All steps were performed at room temperature, and it is important to ensure that the centrifuge does not cool below 20°C. This can affect the conditions for binding of RNA to the membrane in the columns. Result can be reduced RNA yield.

Protocol

- Transfer the homogenate into a RNeasy mini spin-column placed in a collection tube. Centrifuge for 15 sec at >8000 g.
- Discard the flow-through. (Reuse the collection tube).
- Add 700 µL of buffer RWI to the column. Centrifuge for 15 sec at >8000 g to wash the spin column-membranes. Discard the flow-through.
- Before the next step, change to a new collection tube.
- Add 500 µL of buffer RPE to the column. Centrifuge for 1 min. at >8000 g to wash the spin column membrane. Discard the flow-through.
- Add 500 µL of buffer RPE to the column and spin again for 2 min. Discard the flow-through.
- Centrifuge one more time for 1 min. (This centrifugation step dries the membrane, ensuring that no ethanol is carried over during RNA elution).
- Place the column in a marked 1.5 ml RNase free collection tube. Add 50 µL RNase-free water directly to the membrane. Incubate for 1 min and centrifuge for 1 min at >8000 g to elute the RNA.

The RNA should be stored at -80 °C. (In this case the RNA was stored at -20° C until next day).

3.1.2 cDNA synthesis by reverse transcription

Complementary DNA (cDNA) is DNA synthesized from a fully spliced mRNA template in a reaction catalyzed by the enzyme reverse transcriptase (RT). The enzyme operates on a single strand of mRNA, and makes its complementary DNA by base pairing between RNA (A,U,G,C) and DNA (A,T,G,C). Introns are non-coding sequences that have to be removed from the primary transcript of RNA before translation into proteins can start. In this thesis cDNA synthesis has been used for the creation of a cDNA library from mouse cortex and cerebellum, in order to get material for the amplification of the coding sequence of Kir.4.1 by using conventional PCR.

To generate cDNA, "High capacity cDNA Reverse Transcription kit" from Applied Biosystems was used (for primers see table 20). The procedure was performed according to the protocol included in the kit. Before starting, RNase-free eppendorf-tubes were labelled, the buffers used in the master mix were thawed in a water bath at RT, and the enzyme was placed in a cold-box.

Protocol

- 50 µL of total RNA (obtained in the RNA extraction step, see 3.1.1) is mixed 1:1 with a master mix-solution described in table 2. The reagent was added in the order shown. Before adding the enzyme to the master mix, vortex and spin the mix very shortly.
- Incubate the mix for 10 minutes at room temperature.
- Place the samples in 37 °C (water bath) for 1 h.
- Spin the samples down and freeze at -20°C until proceeding with conventional PCR.

3.2 PCR (Polymerase chain reaction)

PCR is a method that allows the production of more than ten million copies of target DNA-sequences from only a few molecules. To amplify the desired DNA sequence, specific primers, DNA polymerase and dNTP are added. After denaturation of the DNA at high temperature, the primers anneal to a complementary sequence in the DNA when lowering the temperature. This makes it possible for the polymerase to initiate DNA replication of the sequence located between the primers (extension step). By exposing the reaction mixture to different thermal cycles, DNA synthesis of the target sequence is repeated in every cycle, giving an exponential synthesis of new copies of the template sequence.

For PCR amplification of DNA fragments used in cloning steps, the Pfu(sion) DNA polymerase (Fermentas) and in conventional PCR the *Taq*-DNA polymerase (Invitrogen) was used to ensure correct amplification. *Taq* DNA Polymerase catalyzes the incorporation of dNTPs into DNA. All PCRs were performed in the Gene Amp® PCR system 9700 (Applied Biosystems). Primers used in the different PCR setups are listed in table 20.

Protocol

- The PCR reaction was prepared in thin walled PCR tubes on ice. A mastermix was made according to the table 3 and multiplied with the number of samples +1
- The reaction mixture was placed in a thermal cycler and the settings described below were applied (Table 30).

Table 30. Temperature, length and cycles of the different steps in the PCR reaction.

Temperature	Action	Time	Number of cycles
	Initial		
94°C	Denaturation	3min	
95°C	Denaturation	30sec	35
56°C	Annealing	45sec	
72°C	Elongation	90sec	
72°C	Extension	2 min	1
4° C	storage	Until program is stopped	

The PCR products were analyzed by gel electrophoresis as described in 3.3 to confirm correct amplification.

3.3 Agarose gel electrophoresis

Agarose-gel electrophoresis is an easy and fast method for verifying the quality and quantity of DNA. This is a separation method used to visualize and identify DNA according to size. When adequate migration has occurred, DNA fragments are visualized by a staining-procedure. In our laboratory, we use the nucleic acid gel stain; SYBR Green (S7585, Invitrogen). This fluorescent dye bind efficient to both double and single-stranded DNA. It is less mutagenic than ethidium-bromide, and five times more sensitive (data sheet Invitrogen). The gel can be stained prior to electrophoresis or after. In general the gel was stained by soaking in a dilute solution of SYBR Green and running buffer (1:10000) after electrophoresis. Incubation period was 45-60 min. This procedure gave the sharpest and strongest fluorescing signal. To visualize DNA, the gel was placed under an ultraviolet transilluminator, or a photo was taken by using a laser scanner (Typhoon). The DNA will diffuse within the gel over time, so examination of the gel should

take place shortly after the incubation time. In order to determine the molecular size of DNA, a DNA ladder is always run on the gel.

Protocol

Normally, DNA electrophoresis was performed at room temperature using 2 % agarose gel in 0.5 X TAE buffer (table 16).

- Mix agarose and 0.5 X TAE buffer. Heat the solution in the microwave until the agarose is dissolved completely.
- Cool the agarose solution to approximately 70° C. Pour the solution into a tray (BioRad) where it can harden as the temperature drops. A well-comb with 10 or 15 wells was placed in the agarose gel during hardening.
- The solid gel was transferred to an electrophoresis chamber filled with 0.5 X TAE buffer.
- Samples were diluted to 1 X with 6 X loading dye before loading. 2 µg TrackIt 1Kb DNA ladder from Invitrogen was used as a molecular marker.
- Electrophoresis was carried out for 45 min at 70 Volt.
- When electrophoresis is done, stain the gel in SYBR Green solution for 45-60 min.
- Scan gel using Typhoon scanner or proceed with purification (section 3.3.1).

3.3.1 Purification of PCR products

PCR products were excised from the electrophoresis gel using the GFX purification kit (Qiagen). The DNA fragment was cut out with a sharp, clean scalpel, after running a new 2 % agarose gel with minimized UV exposure time. The size of the gel slice was minimized by removing extra agarose.

Protocol

- The gel slice is transferred to a pre-weighed clean tube.
- 1µL of capture buffer is added for every mg of gel slice.
- The tube is incubated at 60 ° C until the gel slice completely dissolved. To help dissolving the gel slice, the tube is gently mixed every 3rd min during the incubation.

- After the gel slice is dissolved completely, a spin column is placed in a provided collection tube. The sample mixture is applied and incubated for 1 min at room temperature.
- After a centrifugation step (13000 RPM for 1 min), the flow through is discarded.
- 500 μ L of wash buffer is added to the column, followed by a new centrifugation step for 30 sec. The flow through is discarded
- The GFX-column is placed in a clean 1.5 ml microcentrifuge tube. To eluate DNA, 20 μ L MQ-H₂O is added to the center of the GFX-column membrane and the column is centrifugated for 1 min
- All centrifugation steps are performed at 13000 RPM and RT. DNA is stored at -20 °C.

3.4 Preparation of pCR2.1-TOPO plasmid

3.4.1 Sticky end ligation into plasmid by using TOPO TA cloning-kit

This is a method used for insertion of a Taq-polymerase amplified DNA product into a plasmid vector (pCR 2.1-TOPO plasmid). Plasmid with DNA-insertion can then be introduced for cells that are able to incorporate this plasmid/DNA and express it on its surface. The enzyme DNA topoisomerase I, is important in this cloning assay. Topoisomerase I functions as a restriction enzyme and as a ligase, so other DNA ligases for this cloning are not needed. The biological role of the enzyme is to cleave and rejoin DNA when replicated.

In the kit, (TOPO TA cloning, Invitrogen) TOPO-vectors are provided with a topoisomerase I covalent attached to each 3'-phosphate. Topoisomerase I in this assay recognizes a specific sequence 5'--CCCTT found in one strand of the plasmid, and can cleave the phosphodiester-bond behind the last thymine and the strand can unwind. Taq polymerase is used for the amplification in the PCR reaction, and has the ability to add a single deoxyadenosine (A) to the 3' end of the PCR product. The TOPO-vector has an overhanging 3' thymine-residue, and is then compatible to the PCR product. The TOPO-vectors are designed in such a way that they carry this specific sequence (CCTT-3') which can be recognized by the topoisomerase enzyme. The enzyme ligates the compatible ends of the plasmid and DNA insert, and releases it self from the complex.

The vector pCR®2.1-TOPO contains DNA coding sequences for both ampicillin and kanamycin. This is used to select transformed *E.coli* grown on agar with the appropriate antibiotics. The vector also occupies a restriction site for *EcoRI*, which makes it possible to cut out the PCR product after ligation. The T7-promotor in the vector indicates the start sequence for the T7-polymerase used for *in vitro* translation (see appendix 4)

The manual included with the kit was generally followed when using the TOPO TA Cloning kit (Invitrogen). This utilizes bacteria competent for chemical transformation.

Table 31. Reaction mix for TOPO-cloning

Reagent	Volume
ds DNA	4 µL
Diluted TOPO-vector (2 µL TOPO-vector + 2.3 µL MQ-H ₂ O)	1 µL
MQ -H ₂ O	1 µL

Protocol

- Incubate the reaction mixture for 15 min at RT (table 31). During the incubation period, the vial with competent DH5α-bacteria can be thawed on ice.
- Spin the vial briefly and apply 3 µL of the reaction mixture (table 31). Keep everything on ice during a 30 min incubation period.
- Heat-shock the bacteria-vial for exactly 35 sec at 42°C (use a water bath). Rotate the vial every third second.
- After 35 sec, immediately transfer the tube to ice. Add 200 µL S.O.C medium and incubate on a shaker for 45 min at RT.
- After the incubation period, plate out each transformation on pre-warmed selective LB plates. The vector used contains an ampicillin-resistant gene, and ampicillin (50µg/mL) is used as a selective in the agar-plates. Only colonies containing the correct plasmid will grow on the selective plates.
- To avoid too dense colonies, two different volumes were spread using glass-beads prewashed in alcohol and dried. The agar plates are incubated at 37 °C for 12-16 h before proceeding picking colonies and perform miniprep, maxiprep and sequencing (see 3.6 and 3.10)

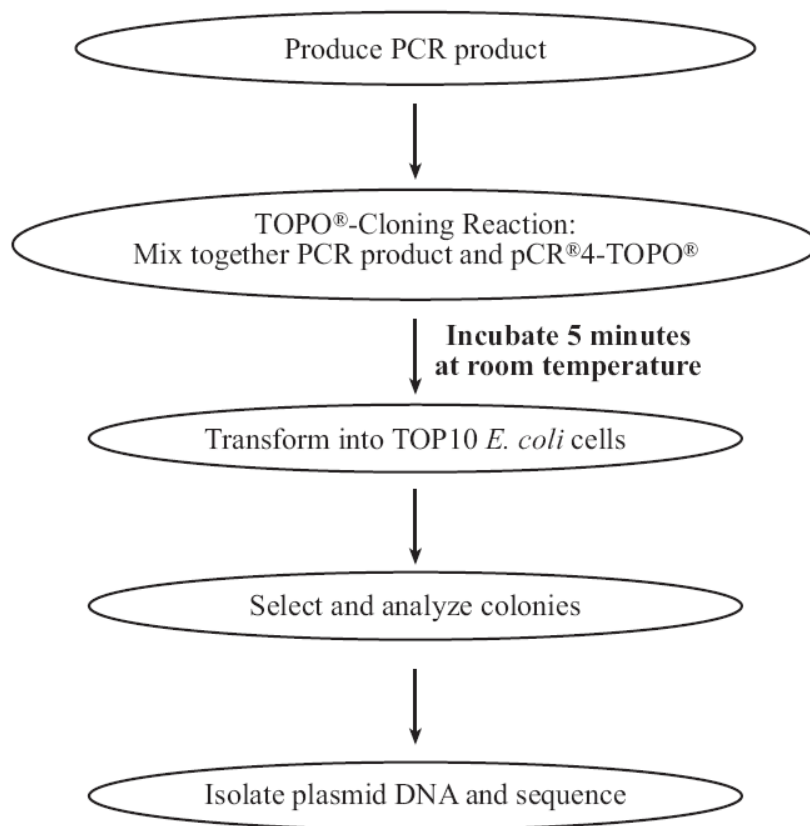


Figure 6. A flow sheet diagram of the TOPO-cloning reaction. (From Invitrogen .com)

3.4.2 Growth of Escherichia coli strain

E.coli cells were grown as overnight cultures in open to air liquid LB media. The incubation was carried out at 37 ° C and with shaking at orbit 160. The DH5-*alpha*- *E. coli* strain was used as a second vector for harbouring of plasmids. The concentration of the antibiotic (kanamycin or ampicillin) used in liquid agar was 100 µg/mL and in solid agar 50 µg/mL. LB medium and LB agar were made by workers at “Substratlaboratoriet”, Rikshospitalet.

3.4.3 Bacterial strains

E.coli bacteria strains arrived from the manufacturers as glycerol stocks and were stored at -80°C. The bacteria vials where thawed on ice when needed for experiments.

Subcloning Efficiency™ DH5 *alpha*™ competent cells (White cap) (Invitrogen) where used for sub cloning and easy transformation of plasmids. DH5 α-cells are very robust, and this method is well established in our lab.

3.5 Overnight (ON) cultures

To make overnight cultures for use in plasmid purification, one bacteria-colony from a LB-plate with appropriate selective antibiotics (ampicillin (50 µg/mL) or kanamycin) was grown in 100 mL LB-agar. The master plate containing all the different colonies was kept at 4 °C for retesting if necessary. The tubes were placed in a table-top incubator with shaking movements (orbit: 250) at 37 °C for approximately 16 h before plasmid preparation.

3.6 Plasmid purification from ON cultures

3.6.1 Miniprep protocol

QIAprep® Miniprep protocol (Qiagen) was generally used for small scale plasmid purification when screening for plasmid inserts. This protocol is designed to give high-copy plasmid DNA from over night cultures of *E.coli* in LB medium. The procedure is based on lysis of bacterial cells by using alkaline buffers, neutralization, followed by adsorption of DNA onto a silica membrane.

Protocol

- 3 mL of an overnight bacterial culture grown in selective LB/antibiotics medium was pelleted by a table-top centrifugation-step at >8000 rpm for 5 min at RT.
- The supernatant was removed and the pellet resuspended in 250 µL of buffer P1 with RNase added.
- The resuspend pellet was transferred to a microcentrifuge tube and 250 µL of buffer P2 (lysis) was added and mixed by inverting the tube eight times.
- The lysis reaction was allowed to proceed for exactly 4 min and 30sec.
- After lysis, 350 µL of buffer N3 (neutralization) was added, and mixed by inverting the tube eight times. Centrifuge the mix at 13000 rpm for 10 min in a tabletop microcentrifuge
- The supernatant from the previous step was decanted into a spin column, and centrifuged at 13000 rpm for 60 sec. The flow-through was discarded.
- All bound DNA was washed by adding 750 µL buffer PE and centrifuged for 60 sec. The flow-troughs were discarded.

- An additional centrifugation step was performed to remove the residual wash buffer, since ethanol in the buffer can inhibit upcoming enzymatic reactions.
- The bound DNA is eluted in a clean eppendorf-tube by adding 50 μ L EB-buffer (10 mM Tris-Cl, pH 8.5), incubating for 1min, and centrifuged for 1 min at 13 000 RPM.
- The pure plasmid DNA can be stored at 4 °C for a short period of time, or -20°C.

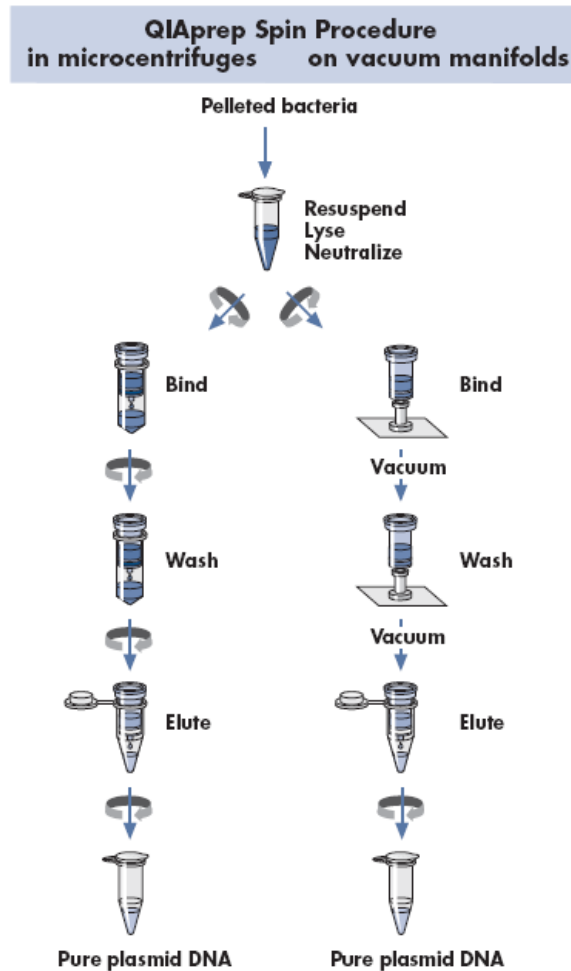


Figure 7. Flowchart of miniprep procedure from www.qiagen.com

3.6.2 Endotoxin-free Maxiprep

Big batches of bacterial plasmid purification were performed using the EndoFree® Plasmid Maxi purification kit (Qiagen). Using this protocol up to 500 μ g endotoxin-free plasmid DNA can be purified. Endotoxins, also known as lipopolysaccharids, are cell membrane components

of bacteria e.g. from *E.coli*. Small amount of endotoxins are released into bacteria- surroundings when they die, thus during lysis these molecules are released into the lysate and can influence transfection efficiencies of DNA into cultured cells later. The procedure is based on an alkaline lysis reaction, followed by binding of plasmid- DNA to an QIAGEN Anion-Exchange Resin, in the presence of low salt and pH conditions.

Before starting

- Buffer P3 should be pre-chilled at 4 °C.
- Make 70 % endotoxin-free ethanol by adding 40 mL of 96 % ethanol to the endotoxin-free water supplied in the kit.
- Make sure that tubes and plastic- wear are endotoxin-free.

Protocol

- Harvest the bacterial cells from the overnight-cultures by centrifugation at 5000 rpm for 10 min in a table top centrifuge at 4 °C.
- Resuspend the bacterial pellet in 10 mL of cold Buffer P1 by using a pipette to activate lysis.
- Add 10 mL Buffer P2 (wash step) to the bacterial lysate. Mix by inverting the tube six times. Let the tube incubate at RT for exactly 4 min 45 sec.
- Prepare the QIAfilter cartridge; lock the cartridge with the cap and place it in a rack with the nozzle down.
- Add 10 mL of chilled Buffer P3 to the lysate. The lysate will be less viscous. Mix by inverting the tube six times, or until the lysate appears clear again. A precipitate will form at the bottom of the tube, containing genomic DNA, proteins and cell debris.
- Transfer the lysate to the QIAfilter cartridge, and incubate at RT for 10 min. Tap carefully on the tube to avoid the precipitate clogging the filter.
- Insert the piston after the incubation period, and remove the cap on the nozzle. Filter the lysate into a 50 mL falcon tube, by pushing the piston down.
- Add 2.5 mL of Buffer ER (endotoxin removal buffer) to the lysate and invert the tube 10 times. Incubate the mix on ice for 30 minutes.
- Prepare a Qiagen-tip filter column by adding 10 mL of the equilibrate-buffer QBT. Let the column empty by gravity.

- After the 30 min incubation step, apply the filtered lysat to the column, and let it flow through by its own gravity.
- Wash by adding 30 mL Buffer QC to the column, twice. The buffer moves by gravity through the column.
- Elute DNA by adding 15 mL of Buffer QN.
- Precipitate the DNA by adding 11 mL of isopropanol (2-propanol) at RT to the eluate. Mix and centrifuge at 13000 for 30 min at 4 °C to prevent overheating. Mark the outside of the tube for more easily visualization of the pellet, before centrifugation. Remove the supernatant by decanting.
- Wash the DNA pellet with 5 mL of endotoxinfree 70 % ethanol and centrifuge at 13 000 g for 10 min. The ethanol removes precipitated salt and replaces isopropanol with ethanol, which evaporates more easily. This will make the DNA easier to redissolve. Remove the supernatant by using a 500 µL pipette.
- Remove any drops of ethanol by using a small pipette, and air dry the pellet for 5 min.
- Redissolve the pellet with 500 µL of TE buffer and rinse the wall with a pipette for good recovery of DNA.
- Determine the DNA yield by spectrophotometric measuring at 260 nm. (section 3.8)

3.7 Restriction enzyme digestion of DNA, pCR2.1-TOPO plasmid and expression plasmid pcDNA3.1/Zeo(+)

A restriction enzyme is an enzyme able to cut a DNA strand within a specific sequence in a nucleotide. They produce a double-stranded cut in the DNA. These specific recognition sites differ for each restriction enzyme, and can therefore produce segments with different length, sequence and orientation. All plasmid used in this thesis contain a "multiple cloning site" that contains many restriction enzyme recognition sequences within its DNA. This allows for insertion of a specific fragment of DNA into a plasmid.

Restriction enzyme digestion was performed by incubating double stranded DNA or plasmid, with an appropriate amount of restriction enzymes, in a buffer (recommended by the supplier) and at the optimal temperature for the specific enzyme. Every tube contains plasmid/DNA, buffer C or D (Sigma), BSA, enzyme and water (table 8).

Protocol

Incubate the “digestion mixture” for 1.5 hours at 37 °C (optimal temperature for HindIII/EcoRI/XhoI).

Digestion mixture

5 µg DNA or plasmid DNA

3 µl 10X Buffer C or D (Sigma)

3 µl 10X BSA

1 µl restriction enzyme (HindIII, EcoRI and XhoI, 10000 units/mL)

Add MQ H₂O up to a volume of 30 µL.

After digestion the samples are frozen at -20 °C for further evaluation.

The result is examined by agarose- gel electrophoresis as described in section 3.3

3.8 DNA concentration measurements

Samples were measured at 260 nm against a blank (MQ-H₂O or elution buffer), to determine DNA concentration. For measurements the Nanodrop 1000 (Thermo Scientific) was used.

OD (optical density) 1.0 correspond to approximately 40 µg/mL and 50 µg/mL of single stranded RNA and double stranded DNA, respectively (Sambrook.J and Russel, 2001).

To determine the purity of the DNA, the calculated ratio between OD 260: OD 280 was used. A ratio of 1.8 is acceptable. A ratio <1.8 will indicate significant contamination of i.e phenol or trizol. A ratio of ~2.0 indicates RNA contamination.

3.9 Sticky end ligation of Kir4.1 into expression plasmid pcDNA3.1/Zeo(+)

After the digestion step, DNA fragments contain 5`-3` overhanging ends. These single stranded overhangs were created by digestion of the vector and target DNA with a restriction enzyme (section 3.7). When the overhanging ends from the plasmid and the DNA fragment are compatible, they can anneal to each other and form a hybrid molecule. Annealing brings the 5`phosphate and the 3`hydroxyl residues on both vector and DNA fragment close together,

allowing for the two parts to anneal. The process of ligation is performed by the enzyme DNA ligase, forming a phosphodiester-bond between the compatible base-pair.

The DNA was eluted with 30 μL or 50 μL of nuclease-free water, depending of the expected yield. The concentration of vector and DNA fragment, respectively, was measured by using the Nanodrop1000 (Thermo Scientific) (section 3.8).

Reaction mixture

120 ng DNA fragment

10 μL 1X Quick ligase buffer (BioLabs)

8 μg plasmid pcDNA3.1/Zeo(+)

1 μL Quick ligase enzyme (10000 units/mL) (BioLabs)

MQ- H₂O up to 30 μL

Protocol

- Add the different components of the reaction mixture in the order described above.
- Let the mixture incubate in room temperature for 15 min and then put the vial on ice.
- The ligation mixture is then transformed into competent DH5-alpha bacteria (section 3.4.1) and plated out on LB agar plates with the appropriate antibiotics (section 3.5)
- Incubate the plates at 37 °C for 16 h before proceeding picking colonies and perform miniprep, maxiprep and sequencing as describes previous (section 3.6 and 3.10))

3.10 Sequencing

DNA sequencing is a method by which the precise order of the nucleotides in a piece of DNA can be determined. A PCR reaction is carried out with only one primer and a mixture of deoxy-nucleotides (dNTPs) and labeled dideoxy-nucleotides (ddNTPs). The dideoxynucleotides can be incorporated into the growing polynucleotide strand just as efficiently as the normal nucleotide. When a ddNTP is incorporated into a growing strand, further synthesis stops. The results are many DNA fragment with various lengths, each ending with a labeled ddNTP. A capillary electrophoresis analyzer can separate and detect the different labeled nucleotides. Each dideoxynucleotide correspond to different colores (ex. all ddATP are green, ddCTP's are red..) in the diagram showing the sequence. This means that every DNA fragment terminated by a specific ddNTP, can be detected. The shortest DNA fragment will be detected first

(moving fastest), and this will be the first nucleotide in the sequence. The second fastest nucleotide will be detected and so on.....(Sambrook.J and Russel, 2001).

Sequencing mixture

150-300 ng template (double stranded)

1µL (3.2 pmol) primer

MQ- H₂O added up to a total volume of 15µL

All the sequencing reactions were performed on a ABI 3100 Automated Capillary DNA Sequencer at the Centre for Molecular Biology and Neuroscience, Institute of Medical Microbiology at Rikshospitalet. The sequencing diagrams are analyzed using the software “Chromas” from the University of Oslo.

3.11 The cellular model system

3.11.1 HeLa -cells

In this study HeLa cells were used as a cellular model for production of AQP4-isoforms, Kir4.1 protein, PatJ protein, α -syn trophin protein and protein variants with myc-tag, using transfection assays. HeLa cells are human epithelial cells from cervical carcinoma transformed by human papillomavirus 18. The cells were originally taken from Henrietta Lacks, who died from cancer in 1951. The HeLa cell line is a classic example of an immortalized cell line and is often used in medical research. They are adherent and maintain contact inhibition *in vitro*. HeLa cells grow in monolayer, and will not grow on top of each other when they touching the adjacent cell. Loss of contact inhibition is a sign of oncogenic cells, so *in vitro* HeLa cells are not oncogenic but can be transformed by an oncogen virus (Van Valen, 1991).

3.11.2 Human Embryonic Kidney (HEK) 293-cells

HEK 293 is a cell line that is easy to grow. The cells transfect well and is a widely used in both research and industry. The cell line is derived from embryonic kidney cells grown in tissue culture. If you compare growth-velocity of this cell line with the HeLa cell line more rapid growth is observed.

3.12 Culture and maintenance of cell cultures

Different cell types and different bacterial strains have different nutritional needs. For optimal growth, we have to ensure that each type of organism have a medium that fulfils its biological needs.

3.12.1 HeLa cells and HEK 293 cells

Both HeLa- and HEK 293- cells were cultured in DMEM medium (Gibco) supplemented with 10 % foetal calf serum (FSC) and 2 mM L-glutamine. DMEM medium contains phenyl red as a pH indicator. The cells were incubated in a incubation chamber at 37 ° with 5 % CO₂ and saturated humidity and passaged when ~ 70 % confluent (two-three times a week). Confluence refers to the percent coverage of the dish or the flask by the cells. When no open space is observed between the cells, total confluence is obtained. In the beginning, confluence was determined by counting cells (see section 3.12.5) but after a while confluence was determined by microscopy. When performing a transfection, cells were split into ~ 50 % confluence with no antibiotics in the media.

3.12.2 Splitting cell lines

Splitting or passaging cells is important to obtain healthy and optimised conditions for experiments. Cell culture medium was heated to 37 °C using a water bath prior to cell culture work, and all cell-work was performed under sterile conditions. HeLa- and HEK293 cells were cultured until they reached ~70 % confluence.

The purpose of washing the cells is to remove rest medium and dead cells. Serum in the medium can inhibit the enzyme trypsin (see below), and influence the amount of cells after the passage. PBS must be free from Ca²⁺ and Mg²⁺ in order to not inhibit the effect of trypsin. All DMEM used in the cell work has no antibiotics added.

Protocol

PBS washing

- Remove media.
- Add PBS and wash gently using a 500 µL pipette.
- Remove excessive fluid.
- Repeat the previous steps three times.

Trypsination

Trypsin is a serine protease who predominantly cleaves peptide bonds at the carboxylside of the amino acids lysine and arginin. When used for detaching cells, bonds between cells and the container will be broken. For optimal function of the enzyme, the container is placed in 37 °C for five to ten min, depending on the cell type and effect of the enzyme.

- Add trypsin (1 mL) to the container with cells to be splitted.
- Make sure the fluid covers the entire surface of the container.
- Leave it at 37 °C for 5-10 min.
- Before proceeding, cells must have detached from the surface indicated by sphere-shaped morphology. To enforce loosening, knock container one time on the bench.

Dilution and distribution off cells

- Prepare 1 new container – make sure to label sufficiently
- Add appropriate volume of DMEM with serum and L-glutamin to the container.
- Add appropriate volume of DMEM with serum and L-glutamin to the container with the cells to be split.
- Mix well by pipetting hard 4-6 times to separate cells from each other
- Check in microscope for single cells. If there are sheets, pipette hard a couple of times more.
- Distribute appropriate volume of cell (after counting) suspension into the new container (175 000 cells/flask)
- Make sure cells are well spaced and non-accumulated before leaving in incubator.
- Place the cells in the incubator at 37 °C until passage or use.

3.12.3 Cell thawing

Whenever a new batch with HeLa or HEK 293 cells were needed, a cryo-tube containing a stock with cells was taken from the liquid nitrogen tank, and thawed as fast as possible using a water bath at 37 °C. The whole content (1 mL) was after thawing pipetted into a T-75cm² container with 14 mL DMEM with 5 % serum, glutamine added and no antibiotics under sterile conditions. The flask was then swirled gently and the cell solution was distributed into a new container after cell counting (section 3.12.5) to obtain the correct dilution of cells. The cells were maintained as described in section 3.12.

3.12.4 Cell freezing

To generate frozen stocks of cells, one confluent T-75 cm²-culture flask was trypsinated as described in section 3.12.2, washed twice with PBS (phosphate-buffered-saline (pH 7.4) to remove dead cells and serum, and mixed with freezing medium (DMSO) using the following protocol under sterile conditions

The dimethylsulfoxid (DMSO) used for preservation of cells, prevents formation of water crystals which can lead to cell disruption. DMSO also protects the cells from further damage during the storage period.

Protocol

- Resuspend cell-suspension in 9 mL DMEM with serum and L-glutamin, and transfer to a 15 mL tube
- Centrifugate at 160 g at 4 °C, for 10 min
- Remove supernatant and resuspend the pellet obtained, in 500 µL DMEM with serum and L-glutamin, using a 500 µL pipette.
- Mix cell solution with 500 µL of cold freezing medium (40 % DMEM with serum and glutamine added and 20 % DMSO) and transfer to a cryo-tube. Make sure the lid is properly tightened.
- Equilibrate the cells in a polystyrene-box at -80 °C for 24 h.
- Freeze down cells for long-term storage in liquid nitrogen (-178 °C).

3.12.5 Counting cells

Counting cells were done on a regular basis, when splitting cells, to obtain comparable conditions when analysing the results.

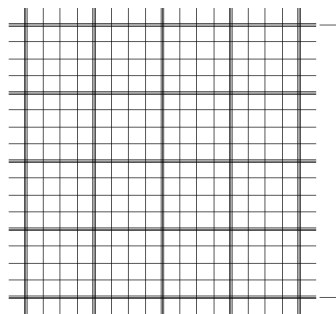


Figure 8. The pattern of the Fuchs-Rosenthal counting chamber. (Figure taken from hausserscientific.com).

The cells were first detached using Trypsine as described in section 3.12.2 .For counting, a “Fuchs-Rosenthal counting chamber” (cell-depth 0.2 mm) with two cover-slips, was used.

The pattern in the chamber consists of 16 one square millimetre areas (A-squares) orientated by triple lines, and each such area sub-divided into 16 squares (Fig.8). Four A squares were counted for each chamber. The volume of one A-square is 0.1 μ L. The optimal amount of cells for performing a good transfection is ~175.000 cells in each flask.

Protocol

- Mix a 1:1 solution of cell-suspension and tryptophan-blue. Vortex and spin.
- Add 5 μ l of the mix to each chamber in the “Fuchs-Rosenthal counting chamber”. Count four A-squares in each chamber and calculate the average number of cells.

Calculation

The example is given to calculate a concentration of 175.000 cells / flask. The average from four squares is 20 cells.

$X = 20 \text{ cells} \times 2 \text{ (dilution factor)} = 40 \text{ cells pr. A-square}$
 $40 \text{ cells} / 0.1 \mu\text{L suspension} \rightarrow 400 \text{ cells}/\mu\text{L} \rightarrow 400.000 \text{ cells}/\text{mL}$
 $\rightarrow 175.000 \text{ cells}/400.000 \text{ cells}/\text{mL} = 0.44 \text{ mL}$

In this specific calculation, 440 μ L of cell-suspension is plated in each flask to obtain ~175.000 cells.

3.13 Transfection of plasmids into cultured cells

Cationic (+) lipid-based transfection is a method for the introduction of genetic material into a cultured cell. Most lipids are negatively charged (anionic) but positively charged (cationic) lipid was first introduced for medical research in 1987 (Felgner et al., 1987). Cationic lipid can interact electrostatic with the negatively charged DNA and make condensed lipid/DNA complexes. The condensed aggregates of lipid/DNA are allowed to fuse with the hydrophobic, and negatively charged cell-membrane in e.g. cultured cells, and the DNA/plasmid is then introduced to the target cell by endocytosis (Sambrook.J and Russel, 2001).

3.13.1 Transfection with Fugene 6

In our lab the reagents Fugene 6 (Roche) is used for the transfection-reaction. The ratio of DNA (μ g): Fugene 6 (μ L) should be approximately 1: 3. Usually we use 6.6 μ g DNA and 19.5 μ L

Fugene 6, for a container with area 75 cm². When cotransfecting plasmids, total amount of DNA is 6.6 µg. Plasmid/DNA complex is prepared by using serum-free Opti-MEM (Invitrogen), since serum disturbs the complex formation for Fugene 6.

Protocol

Complex preparation

- Add 200 µl serum-free Opti-MEM into two different, clean tubes.
- Add 20 µL of Fugene 6 into the first tube, and 6.6 µg plasmid to the other. (DNA prepared from maxiprep). Mix gently by pipetting six times with a 500 µL pipette and incubate in room temperature for five min.
- Mix the two solutions (plasmid and Fugene 6-solution)
- Incubate at room temperature for 20 min (complexion step).
- Add 9 mL of serum free DMEM in a new tube. Mix the complexion solution (1mL) with 9 mL of prewarmed DMEM containing serum. Total volume is 10 mL.

Transfection

- Remove the media in the cell culture container .Wash the cells with PBS a couple of times to remove dead cells and debris.
- Add the complex/ DMEM solution from the complexion step into the cell flask, and incubate for 24 h at 37 °C before harvesting.

3.13.2 Harvesting of DNA from 75cm² cell-culture containers

This is a method describing how to get a cell pellet from cultured cells containing your DNA of interest. It is important to count the cells harvested, to not exceed the yield limit of the purifications column .Count the cells in the control container prior to harvesting. A maximum of 175.000 cells / flask should be used according to our transfection procedure (section 3.13.1).

After 24 h. of growth, the cells were washed and trypsinated as described in section 3.12.2

Protocol

Add appropriate amount volume of DMEM with serum and glutamine, to the trypsinated cells. Transfer the suspension into a 15 mL falcon tube, and pellet by centrifugation at 160 RCF for 10 min at 4 °C.

- Decant off the supernatant
- Resuspend the pellet in a clean eppendorf by adding 1 mL PBS.
- Pellet by a new centrifugation step.
- Remove the last drop of supernatant with a pipette.
- Homogenize the pellet (section 3.14) for performing Western blot/BN-PAGE or store at -20°C until use.

3.14 Preparing protein homogenate from cultured cells

In order to prepare protein extracts for use in Blue Native-Page or SDS-PAGE, a homogenization protocol established in the laboratory was used. The cells were harvested from 75cm² container as described in section 3.13.2 and frozen cell pellets were thawed on ice before proceeding.

Protocol

- Add 200 µL lysis buffer (0.32 mM sucrose, 10 mM Hepes pH 7.4, 2 mM EDTA, 4 µL PIC (Protease inhibitor cocktail (Roche)) to the thawed pellet.
- Resuspend the pellet and transfer to a Kontez Homogenizer (size16).
- Homogenize with 20 strokes. Lysate is transferred to a clean eppendorf tube
- Spin the samples at 1000g, 4 °C, for 10 min
- Transfer the supernatant (S1) to a new eppendorf-tube and freeze both S1 and pellet (S2) at -20 °C.
- Protein yield estimation was performed as described in section 3.15.1

3.15 Preparing of samples for SDS-PAGE and Western blot

3.15.1 Total protein concentration determination

The detergent compatible (DC) protein assay (Bio-Rad) was used for total protein concentration determination of cell extracts lysed in homogenization buffer. This assay is based on a colorimetric reaction of protein with an alkaline copper tartrate solution. By adding a Foline reagent color development will occur. The colour development is primarily due to the appearance of amino acid tyrosine (V) and tryptophan (W). When protein react with the Folin reagents, a reduction by loss of one to three oxygen atoms occur. These reduced species have a blue colour which can be measured by absorbance (405-750 nm). In general, samples were diluted (setup below), and a standard curve of BSA ranging from 0-2 g/L was prepared in MQ-H₂O. 5µL of each standard and samples were measure in triplicate at 655 nm with the Bio-Rad Benchmark reader. The protein content in the samples was estimated against the Bovine Serum Albumin (BSA) standard curve.

Protocol

- Thaw the protein lysate samples and take out BSA standards (0-2000 µg/ml) from the fridge. Prepare one eppendorf tube per sample subjected to total protein measurement and make a dilution series of each sample. Calculate with 20 µl for each sample as the samples are measured in triplicates.
- Prepare reagent “A” from the kit: Mix 2 ml reagent A and 40 µl reagent S (the small bottle) in a 15 ml tube. Mix. The reagent S is only added when you have membrane protein (not liquid soluble).
- Pipette 5 µl of each diluted sample, and BSA standards into a 96 well plate. See table 32)
- Pipette 25 µl of reagent A into each well.
- Pipette 200 µl of reagent B into each well.
- Incubate for 15 min at RT.
- Measure absorbance at 655 nm with the Bio-Rad Benchmark reader and save file/print reports.

Table 32. Setup of the protein dilution series

	1	2	3	4	5	6	7	8	9	10	11	12
A	2000	2000	2000	1500	1500	1500	1000	1000	1000	750	750	750
B	500	500	500	250	250	250	125	125	125	25	25	25
C	Lysis buffer	Lysis buffer	Lysis buffer									
D	Sp. 1:1	Sp. 1:1	Sp. 1:1	Sp. 1:10	Sp. 1:10	Sp. 1:100	Sp. 1:100					

3.15.2 Preparation of lysate from cultured cells

The lysate is mixed with 1 x SDS loading buffer and reducing agent (DTT or β -mercaptoethanol, 0.1M). The reducing agent reduces sulphur bridges in proteins and contributes to protein denaturation.

Protocol

- Estimate 10-50 μ g of protein in each lane in the gel. One well in a 10 well /1.5 mm gel, have a volume of 60 μ L. Equal volumes should be loaded in each well.
Tip; dilute the 6 X loading buffer to 1 X and prepare a sample stock of 1 g/L protein. Use the diluted 1 X loading buffer.
- Heat the samples containing water soluble proteins (not membrane proteins) in a heating block at 60 °C for 5 min
- Set up a gel rig

3.15.3 Making SDS-PAGE gels

- 1.5 mm thick gels were made by using an arrangement from MINI Protean (Bio-Rad). All parts used in the arrangement were clean.
- A resolving gel (Table 17) was made and transferred to the chamber made of two glass covers in the arrangement.
- When adding TEMED, the gel polymerizes and it is important to work fast. Butanol was overlaid the resolving gel to straighten the edge.

- The gel was allowed to polymerize in room temperature for at least 30 min. When the gel was polymerized, the stacking gel was made and applied on top.
- A plastic comb was put between the two glass covers, making wells into the stacking gel.

3.16 Western Blots and SDS polyacrylamide gel electrophoresis (SDS-PAGE)

SDS-PAGE followed by Western Blotting (section 3.16.2) is a method for separation and detection of specific proteins from in this case, a transfected cell culture- or brain- homogenate, using electrophoresis. Electrophoresis (section 3.17.3) is a process where charged particles migrate through a solid gel in response to an electric field. The rate of movement is influenced of frictional resistance (pore size) and the charge: mass ratio of the protein.

The SDS-PAGE system uses a discontinuous buffer system with two gel types with different pore sizes. In this case migration is influenced of both size and shape of the protein. Smaller proteins are retained less than bigger, and thus move faster.

In SDS-PAGE the influence of charge on protein migration is eliminated by providing all proteins a negative net charge. Sodium dodecyl sulphate (SDS) is an anionic detergent that binds to proteins. SDS is added for at least two reasons. One action is to denature the protein by braking non-covalent bonds in the proteins. This destroys the tertiary structure (not the primary), giving each protein similar shape. The other one is to give proteins a negative charge. This also blocks the possibility for the protein to interact with other anionic polymers, such as lipid or nucleic acids, which give rise to a different protein shape affecting electrophoretic migration.

The gel matrix used in this protocol is polyacrylamide. These gels are formed when monomeric acrylamide is polymerised by use of two forming agents, ammonium persulfate (APS) and tetramethylethylenediamine (TEMED). Acrylamide polymerize to long linear products and for the formation of a three-dimentional gel, a cross linker is added (bisacrylamide). The pore size can be varied by changing the ratio between acrylamide and bisacrylamide.

Most of the gels used in the SDS-PAGE protocol, are hand made in the laboratory. The self made gels consist of 1/3 part stacking gel and 2/3 part resolving gel. Stacking gel is used to

increase the resolution of the protein bands during electrophoresis. The stacking gel contains chloride ions, which migrate faster through the gel than the protein sample applied. In the electrophoresis buffer, glycine is added, and these ions migrate slower than the protein sample. In the stacking gel, the protein molecules will therefore be trapped as a sharp band between these two ions. (Sambrook, J and Russel, 2001)

The resolving gel is a separating gel underlying the stacking gel. When the protein sample enters the resolving gel, which has a smaller pore size, the glycine is ionized because of higher pH and a different salt concentration. This leads to no voltage gradient in the system and the proteins can be separated based on size only (Table 17).

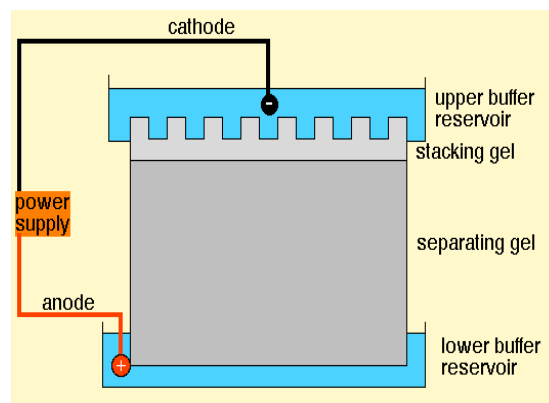


Figure 9. An figure showing the SDS-PAGE set up with stacking gel and resolving gel (here: separation gel). Picture from www.bioon.com.

3.16.1 Electrophoresis on SDS-PAGE gels

The proteins were separated on SDS-PAGE gel electrophoresis (MINI PROTEAN II, Bio Rad) containing 12-14 % polyacrylamide, and in some cases urea (Table 17).

- All samples were thawed on ice and diluted to the concentration 1 g/L with loading buffer (section 3.15.2).
- 10 µg-50 µg proteins were loaded in each well.
- Electrophoresis was run at 150 V for one h or to the proteins ridge the bottom of the gel, by the use of diluted Laemmli buffer. Diluting the samples to the same protein concentrations made it possible to load equal amount of proteins in each lane.
- To enable identification of protein mass, 5 µL of prestained Dual color Protein Standard (Bio-Rad) were run alongside the samples.

- Glyceraldehyde-3-phosphate dehydrogenase (GAPH) was used as a loading control.
- MagicMark XP (Invitrogen) or Presicion Plus Protein Standard (BioRad) was used as molecular weight marker. 2 μ L MagicMark XP was applied in the first lane (only visible on the membrane), together with 5 μ L of SeeBlue Plus –marker (Invitrogen) added in lane number two (only visible in the gel). The MagicMarkXP is a molecular weight marker with a IgG binding site. This is the reason why the marker is not visible before the immunodetection is completed.

3.16.2 Western Blotting

Western blotting is a technique that use antibodies for protein detection. The proteins are resolved by SDS-PAGE electrophoresis, and made available for antibody hybridization, by transfer from a gel to a polyvinylidene fluoride (PVDF) membrane. Blotting is performed by applying an electric current that transfers the protein from the gel to the membrane.

The electrophoretic transfer of proteins from the gel to the membrane was performed in cold, diluted, transfer / Towbin buffer with 20 % w/v methanol, by using a gel ridge (Criterion blotting system). A blotting sandwich was made consisted of pads, filters, the gel and a PVDF membrane (Fig.10).

Protocol

- The PVDF membranes are hydrophobic and must be activated in methanol for 10 sec prior to blotting.
- All sponges and filters used in the sandwich must be wetted with Towbin buffer.
- Assemble the Criterion blotting cell and fill up with Towbin buffer.
- Set up the blotting sandwich according to figure 10.
- Insert the blotting sandwich and add a magnetic stirrer into the cold buffer.
- Blot at 100 V for 30 min.
- After blotting, rinse the membrane in MQ-H₂O, briefly. Label the membrane.

The efficiency of the protein transfer from the gel to the membrane was checked by incubation with Coomassie G-250 staining (Bio-Rad) for 12-24 hour prior to scanning in a table top scanner.

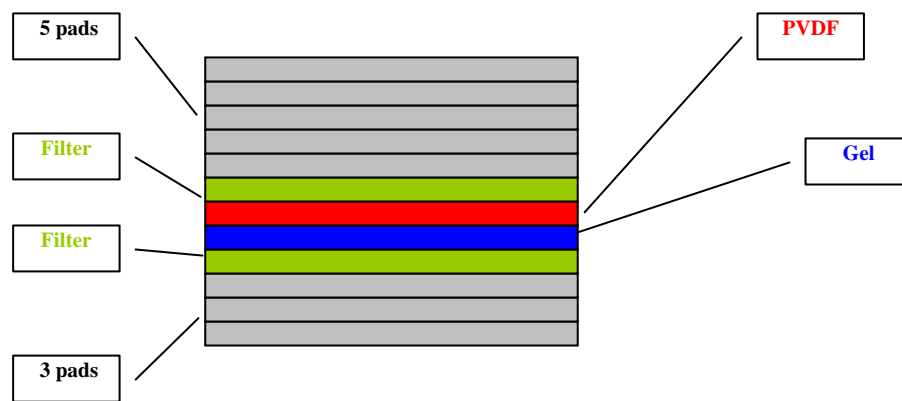


Figure 10. This figure shows the assembly of the SDS-PAGE blotting sandwich.

3.16.3 Immunolabelling and detection of proteins in SDS-PAGE

Antibodies bind to the target protein with a certain affinity. Neither the target protein or primary antibodies are visible on the PVDF membrane. To visualize the protein of interest, secondary antibodies coupled to the enzyme alkaline phosphatase (AP) are used. These antibodies are raised against one specific species. E.g. if the primary antibody is raised in rabbit, the secondary antibody should be anti-rabbit.

AP is a phosphatase/enzyme that cleaves off a phosphate-group from the AP substrate (ECF-substrate (GE Healthcare), which will be added for immuno-detection. This substrate reacts with the secondary antibody and produces a light signal at approximately 630 nm. The light signal from the membrane is scanned by a detector and the resulting image shows whether the protein of interest has been detected.

Protocol

Before immunodetection, membranes were blocked for at least one hour in 5 % milk solution with w/v 0.05 % NaN_3 , to avoid unspecific labeling of the primary antibody.

- The membranes were washed in TBS-T for one hour and incubated ON with primary antibody at 4°C in a roller-drum. For mini-gels a 50 mL falcon tube was used as incubation chamber (concentrations and dilutions of primary antibodies are listed in table 22 and 23).
- After ON incubation with primary antibody diluted in block solution, the membrane is washed for three times for 10 min in TBS-T.

- The membrane was then incubated at room temperature for one hour in secondary anti-specie conjugated alkalic phosphatase AP (Sigma) diluted in TBST (1:10000)
- After incubation with secondary antibody, the membrane is washed in TBS-T for at least two h with frequent changes of TBS-T.
- Immunodetection was carried out by adding 1 mL of ECF-substrate on the membrane, put folio-coated lid over and incubate at exactly 5 min. Wrap the membrane in a transparent plastic sheet, after pouring off excessive substrate.
- Blots are scanned using “Typhoon-scanner” and software settings are as followed:
 1. Acquisition mode: Fluorescence
 2. PMT: 400-600V
 3. Sensitivity: Normal
 4. Press sample activated
- Membranes were either scanned dry or wet. For storage, the membranes were dried and kept at 4 °C. If membranes needed to be reprobed, a stripping protocol was used (3.16.4 and Table 17).
- In some cases, urea was added to the SDS-PAGE gel. Urea is supposed to improve resolution of membrane protein, such as AQP4 (Neely et al, 1999), and is commonly used as a reagents which disrupt the three-dimensional structure in proteins. Urea interferes with stabilizing intra-molecular interactions, such as hydrogen bonds and hydrophobic effects.

3.16.4 Membrane stripping

- Prior to stripping, membranes were washed in 40 % methanol, and then stripped in β -mercaptoethanol (7 μ L / 1 mL stripping buffer) and strippingbuffer at 60 °C for 1.5 hour.
- Wash briefly in distilled water and block in 5 % milk solution with w/v 0.05 % NaN₃ for one hour.
- The membrane is now ready for reprobing with primary antibody ON.

3.17 Blue Native PAGE (BN-PAGE) gel electrophoresis

BN-PAGE is a technique for electrophoretic separation of proteins with their native structure and activity intact. In standard SDS-PAGE, SDS denatures proteins and gives them a net negative charge by binding to the protein. This allows the protein to migrate in one direction towards the positive anode. SDS is present in both sample and buffers (section 3.16).

However, in BN -PAGE, the charge-shift molecule used is the dye Coomassie G-250, developed by Schagger & von Jagow in 1991(Schagger and von, 1991). The dye binds to the hydrophobic areas of the proteins and gives them a negative charge while still maintaining their native state. No denaturation will occur. The G-250 is present in the cathode buffer and the running buffer, but not in the gel itself.

A common problem when performing Blue Native Page with membrane proteins is solubilisation of the proteins and how to avoid aggregates. For good separation, membrane proteins require a mild detergent that does not disrupt the higher order structures of the protein. If the solubilisation is just partial, or the detergent has damaging effects on the three dimensional structure, this could influence the results in a negative way. Our group have investigated 55 different detergents in order to find the best solubilisation reagents (6 detergents published in Sorbo et al 2007), and in this protocol the detergent n-dodecyl-Beta-D maltoside (DDM) is the chosen one.

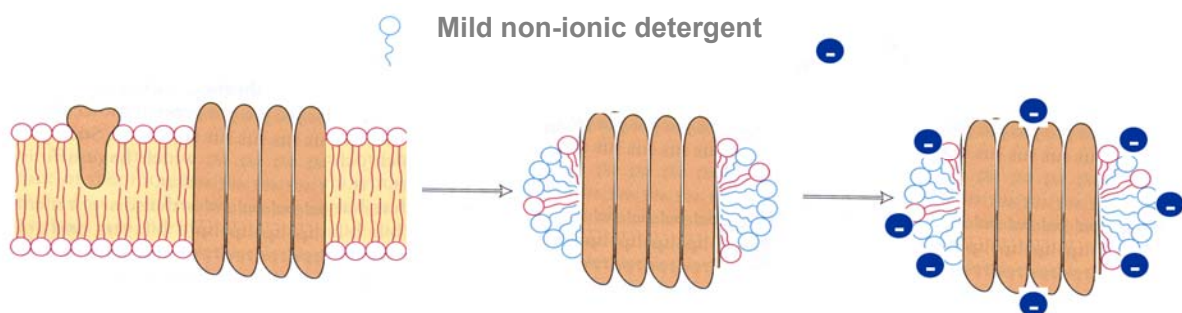


Figure 11. This figure shows a membrane protein surrounded with detergent and commasie G-250. (Reprinted from J.G Sørbo).

3.17.1 Collection of samples for BN-PAGE

Samples for BN-PAGE were collected by harvesting cell cultures as described in section 3.13.2 followed by homogenization. Protein determination was carried out using the Bio-Rad DC kit and a microplate reader as described in section 3.15.1.

3.17.2 Sample preparation for BN-PAGE

Protocol

- 5-10 µg of protein is mixed with 1 % DDM (Invitrogen) total, ready made Native-PAGE 4 X sample buffer (Invitrogen) and MQ H₂O according to the table 18.
- The prepared samples should incubate at RT for 10 min
- Spin down on a table top centrifuge for 10 min at 4°C (10000 RCF). Transfer supernatant to a new tube.
- Set up a gel ridge (X Cell Sure Lock Mini-Cell) and continue with section 3.17.3

3.17.3 Electrophoresis on BN-PAGE assay

The electrophoresis is performed in a XCell Sure Lock Mini-Cell ridge from Invitrogen.

The buffer system used in BN-PAGE assay, involves different ions. The gel matrix is added with chloride ions, which serves as a leading ion due to mobility and move fastest.

Protocol

- Samples from section 3.17.2 are loaded on a pre-cast 4-16 % NativePage Novex Bis-Tris Gel (Invitrogen). Prior to loading the samples are mixed with 1 µL Coomassie G-250, and the wells are washed with water and 1X “Dark blue”- cathode running buffer (Table 18) three times.
- Fill up the wells with “Dark blue”-cathode-buffer and displace air bubbles before loading samples with a Hamilton syringe (20 µL).
- All samples are handled quickly in room temperature, because of easy aggregation.
- To provide easy visualizations when loading samples, do not fill up the inner chamber of the gel rigde with cathode buffer prior to loading
- 3 µL of NativeMark Unstained Protein Standard (Invitrogen) is loaded in lane 1. 20 uL of protein-solution is loaded in the other wells.
- After loading samples, fill up the inner chamber (covering the wells) of the gel-rigde with dark cathode buffer. The outer chamber contains 1 X anode buffer.
- The electrophoretic separation of proteins is run at 150 V for 160 min. Change from dark to light running buffer after 1/3 migrated distance (after~ 20 min) with constant current. The dark cathode buffer contains more negative charge, and will help the big protein complexes in entering the gel.
- Make Anode buffer /BN-running from 20 X stock-solutions according to table 18.

3.18 Protein transfer (blotting) and immunolabelling in BN-PAGE

3.18.1 Blotting

Protocol

- Make Transfer/ BN-blotting buffer according to table 18.
- When the electrophoresis run is finished, let the gels rest in transfer / BN-blotting buffer for 5 min.
- In the meantime, sponges are prepared by soaking in transfer buffer. PVDF membrane used for the immuno detection must be activated in methanol, and the XCell II Blot Module (Invitrogen) are used for building up a blotting sandwich (as for SDS-PAGE, Fig.10)
- Blotting is performed at 50 V for 60 min. Tap water is used as a cooler in the outer compartment in the blot module.
- When the run is done, the membranes are washed in methanol for three times. The gels are discarded. Visualize the marker (and protein) by staining with Ponceau S Acid red 112, for 10 min. Reverses the stain by washing with tap water.
- The membranes are cut at one edge for easy identification.

3.18.2 Immunolabelling and detection for BN-PAGE

Protocol

- The membranes are blocked for at least 30 minutes in 5 % milk solution with w/v 0.05 % NaN_3 , to avoid unspecific labelling of the primary antibody.
- Incubation with primary antibody was performed in the cold room ON (constant rotating). Concentrations and dilutions of primary antibodies are listed in table 22. Before proceeding with secondary antibody- incubation the following morning, the membranes are washed in TBS-T for 10 min, three times.
- Incubation with 1:10000 dilution of secondary anti-specie conjugated AP (Sigma) antibody in TBS-T, is performed in room temperature for one hour.
- Remove unbound antibody with frequently changes of TBS-T buffer for 2-3 h.
- Remove excess TBS-T (use clean bench paper) before applying 1 mL of ECF-substrate (GE Healthcare) for immuno-detection.

- Incubate the membranes in the dark for exactly 20 min between to plastic sheets. Dry the membranes at 37 °C for 10 min and use the “Typhoon 9410 Scanner” for signal detection.

Analytical tools for processing images; “Image Quant TL version 2003.02” (Amersham)

Software settings on “Typhoon 9410 scanner” are as followed:

1. Acquisition mode: Fluorescence
2. PMT: 400-600V
3. Sensitivity: Normal
4. Press sample activated
5. Laser; Blue 1457nm, Filter: 560LP Gen Purple

4 RESULTS

The results are divided into three different parts. The first part (I) is a step-by step section where the construction of the Kir4.1 expression plasmid is described. The different section in part I was to a certain degree dependent on successful results from the proceeding section. Therefor part I contains some discussion of the challenges each step in the plasmid construction procedure had to overcome. The second part (II) contains the different studies of Kir 4.1 as a possible interaction partner, and the third part (III) comprises the assembly of square arrays and protein-protein interactions in isoforms of aquaporin 4.

Part I

4.1 Construction of Kir4.1 expression plasmid

There has recently been uncertainty about the specificity of anti Kir4.1- antibodies in the detection of Kir4.1 protein *in vivo*. Since specificity is crucial in studies where antibodies are involved, it was decided to generate a system to test whether the Kir4.1 antibody really binds Kir4.1 protein and whether the binding is specific. To do so, we decided to express Kir4.1 in a cell line and test the available antibodies against Kir4.1 in this system. At first a plasmid for expressing Kir4.1 was constructed, as described in chapter 3.

4.1.1 Designing primers and PCR amplification of the Kir4.1 gene

BLAST-analysis of the Kir4.1 mRNA (NM_001039484) showed that cDNA from mouse could be used as starting material in a PCR amplification of Kir4.1. The coding sequence (CDS) of Kir4.1 gene is from nucleotide 243 to nucleotide 1382 in the mRNA. This corresponds to a Kir4.1 protein of 379 amino acids and 42 kDa size.

The PCR primers were designed to amplify the area on both sides just outside the CDS region. Two forward-primers and two reverse primers were made, as PCR sometimes can fail or can be unspecific (Table 20). In the primer design, restriction enzyme sites were added to each primer. Furthermore, an optimal Kozak sequence was added to the 5' primers, which is important for the initiation of the translation by the ribosome. The PCR was carried out on both mouse cDNA template and a SPORT-Kir4.1- plasmid from Open Biosystem (Bc

099932). Four combinations of primers were tried and two different hybridization temperatures were tested. The enzyme used was “Taq DNA polymerase (New England Biolabs).

Figure 12 shows a stained 2 % agarose gel after electrophoresis, where the amplified DNA obtained in the PCR is visualized. The gel shows that all combinations of primers gave product on the pSPORT1_Kir4.1-plasmid (Fig.12 A). The size of the bands correspond to the correct size (1139 bp), as it is larger than the 1018 bp band and smaller than the 1636 bp band of the TrackIt 1kb ladder.

There are some minor extra bands visible, indicating that the primers used are not perfectly specific to the target area. At the bottom of the lanes, primer-dimer bands are visible, indicating that primers interact. This might be a result of PCR conditions being not optimal due to the constrained positioning of the primers at start and stop of the CDS.

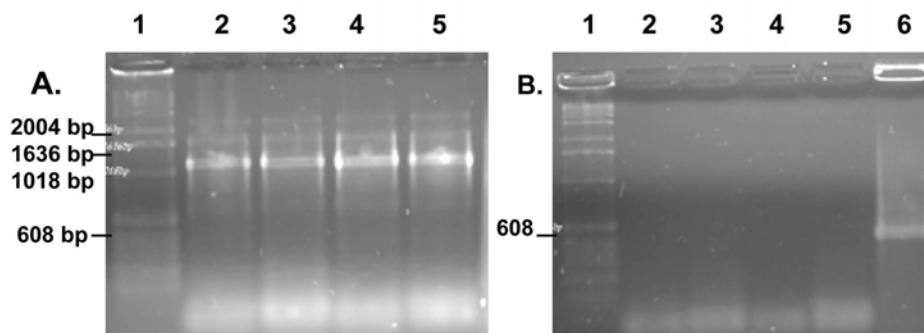


Figure 12. Agarose gel electrophoresis of primers tested on pSPORT_Kir4.1-plasmid and mouse cDNA. Lane 1 in both panels contains 1Kb DNA ladder (Invitrogen). Panel A: Lane 2-5 show four different combinations of Kir4.1-Kh2 and Kir4.1-Kh243 (forward primer) and Kir4.1-X2 and Kir4.1_X1367 (reverse primers) on pSPORT_Kir4.1- plasmid. The expected product of Kir4.1 is 1139 bp. Panel B: Lane 2-5 has same combinations of primers as in panel A, but the template is mouse cDNA. No bands visible when using cDNA. Lane 6 shows the positive control with Fen-1-897 and Fen-1-1314 primers on Fen1-plasmid. Expected product is 517bp (417bp + primers). Negative control with MQ water did not show any bands and is not shown.

Figure 12 B shows that the reactions with mouse cDNA were not successful .The failure of PCR on mouse cDNA might indicate problems with the synthesis or degraded RNA. RNA easily degrades and should always be stored at -80°C , and not at -20°C as in this case. Unfortunately the RNA was not analyzed for degradation prior to cDNA synthesis. Still, our strategy with multiple primers tested on two different templates and at different annealing temperatures was successful, since a PCR product at the expected size of 1139 bp was obtained.

The PCR product was then purified from an agarose gel (not shown), and cloned into a TOPO-vector for further amplifications and sequencing, as described below.

Figure 13 shows stained and purified DNA from figure 12. Visible bands on the control-gel (Fig.13) indicated enough yield of DNA for proceeding with the next step.

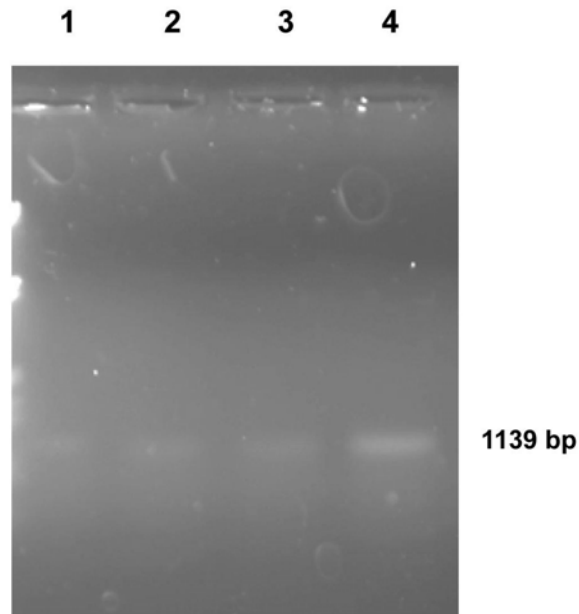


Figure 13. An 1% agarose gel electrophoresis of stained and purified DNA. Lane 1-4 contains GFX purified PCR product with expected size of 1139 bp.

4.1.2 Cloning of Kir4.1 PCR-products into a pCR2.1TOPO plasmid

The amplified Kir4.1 fragment was cloned into a plasmid vector called 2.1-TOPO plasmid. By using the TOPO TA cloning kit (see section 3.4.1) the PCR fragment can be directly incorporated into the vector without use of ligases.

Purified DNA from the PCR amplification was mixed with the pCR2.1-TOPO plasmid, incubated at room temperature and then DH5 α *E.coli* bacteria where chemically transformed. The TOPO vector contains genes coding for ampicillin- and kanamycin resistance, so bacteria with vector, with or without insert, can grow on agar plates containing these antibiotics. Bacterial colonies obtained after 24 h of growth, should contain a TOPO-vector. After 16 hours, the colonies were counted and the results are shown in table 33.

Table 33. Number of colonies obtained after TOPO-cloning. The table shows the results from four different transformations with different inserts (i.e the four different PCR products shown in lane 2-5 in Fig. 12A, and , in purified form, in lane 1-4 of Fig. 13). Cells were grown at 37° C for 16 h before counting.

Sample	Number of colonies
TOPO 1_243_1367	75
TOPO 2_243_X2	116
TOPO 3_Kh2_1367	121
TOPO 4_Kh2_X2	200

The plasmid sometimes religates without target insert, so the plasmid in the growing cells could be empty. However, the number of colonies for the ligation reaction, compared with previous control experiment where no insert DNA was added, was approximately ten times higher, indicating successful cloning of the PCR products.

4.1.3 Purifying and analyzing the pCR2.1-TOPO-Kir4.1 plasmids

4.1.3.1 Purifying plasmids from bacterial colonies using Miniprep and quantifying DNA yield using NanoDrop spectrometry

From each transformation, four colonies were picked and cells were grown for plasmid isolation, as described in section 3.5. Simultaneously, the selected colonies were inoculated on a masterplate for storage and later control. After the isolation of plasmid using the MiniPrep method (section 3.6.1), DNA concentration were measured, as this is helpful for subsequent restriction enzyme analysis, insert sequencing and further sub-cloning. The DNA yield was good, varying from ca. 3.5 to ca. 7 microgram of DNA. These amounts were sufficient for all subsequent steps.

4.1.4 Restriction analysis of plasmid to demonstrate KIR4.1 inserts

In order to demonstrate Kir4.1 insert presence in the TOPO-Minipreps, restriction analysis with the enzymes HindIII and EcoRI was performed. To visualize the cutting fragments, samples were run on 1% agarose gel electrophoresis (for plasmid chart see appendix 4).

Figure 14 contains the different digested Minipreps. Two bands are present in all lanes. Bands with molecular weight of 4281 bp (3931bp + 950 bp), correspond to the pCR2.1-TOPO

plasmid with insert. The Kir4.1 insert with restriction sites will here have a molecular weight of 950 bp since an internal HindIII site in Kir4.1 cut close to ends of CDS. According to the molecular weight marker, correct sizes on insert have been detected, and we have successfully demonstrated presence of Kir4.1 insert

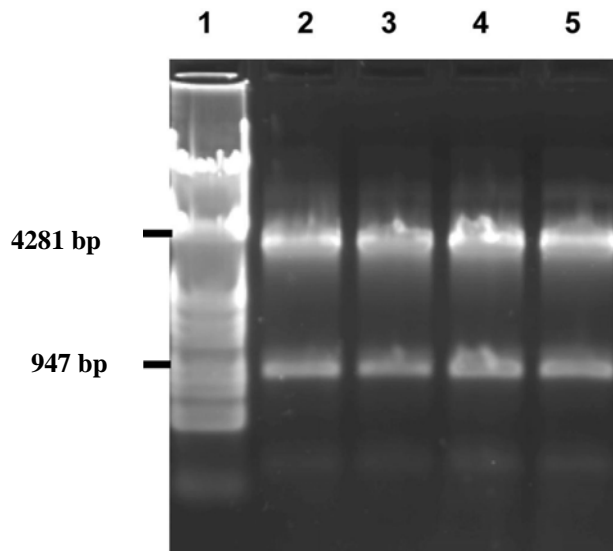


Figure 14. Picture showing the digested plasmid. Lane 1 contains the Lambda-HindIII-EcoRI ladder. Lane2-4 contains digested plasmid where the upper band in every lane corresponds to the plasmid. The lower band corresponds to the Kir4.1 insert.

4.1.5 Sequencing results from cloning of Kir4.1 into TOPO plasmid

The 16 purified plasmids with insert were sent for sequencing, to see if the Kir4.1 insert had any mutations before sub-cloning was performed. In general, the sequences were aligned with the mouse mRNA sequence NM_001039484, using the online alignment tool 2BLAST from NCBI. The sequence matched nicely in four overlapping alignments, thus we concluded that we had managed to clone Kir4.1 into the TOPO- plasmid successfully.

However, there were two persistent changes at position 380 bp and 820 bp in all four clones (Fig.15 for alignment). Since the changes were present in different PCR products, the changes probably originated from the plasmid template and not in the PCR process or the TOPO-cloning. Furthermore, translation analysis in Vector NTI hardware on pCR2.1-TOPO-mKir4.1- and NM_001039484 files show that the two mutations present in position 380 bp and 820 bp are silent, with no change from the amino acids lysine and histidine. This indicates that the mutations in position 380 and 820 might be natural occurring polymorphisms.

```

Query 244 TGACGTCGGTCGCTAAGGTCTATTACAGTCAGACGACTCAGACAGAGAGCCGCCCCCTAG 303
          |||
Sbjct 37 TGACGTCGGTCGCTAAGGTCTATTACAGTCAGACGACTCAGACAGAGAGCCGCCCCCTAG 96

Query 304 TGGCCCCAGGAATACGCCGGAGGAGGGTCCTCACGAAAGACGGCCGGAGCAATGTGAGAA 363
          |||
Sbjct 97 TGGCCCCAGGAATACSCCGGAGGAGGGTCCTCACGAAAGACGGCCGGAGCAATGTGAGAA 156
                    polymorphism

Query 364 TGGAGCACATTGCTGACAAACGTTTCCTCTACCTCAAGGATCTATGGACGACCTTCATTG 423
          |||
Sbjct 157 TGGAGCACATTGCTGACAAACGTTTCCTCTACCTCAAGGATCTATGGACGACCTTCATTG 216

Query 424 ACATGCAATGGCGCTACAAGCTTCTGCTCTTCTCTGCAACCTTTGCAGGCACGTGGTTCC 483
          |||
Sbjct 217 ACATGCAATGGCGCTACAAGCTTCTGCTCTTYTCTGCAACCTTTGCAGGCACGTGGTTCC 276

Query 484 TCTTTGGTGTGGTGTGGTATCTGGTAGCTGTGGCCCATGGGGACCTGTTGGAGCTGGGAC 543
          |||
Sbjct 277 TCTTTGGTGTGGTGTGGTATCTGGTAGCTGTGGCCCATGGGGACCTGTTGGAGCTGGGAC 336

Query 544 CTCCTGCCAACCACACGCCTTGTGTGGTGCAGGTGCACACGCTCACCGGAGCCTTCCTCT 603
          |||
Sbjct 337 CTCCTGCCAACCACACGCCTTGTGTGGTGCAGGTGCACACGCTCACCGGAGCCTTCCTCT 396

Query 604 TCTCCCTGGAATCCAGACCACCATCGGCTATGGCTTCCGCTACATCAGTGAGGAATGCC 663
          |||
Sbjct 397 TCTCCCTGGAATCCAGACCACCATCGGCTATGGCTTCCGCTACATCAGTGAGGAATGYC 456

Query 664 CACTGGCCATCGTGCTTCTTATTGCGCAGCTGGTGCTCACCACCATTCTGGAAATCTTCA 723
          |||
Sbjct 457 CACTGGCCATCGTGCTTCTTATTGCGCAGCTGGTGCTCACCACCATTCTGGAAATCTTCA 516

Query 724 TCACAGGTACCTTCCTTGCAAAGATTGCCCGCCTAAGAAGAGGGCCGAGACGATCCGCT 783
          |||
Sbjct 517 TCACAGGTACCTTCCTTGCAAAGATTGCCCGCYCTAAGAAGAGGGYCGAGACGATCCGCT 576
                    Polymorphism

Query 784 TCAGCCAGCATGCCGTTGTGGCTTCCCAATAACGGGAAGCCTTGCCTTATGATCCGGGTTG 843
          |||
Sbjct 577 TCAGCCAGCATGYCGTTGTGGCTTCCCAACAACGGGAAGCYTTGCCTTATGATCYGGGTTG 636

Query 844 CCAATATGCGGAAGAGTCTCCTCATTTGGATGCCAGGTGACA-GGCAAACCTGCTTCAAACG 902
          |||
Sbjct 637 YCAATATGCGGAAGAKTCTCCTCATTTGGATGCCAGGTGACAAGGCAAACCTGYTTCAAACG 696

Query 903 CACCAGACAAAGGAGGGTGAGAAATATTCGGCTCAAC-CAGGTCAACGTGACTTTCCAAGT 961
          |||
Sbjct 697 CACCAGACAAAGGAGGGTGAGAAATATTCGGCTCAACYCAGGTCAACGTGWCTTTCCAAGT 756

Query 962 AGACACAGCCTCAGACAGCCCCTTCTCATCCTACCCCTGACTTTCTACCACGTGGTAGA 1021
          |||
Sbjct 757 AGACACAGYCTCAGAC-RCYCYCTTKCTCATCCTACYCCTGACTTTCTACCWTGTGGTAGA 815

Query 1022 TGAGACCAGCCCCTTAAAAGATCTCCCGCTCCGAGTGGGGAGGGGGACTTTGAGCTGGT 1081
          |||
Sbjct 816 TGAGAGYAGYCYCTTAAARGATCTCCCGCT-CGCA-TGGGGAGGGGGAM-TTGAGCTGGK 872

Query 1082 GCTGATC 1088
          |||
Sbjct 873 GCTGATC 879

```

Figure 15: Multiple alignment of sample sequence form Miniprep from TOPO 1 (upper sequence), with mKir4.1 NM_001039484 (CDS = 243-1382) (lower sequence). Sequence mistakes labelled in red, which increase strongly at end of sequence. Possible polymorphisms in position 380 and 820 indicated in purple.

The sequencing results revealed four clones with the right insert. There was one positive clone from every set of TOPO reaction.

We successfully amplified the restriction enzyme sites inserts into the PCR primers (data not shown). At the 5`end of the CDS we identified the *EcoRI* site, and the optimal Kozak sequence. At the 3`end of the CDS we identified the *XhoI* restrictions site. Since our Kir4.1 insert contained the correct sequence, the next step was subcloning of the Kir4.1 insert into the expression vector pcDNA3.1/Zeo(+) utilising the *EcoRI* and *XhoI* restriction enzyme sites.

4.1.6 Sub-cloning Kir4.1 insert from pCR2.1-TOPO to pcDNA3.1/Zeo(+)

The Kir4.1/Topo plasmid prep was excised from the TOPO vector with *EcoRI* and *XhoI* restriction enzymes and analyzed on agarose gel (Figure16 A and B).

As shown in figure 16, two bands in every lane, with different sizes were observed when digesting with *EcoRI* and *XhoI*. The main band (plasmid) is around 4000 bp. The second band is around 1000 bp which corresponds to the correct size of the DNA insert (1139 bp). The pCR2.1-TOPO plasmid is 3.9 kb and the insert has a size of 1139 bp, the expected ratio between digested plasmid band and insert band is in this case 1:3.4. In lane 2, 834 ng of plasmid is loaded. The 1139 bp band should then contain ~245 ng of plasmid. The yield is important for the subsequent ligation reaction setup. Here, with 50 % yield in purification, and elution in total volume of 20 µL, we would expect 6.1 µg/L concentration of purified insert DNA.

The bands in lane 7 and 8 (Fig.16) are slightly higher than in lane 3-6. In lane 7, the band correspond to the plasmid digested with *EcoRI*, with the expected size 3923 bp (vector) plus 1139 bp (insert) for a total of 5062 bp. In all lanes, small bands < 100 bp in size were observed (but not visible in figure 16). These small fragments are probably fragments of the TOPO-plasmid itself, as it contains several restriction sites for *EcoRI* and *XhoI*.

In conclusion, these data shows successful amplification and cloning of Kir4 into the TOPO vector. The next step was cloning of Kir4.1 into the expression plasmid, pcDNA3.1/Zeo(+), by the use of the same restriction enzymes.

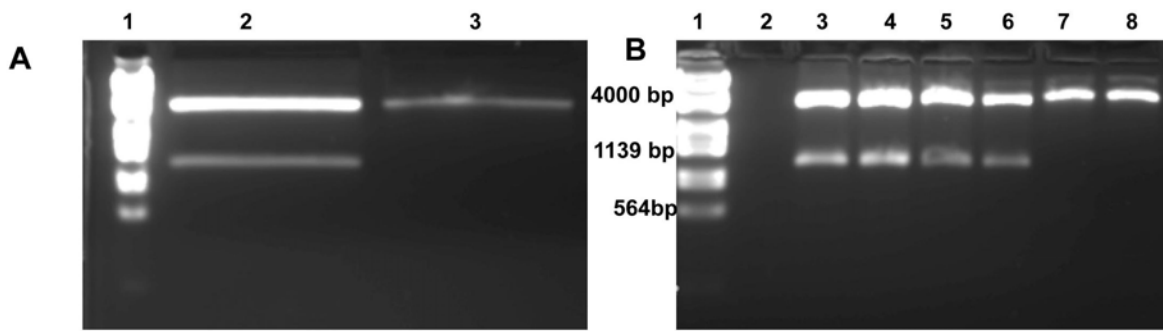


Figure 16. Digested plasmid fragments separated on an agarose gel. In Fig.16A, lane 1 contains the 21kDa Lambda DNA ladder. In lane 2 the upper band corresponds to the cut plasmid of ~4000 bp. The lower band corresponds to the DNA insert of ~1000 bp. In panel B, lane 1 contains the same ladder as in panel A. Lane 3-6 contains different eluates digested with both restriction enzymes. The same patterns as in panel A are seen. Lane 7-8 contains eluate digested with only one restriction enzyme, EcoRI and XhoI, respectively.

4.1.7 Digest of the expression plasmid pcDNA3.1/Zeo(+) with EcoRI and XhoI

The expression plasmid (pcDNA3.1/Zeo(+)) will act as a carrier for the Kir4.1 insert when transfected into cells. The plasmid contains a CMV-promotor driving the expression of the Kir4.1 mRNA and protein. The vector also contains a T7 promoter region which could make an in vitro transcription / translation possible by indicating the start sequence for a T7 polymerase in the transformation *E.coli* assay.

The pcDNA3.1/Zeo(+) plasmid was cut with *EcoRI* and *XhoI*, as shown in Figure 17. Lane 2 and 3 show the plasmid digested with both *EcoRI* and *XhoI*. The band size corresponds to the expected size of the plasmid (5015 bp), according to the molecular weight marker in lane 1. The small fragment of ~40bp (position 912-953, which corresponds to the fragment between the two restriction enzyme sites), is not visible on the agarose gel. GFX purified plasmid digested with only one restriction enzyme at a time and undigested plasmid, were used as controls of the digest reaction (not shown).

The bands from lane 2 and 3 were excised from the gel and purified. The control gel in figure 18 shows the expected size of the plasmid, and indicates enough yield for the next step, which was ligation of Kir4.1 insert and pcDNA3.1/Zeo(+) plasmid.

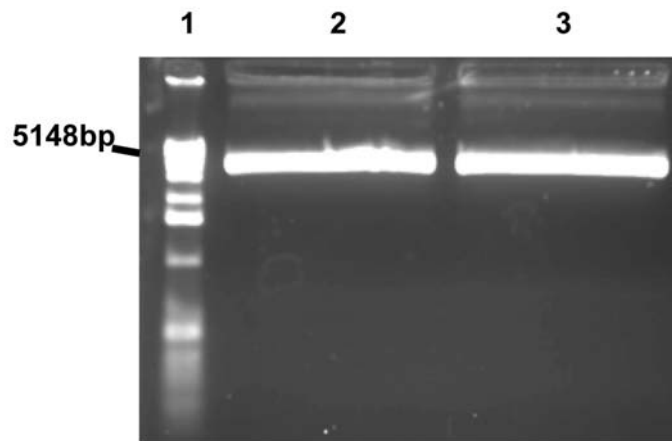


Figure17. Digested eluate of plasmid pcDNA3.1/Zeo(+)- separated in an agarose gel.Lane 1 contains the Lambda DNA ladder and the sizemarker 5148 kDa is indicated. Lane 2-3 contains plasmid digested with both EcoRI and XhoI. The bright band at ~5000 bp has the correct size.

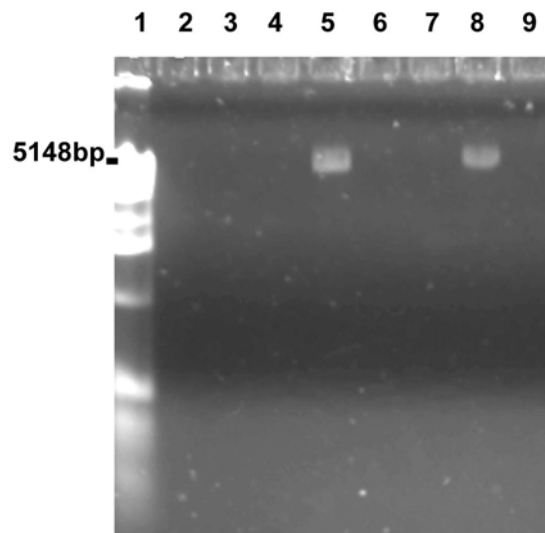


Figure 18. Control gel of purified plasmid pcDNA3.1/Zeo(+)- plasmid digested with EcoRI and XhoI. Lane 1 contains Lambda DNA ladder. With sizemarker 5148 kDa indicated. Lane 5-8 contains purified plasmid with size ~5000 kDa.

4.1.8 Ligation of Kir4.1-insert and expression plasmid pcDNA3.1/Zeo(+)

The Kir4.1 insert and the expression plasmid now had complementary end junctions. When mixed together, along with ligation buffer and the T4 DNA ligases, some of the DNA fragments will be ligated into a complete plasmid. Transformation into bacteria and selection for ampicillin resistance will identify the bacterial colonies containing the successful ligations, along with some mistaken ligations. Four different ligation reactions were made where purified Kir4.1 digested with XhoI and EcoRI, were mixed with the vector

pcDNA3.1/Zeo(+). After several unsuccessful attempts to ligate various Kir4.1 fragments resulting from different restriction enzyme digests and purifications, into the expression plasmid pcDNA3/Zeo(+), we finally obtained a few colonies after *Dh5alpha* transformations (Table 35).

Table 35. Number of colonies obtained from ON cultures after transformation reaction of Kir4.1 fragment and expression vector

	Fragment (1uL)	Vector (9uL)	Number of colonies
1	Kir4.1/19.12.07 Mp1 119ng/uL	pcDNA3.1 /6.3ng/uL _1	4
2	Kir4.1/19.12.07 Mp1 119ng/uL	pcDNA3.1/ 6.3ng/uL _2	5
3	Kir4.1/19.12.07 Mp4 69.5ng/uL	pcDNA3.1 /6.3ng/uL _1	3
4	Kir4.1/19.12.07 Mp4 69.5ng/uL	pcDNA3.1/ 6.3ng/uL _2	6
5	Nothing/ Negative control	pcDNA3.1 /6.3ng/uL _1	0
6	Nothing/ Negative control	pcDNA3.1/ 6.3ng/uL _2	2

The number of colonies is low (3 to 6 colonies in ligation 1-4) but higher than the background level seen in the control ligation without fragmen (ligation 5-6). This can indicate a few successful ligations. Two colonies arose from one of the ON negative controls (no fragment added) (ligation 6). This is probably colonies from plasmids with no insert. Since the probability of empty plasmids was present, we had to purify DNA from colonies by Miniprep, and check the DNA by sequencing.

4.1.9 Sequence analysis and Maxiprep purification of pcDNA3.1/Zeo(+)-Kir4.1

4.1.9.1 Sequencing results of plasmid after performed ligation assay

The purpose of sequencing the plasmids was to verify correct amplification and cloning of the Kir4.1 insert into the pcDNA3 vector. Two different primers (T7 and reverse primer BGH) where used. The sequencing output was analyzed with “Cromas Lite”, and a multiple alignment using 2BLAST (<http://www.ncbi.nlm.nih.gov>), were performed. Four different clones contained the correct insert (table 36), containing the Kir4.1 insert, ATG start codon, Kozak-sequence (GCCACC), XhoI restriction site (AAGCTT), EcoRI restriction site (GAATTC) and Topo-vector sequence (GCCCTT) (Appendix 5).

As these four plasmids had the correct sequence, their corresponding bacteria from the MiniPrep Masterplate were used for the final large-scale purification of plasmid by the use of Qiagen Endotoxin-free MaxiPrep, according to section 3.6.2.

4.1.10 Yield and quality of Endotoxin-Free MaxiPrep

After the purification step, DNA yield were measured. The concentrations in the eluates were too low for proceeding with transfection of plasmid into the cell lines, so new fresh colonies for ON cultures had to be made. The reason for the purification failure might have been clogged columns or loss of plasmids in bacterial Masterplate colonies. New bacteria containing the plasmids were prepared by bacterial transformation. The second large-scale purification was successful. Results and yield from the new transformation of Kir.4.1 in competent cells are shown in table 36.

Table 36. DNA concentration after Endo-MaxiPrep eluation

Endo-maxiprep eluat	Concentration
Mx 8	815 µg /µL
Mx 9	1421 µg /µL
Mx 24	901 µg /µL
Mx 25	1364 µg /µL

Since the plasmids were reconstituted in 500 uL total volume, the total yield varied from ca 400 to 710 µg, which was more than enough for the subsequent transfection into HeLa cells.

The four Maxiprep eluated from table 36 were again sequenced. The result files where analyzed with “Cromas Lite” hardware, and a multiple alignment using 2BLAST (<http://www.ncbi.nlm.nih.gov>), where performed as in section 4.4.1. All alignments contained the insert (Kir4.1) and had no mutations.

In conclusion, the cloning of Kir4.1 into the pcDNA3.1/Zeo(+)-expression plasmid was successful, and the plasmid could be transfected into cell lines.

4.1.11 Transfection of Kir4.1- pcDNA3.1/Zeo(+)- plasmid into HeLa cells

As the first transfection experiments failed, we decided to run a control experiment to verify the transfection efficiency of the HeLa cells. In the second transfection experiment, two MaxiPreps (MX 8 and MX 9) were transfected into the HeLa cells. As a control of the transfection assay, a control plasmid (pHIVmAQP4shRNAmir) containing a green fluorescent protein (GFP) was used. Cells expressing the control plasmid exhibits bright green fluorescence when exposed to blue light. Images of cells transfected with the control plasmid were taken, showing cells expressing the GFP protein (Fig.19). In figure 19 white cells corresponds to green cells.

By counting the transfected cells (Fig.19A) and comparing this with the count of total number of cells present (Fig. 19 B) the transfection efficiency can be computed.

- $35 \text{ green cells} / 235 \text{ non-green cells} * 100 \% = 15 \% \text{ transfection efficiency}$

15% transfection efficiency was lower than expected, however thought to be sufficient for the experiment. It was assumed that the transfection reaction of HeLa cell with Kir.4.1/pcDNA plasmid would be the same or a better efficiency than the control transfection. The control plasmid is larger in size than the Kir.4.1/pcDNA plasmid, and therefore more difficult to transfect. In addition, the control plasmid also uses the same promoter, CMV and has only been exposed for the same conditions as the pcDNA3.1/Zeo(+)-Kir.4.1 plasmid.

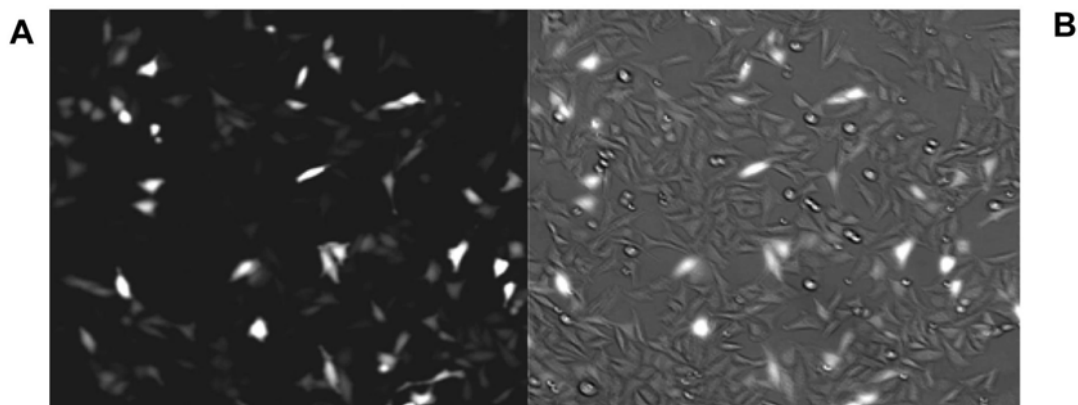


Figure 19. Panel A shows transfected HeLa cells expressing GFP control plasmid exposed to blue light. Bright cells express GFP protein. Panel B shows a picture taken by light microscope of the same cells as in panel A. Pictures taken 24h after transfection by a laser Olympus camera and visualized by “Wasabi” software. Round cells are dead cells.

PART II

4.2 Testing antibodies against Kir4.1 and AQP4 in SDS-PAGE and BN-PAGE assay

The next aim of this thesis was to test and validate Kir4.1- and AQP4-antibodies in the SDS-PAGE- and the BN-PAGE system, as the Kir4.1 construct was made to test possible cross reaction of AQP4 and Kir4.1 with the antibodies available in our laboratory. After homogenization of harvested HeLa cells transfected with the Kir4.1 construct, samples were prepared for Western blot analysis.

4.2.1 Kir4.1 labelling in SDS-PAGE

Self made polyacrylamide gels were used in this experiment. For the determination of molecular weight of the appearing bands “Precisions Plus Protein Standard, Dual Colour was used. Homogenates from mouse brain were used as positive control for all antibodies, and untransfected HeLa cells were used as negative control. The samples containing AQP4, were oocyte sample Aqp4a-3d or the AQP4 isoform M23 expressed in HeLa cells. In table 37, the results of labelling from different antibodies tested in the SDS-PAGE system are listed.

According to the scientific literature (see discussion part) the anti-Kir4.1 antibody from Abcam, has been widely used as antibody for determination of Kir4.1 presence in SDS-PAGE assays and light microscope (LM) assays. The results listed in table 37 have been compared with labelling using the Abcam antibody.

Two different antibodies against Kir4.1 (Kir4.1 “NordicBiosite” and Kir4.1 “Alomone labs,

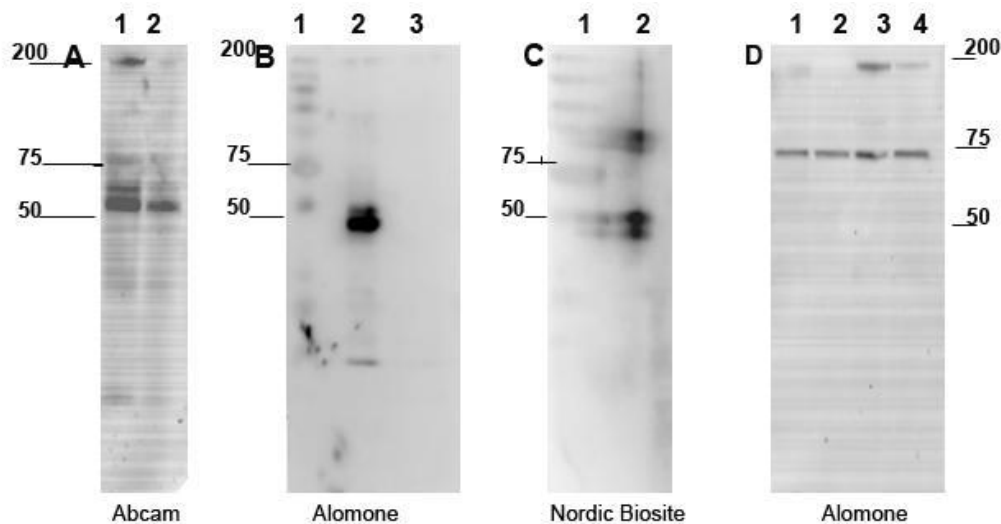


Figure 20. Panel A, B, C and D are labelled with different antibodies. Molecular weight marker is indicated in every panel. Panel A, lane 1 and 2 contains homogenate from wild type Kir4.1 mouse-brain and heterozygote Kir4.1 mouse brain respectively. Panel B, lane 2 contains homogenate from HeLa cells transfected with Kir4.1. Lane 3 contains untransfected HeLa cells. Panel C, lane 2 contains Kir4.1 transfected HeLa cells. Panel D, lane 1-4 contains homogenate from heterozygote Kir4.1 mouse, KO-Kir4.1 mouse, homogenate from mouse-brain and HeLa cells transfected with Kir4.1 construct, respectively. Heterozygote and KO-mouse material from E.Nagelhus (unpublished).

Jerusalem Israel”), were available for use at present time. In addition the results were compared to SDS-PAGE labelling with another Kir 4.1 antibody (Abcam). The results from labelling with Abcam antibody is from an unpublished study by other group members (N.Nabil Haj Yasein and E. Nagelhus) when this antibody was available in the lab.

Figure 20 A shows the protein bands detected using the antibody purchased from Abcam. Lane 1 and 2 show a previous, unpublished study from another group member. (N.Nabil Haj Yasein and E. Nagelhus). The ~50 kDa band in lane 1 corresponds to the Kir4.1 monomer (43 kDa). Another band with size ~200 kDa is also visible, and is possibly a Kir4.1 tetramer. Lane 2 shows the same ~50 kDa band as in lane 1, indicating the presence of the Kir4.1 monomer. No tetramer band with molecular weight ~200 kDa is visible in lane 2, and is consistent with no Kir4.1 tetramer formation in a heterozygote Kir4.1 mouse.

In Fig.20 B, the proteins are labelled with anti Kir4.1 from the Alomone laboratory. Two bands are visible in lane 2, corresponding to 37-50 kDa, which also are visible in lane 2,

Fig.20 C. There are no bands visible corresponding to Kir4.1 dimer or unspecific labelling as in lane 2, panel C. No bands indicating labelling of Kir4.1 tetramer is present in lane 2. The protein samples in Fig.20 B are heated to 95 °C, as opposed to the samples in Fig.20 D which were unheated.

In Fig.20 C the anti Kir4.1 from Nordic Biosite has been used. In lane 1, the molecular weight marker is indicated. Three or four bands are visible in lane 2. Two of these appear in the region corresponding to molecular weight 37-50 kDa. The upper band in this region possibly corresponds to a Kir4.1 monomer of 43 kDa. The lower band might be a posttranslational modified Kir4.1 protein. The bands with molecular weight between 75-100 kDa may correspond to a Kir4.1 dimer (86 kDa) or an unspecific band as shown in lane 4, panel D. No bands indicate presence of Kir4.1 tetramer.

In Fig.20 D, the antibody from Alomone lab is used. In lane 1-4, a band with size ~75 kDa is present. This is probably unspecific binding, as the same band appears in lane 2 (extract from KO mouse). Lane 3 and 4 show the ~200 kDa band corresponding to Kir4.1 tetramers. Protein loaded in lane 1-4 are not heated, so the unspecific bands with size 75 kDa are not due to membrane protein aggregation (see discussion part).

Table 37. Summary of labelling of Kir4.1 and AQP4 with different antibodies in SDS-PAGE. “Yes” means strong labelling. “No” means no visible labelling. “Weak” means visible but not strong labelling, or unspecific labelling

Samples	Antibodies against Kir 4.1			Antibodies against AQP4	
	Kir4.1 Abcam	Kir4.1 NordicBiosite	Kir4.1 Alomone lab	AQP4 SantaCruz	AQP4 LifeSpan Biotech
Dual colour marker	Weak	Weak	Weak	Yes	No
Homogenate cerebellum Kir4.1 200kDa	Yes	Yes	Yes	No	No
Homogenate cerebellum Kir4.1 43 kDa	Yes	Yes	Yes (when heated)	No	No
Unspesific labelling Kir4.1 75kDa	No	Yes	Yes	No	No
HeLa cells Kir4.1 200 kDa	N/A	Yes /BN PAGE No / SDS PAGE	Yes /BN PAGE No / SDS PAGE	No	Weak
HeLa cells Kir4.1 45 kDa	N/A	Yes	Yes	No	Weak
AQP4a and AQP4c	N/A	Weak	No	Yes	Weak
HeLa negative	No	No	No	No	Weak

To summarize figure 20 in light of my experiments, these results are important:

1. The Kir4.1 construct work
2. We have demonstrated that some Kir4.1 antibodies work and others do not. In conclusion the Alomone antibody is the only antibody labelling both Kir4.1 monomer and tetramer. A disadvantage is a unspecific labelling at ca. 75 kDa.
3. Kir4.1 can be expressed along with AQP4 to test an interaction.

4.2.2 AQP4 labelling in SDS-PAGE assay

In order to test a possible interaction between Kir4.1 and AQP4, optimisation of AQP4 antibodies was necessary. Two different AQP4 antibodies were available; the AQP4 antibody from Santa Cruz, was used in the experiments of Strand and coworkers (2009), and the other AQP4 antibody was from LifeSpan Biotech. In addition, we wanted to investigate whether there was cross reaction between AQP4 antibodies and the Kir4.1 protein expressed in HeLa cells (see also table 37)

Fig.21A, lane 1 contains mouse brain homogenate from cerebellum and the main band corresponds to the ~32 kDa AQP4 monomer. The weaker bands just above indicates presence of other AQP4 isoforms. Lane 2 contains untransfected HeLa cells shows no signal. Lane 3 contains homogenate of AQP4 (M23 isoform) transfected HeLa cells, and the band corresponds to a AQP4 monomer.

Fig.21 B and C are probed with two different antibodies. Panel B, lane 1 shows signal of what probably is the AQP4 monomer (32 kDa) from a cotransfection with Kir4.1 and AQP4. Lane 2, panel C shows the Kir4.1 monomer band (42 kDa). There is some weak background labelling in this lane, but no labelling where an expected AQP4 band should be. Thus, the Alomone Kir4.1 antibody does not seem to bind to AQP4 using Western blot detection.

Another anti-AQP4 antibody from LifeSpan Scientific was also tested for cross reaction with Kir4.1. This antibody was discarded because of unspecific binding on the membrane and with very weak labelling of AQP4-protein (results are not shown).

In conclusion, the anti- AQP4 antibody from Santa Cruz shows no cross labelling with Kir4.1 and usually gave strong signal for the AQP4 protein in both homogenate and HeLa cells using SDS-PAGE. Thus, this antibody was used for the work described this thesis.

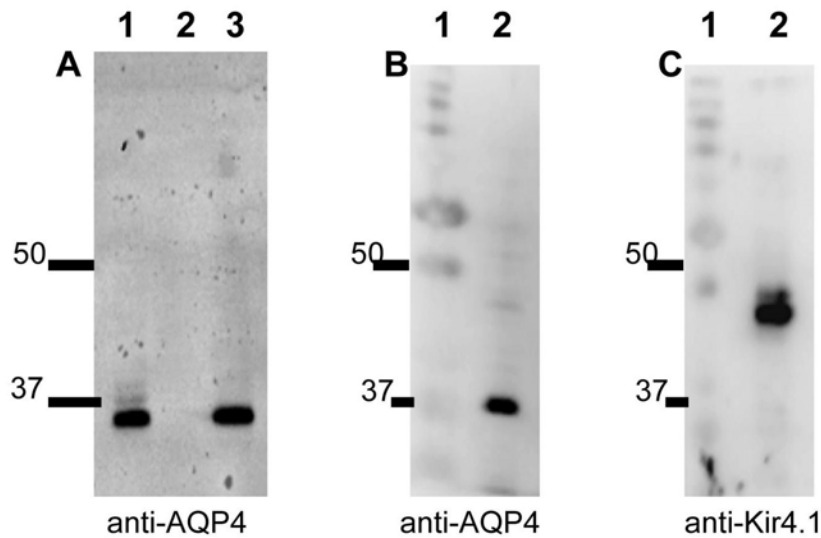


Figure 21. This figure shows SDS-PAGE assay of AQP4 and Kir4.1. Panel A is labelled with anti-AQP4 and molecular weight marker is indicated on the right. Lane 1 contains mouse-brain homogenate, lane 2 contains untransfected HeLa cells and lane 3 contains AQP4-transfected HeLa cells. Panel B contains molecular weight marker in lane 1, and lane 2 contains lysate from cotransfection of AQP4 and Kir4.1 in HeLa cells labelled with anti-AQP4. Panel C is the same membrane as in panel B. reprobred with anti-Kir4.1

4.2.3 Cotransfection of AQP4 and Kir4.1 in BN-PAGE assay

Another important aim in this thesis was to investigate a possible protein-protein interaction between AQP4 and Kir4.1. In Sorbo and collaborators (2008), BN-PAGE was used to detect AQP4 isoform interactions in square arrays. The same series of anti-Kir4.1 antibodies tested in the SDS-PAGE assay (Fig.20) were tested on AQP4a- and AQP4c protein co-expressed with Kir4.1 protein in HeLa cells (Table 37).

Figure 22 A shows a typical pattern of AQP4a and AQP4c on BN-PAGE. AQP4c contains higher order bands as expected (section 1.2.3). Fig. 22 B, lane 1 and 2 are negative controls, with isoforms AQP4a and AQP4c loaded. When scanning this picture, only weak, background labelling was seen in a region above 242 kDa. In lane 3 and 4, homogenate from cotransfected Kir4.1 and AQP4 give rise to one bright, wide band which was detected between 242 kDa and 480 kDa. A Kir4.1 tetramer is ~310 kDa, thus the main band corresponds to the size of a

Kir4.1 tetramer. The small band above the main band in lane 3 and 4 is also weakly present in lane 1 and 2, and is thus probably unspecific labelling.

Since the Kir4.1 labelling did not overlap with the AQP4 isoform bands (Fig.22 A), we concluded that Kir4.1 does not seem to interact with AQP4 in our BN-PAGE assay. Furthermore, since we saw no shift in the size of AQP4 bands when cotransfected with Kir4.1, there is no indication of interaction. No molecular weight marker was used on these membranes, since problems occurred when using secondary antibody from goat for visualization. The result was a smear where the marker was loaded. Many different conditions were tried for better resolution and results. After several attempts, we decided to run BN-PAGE without molecular marker when labelling with primary antibody against AQP4. However, since it was not certain whether the Kir4.1 and AQP4-antibodies signal was specific enough in the BN-PAGE assay we decided to design a myc-tagged version of the Kir4.1-construct for use in Kir4.1/AQP4 cotransfections.

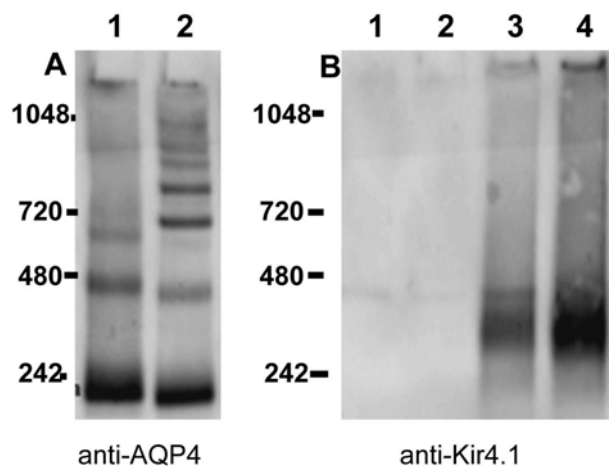


Figure 22. This figure shows cotransfection of AQP4 and Kir4.1. Panel A, labelled with anti-AQP4, shows in lane 1 and 2 AQP4a and AQP4c coexpressed with Kir4.1 respectively. In panel B, lane 1 and 2 contains AQP4a and AQP4c, respectively. Lane 3 and 4 is the same lanes as in panel A, lane 1 and 2, reprobred with anti-Kir4.1. Homogenate from two different transfections are shown.

4.2.4 Cotransfection of AQP4c-myc and Kir4.1

An AQP4c-myc construct was already available in the laboratory. The Kir4.1-AQP4 interaction hypothesis using another set of antibodies were therefore tested. The AQP4c-myc protein was already verified by Strand and coworkers (2009) (Strand et al., 2009). C-myc tag is a polypeptide protein tag of 10 amino acid which can be added to either the N- or C-terminal

of the protein. In this case, the tag is on the C-terminal of both AQP4 and Kir4.1 (see appendix 3 for AQP4- myc tag). By the use of the well tested primary c-myc antibody (Santa Cruz), one hoped to observe a protein-protein interaction of Kir4.1 and AQP4, in the BN-PAGE system.

AQP4c and Kir4.1 were cotransfected into HeLa cells to test protein-protein interaction. Fig. 23 A shows a BN-PAGE blot using the primary antibody against AQP4. Control lanes 1 and 2 contain AQP4a and AQP4c. The AQP4 antibody can still detect AQP4-protein with myc-tag (lane 3), and the myc tag does not seem to influence the assembly of AQP4 higher order bands, since the bands forms normally. The bands in lane 3 shows a higher molecular weight compared to the bands in lane 2, and is due to the additional myc-tag added.

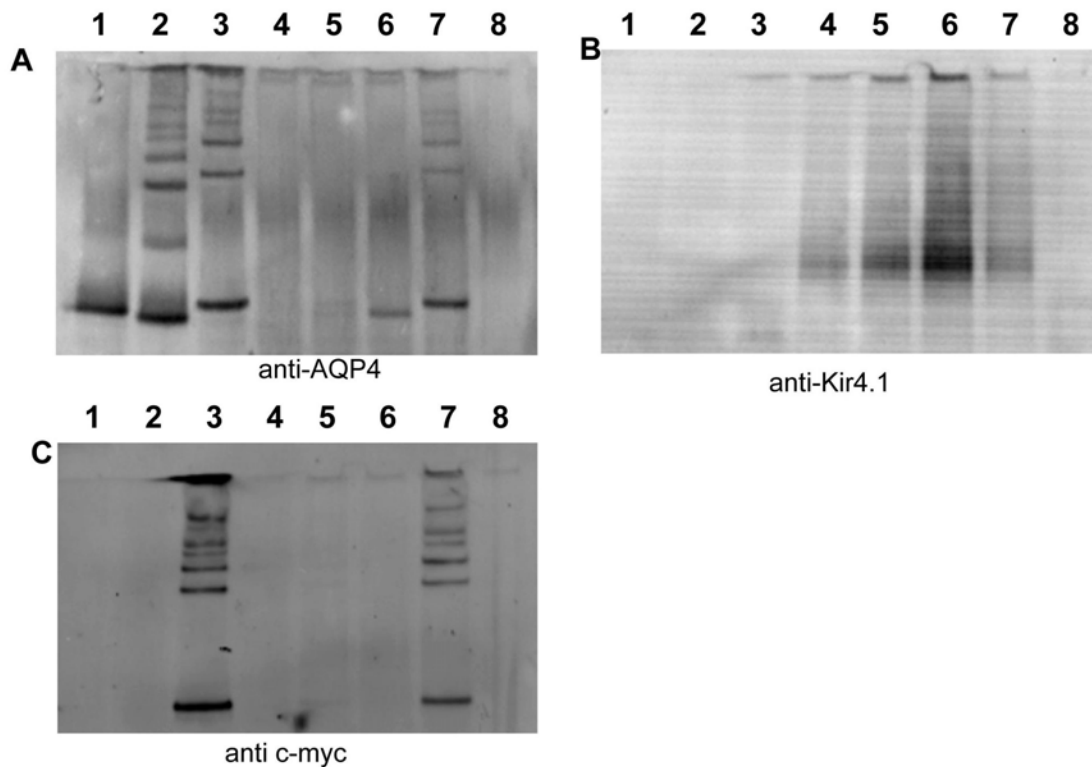


Figure 23. In this figure cotransfection of AQP4c-myc and Kir4.1 is shown. All lanes in all panels contain the same homogenates, respectively. Lane 1 contains AQP4a, lane 2 contains AQP4c, lane 3 contains AQP4c-myc, lane 4 contains Kir4.1, lane 5 contains cotransfection of AQP4a and Kir4.1, lane 6 contains cotransfection of AQP4c and Kir4.1 and lane 7 contains AQP4c-myc and Kir4.1. Lane 8 contains untransfected HeLa cells. Panel A is developed with anti-AQP4, panel B with anti-Kir4.1 and panel C with anti-cmyc antibody.

In figure 23 C the membrane is reprobed with anti c-myc primary antibody. Lane 3 and 7 contains AQP4c-myc alone and together with Kir4.1, respectively. The myc signal is also detected in the higher order bands. The loss of expression of AQP4 protein in Fig.23A lane 5

and 6 due to incomplete transfection, was experienced occasionally for unclear reasons, and emphasized the need for multiple controls in these experiments. The negative data in lane 5 and 6 is included since whole membranes in this case gives more information. Figure 22 shows coexpression without the myc-tag.

However, cotransfection and expression of Kir4.1 and AQP4c-myc were successful, as shown in lane 7, Fig 23 C. In addition, higher order bands are assembled, despite of Kir4.1 presence. Figure 23B shows the membrane probed with anti Kir4.1 (Alomone lab). Lane 4, 5, 6 and 7 show wide bands corresponding by size to Kir4.1 tetramers, similar to those seen in Fig. 22. The intensity of the bands differs. The signal in lane 6 is more intense, for reasons which are unclear. All the transfections are done with similar cell concentrations and should not give rise to a higher expression of Kir4.1 protein in the HeLa cell system.

Importantly, lane 7 has no signals above the main band a ~302 kDa, in the area to expect higher order bands. This indicates no protein-interactions between AQP4 and Kir4.1 using this assay. In conclusion, these data show no protein-protein interaction between AQP4-myc and Kir4.1 by the use of BlueNative-PAGE assay

4.2.5 Cotransfection of AQP4 and Kir.4.1 c-myc

A myc tagged version of Kir4.1 construct was designed and synthesized by the same methods as for the Kir4.1 construct. Unfortunately, the Kir4.1- myc version failed as no labelling using anti-myc antibody was seen in cotransfection with AQP4 (results not shown). The transfection worked well, since AQP4c with higher order band were visible using the anti AQP4 antibody. Kir4.1 was present with anti-Kir4.1 antibody, but when stripping and reprobing the membrane with anti-cmyc antibody, no signal was detectable. Due to the time limitations of this work this problem has not been solved yet.

4.2.6 Cotransfection of Kir4.1 and α -syntrophin

In order to test protein-protein interactions between Kir4.1 and α -syntrophin, cotransfection into the HeLa cell system was performed according to sections 3.13. The syntrophin plasmid was a gift from a collaborating laboratory, and the transfections were performed as for the Kir4.1 plasmid. The anti-syntrophin antibody and transfectants were tested in the SDS-PAGE and BN-PAGE system. The transfection lysates in figure 24 A were also tested in the native

BN-PAGE system in order to investigate if the syntrophin antibody would recognize the target protein under non denaturing conditions. No labelling of α -syntrophin protein was observed (not shown), but the presence of Kir4.1 was verified (Fig. 24 B).

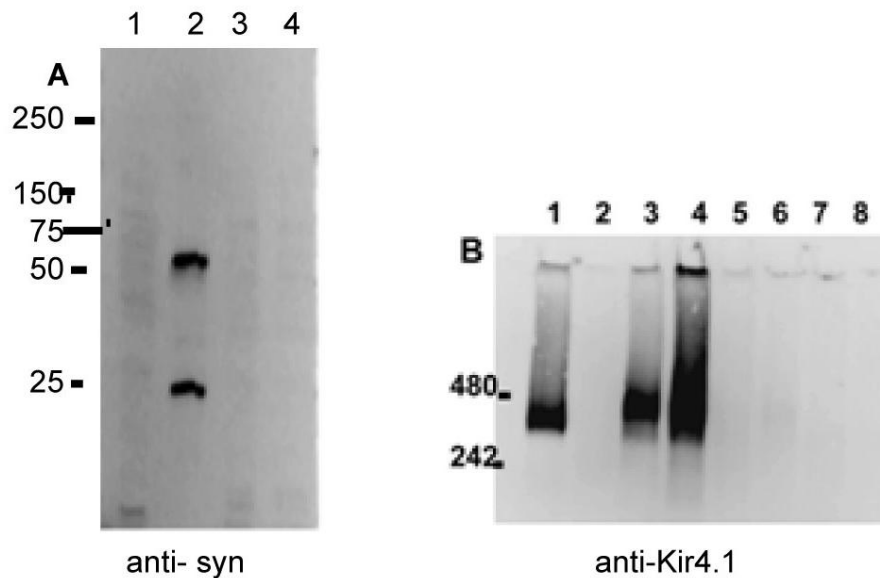


Figure 24. This figure shows cotransfection of α -syntrophin and Kir4.1. Panel A is a SDS-PAGE assay probed with anti-syntrophin. Lane 1 contains Kir4.1. Lane 2 contains mouse brain homogenate. Lane 3 and 4 contain α -syntrophin and cotransfection of α -syntrophin and Kir4.1, respectively. Panel B shows and BN-PAGE labelled with anti- Kir4.1. Lane 1 and 4 contains Kir4.1 alone. Lane 2 contains α -syntrophin alone, and lane 3 contains the coexpression of Kir4.1 and α -syntrophin. Lane 5 and 6 contains AQP4a and AQP4c. Lane 7 contains untransfected HeLa cells and lane 8 is empty.

One interesting observation was a possible shift of band size in the cotransfection with Kir4.1 and syntrophin (Fig.24 B, lane 3). This could indicate an interaction of Kir4.1 with α -syntrophin, since the protein complex in this transfection is larger and retained in the gel. This can not be verified since α -syntrophin not has been detected using the available α -syntrophin antibody.

In conclusion, no protein interaction between Kir4.1 and α -syntrophin could be revealed in these experiments. Since only transfections in HeLa cells were performed, HEK293 cell transfections could have been tested to exclude the possibility of an unsatisfactory cell system. However, the possible band shift in Fig.24 B might be a sign of an interaction, and further investigation has to be performed in order to test this hypothesis.

4.2.7 Cotransfection of AQP4 and α –syntrophin

Cotransfection of AQP4c and α –syntrophin was performed in HeLa cells as described in section 3.13. Despite of two attempts to co-express the proteins, no results were obtained. AQP4 was present and detected with anti-AQP4 in the SDS-PAGE assay (data not shown), however no signal of α - syntrophin could be detected. No further investigations were performed due to lack of time.

4.2.8 Cotransfection of Kir4.1 and PatJ c-myc

PatJ is a large protein associated with interaction to other proteins through the PDZ domain. PDZ domains often organize multimeric complexes at the plasma membrane. A recent study (Sindic et al., 2009) has shown an interaction between a protein complex, MUPP1, which is an paralog to PatJ, with inwardly rectifying potassium channels in the kidney, Kir4.2.

In order to test for interactions between PatJ and Kir4.1, a myc tagged version of the PatJ-expression plasmid was used and cotransfected with the Kir4.1 expression plasmid into two different cell lines, HeLa and HEK 293. HEK293 cells were used in the study by Sindic and coworkers (2009). The PatJ construct was a gift from a collaborating laboratory, and made from the full-length CDS of PatJ protein. The construct should give rise to at least one isoform with molecular weight 200 kDa. According to Lemmers and coworkers, known isoforms in HEK 293 cells have the approximate size of ~200kDa, ~100kDa and ~55 kDa (Lemmers et al., 2002).

4.2.8.1 SDS -PAGE on PatJ-myc and Kir4.1 cotransfection

Figure 25 A and B, show two SDS-PAGE membranes with PatJ protein and Kir4.1 protein in two different cell lines. The Kir4.1 monomer (43 kDa) and PatJ monomer (55 kDa + 2 kDa myc-tag) are quite similar in size, thus can be hard to distinguish.

Figure 25 A, lane 1 and 2 contains HEK 293 cells transfected with PatJ-cmyc alone and detected using the Kir4.1 antibody (Alomone lab). Lane 1 and 2 depict samples with boiled and unboiled protein, respectively. No difference is seen. The signals in lane 1 and 2 are due to background staining of the secondary antibody. Lane 3 and 4 contain protein from cotransfection of PatJ-myc and Kir4.1, boiled and unboiled respectively, no difference is observed. Both show bands in the area of 200-250 kDa and 55 kDa. The two bands in the area

of 50 kDa are most probably monomers of Kir4.1 (43 kDa). Additional modified proteins can also be present, but no interaction with PatJ is seen when comparing with figure 25 B.

Figure 25 B, lane 1-4 have the same lysates as lane 1-4 in panel A. The antibody used for detection is anti-myc. In lane 1 and 2 the different isoforms of PatJ are present. Patj-cmyc protein is stronger expressed when transfected alone than when cotransfected. The isoform of 55 kDa is only present when PatJ-cmyc is transfected alone. Lane 3 and 4 show lysate from the cotransfection, and shows weak bands in the area of PatJ-isoform ~200 kDa and ~100 kDa. The lower band can be another isoform of PatJ, expressed from endogenous mRNA coding for this isoform. In the cotransfection, Kir4.1 gives more signal than the PatJ-cmyc protein. The weak upper bands (200 kDa) in lane 3 and 4 have the same localization as PatJ in lane 1 and 2 and Kir4.1 in panel A.

A band of AQP4 in mouse cerebellum homogenate is present in lane 2, figure 25 C. It functions as a molecular weight marker in addition to Precision Plus Protein standards from BioRad. Since the transfer efficiency of the Precision Plus marker has been varying, AQP4 was added for better protein size identification.

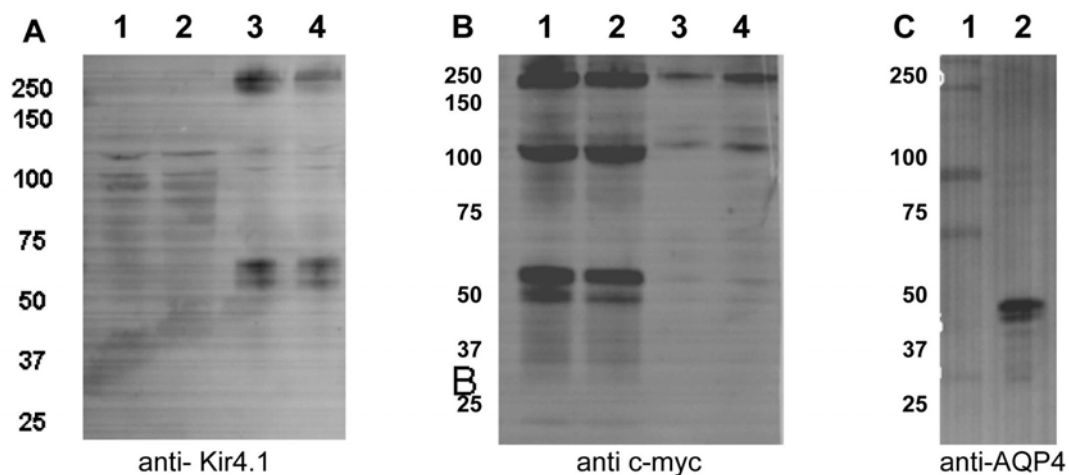


Figure 25. This figure shows HEK 293 cells transfected with Kir4.1 and PatJ-cmyc in a SDS-PAGE assay. Panel A is labelled with anti-Kir4.1 antibody. Lane 1 and 2 contains PatJ-cmyc alone, heated and non-heated respectively. Lane 3 and 4 contains protein from the cotransfection of PatJ-cmyc and Kir4.1, heated and non-heated. Panel B, lane 1 and 2 contains the same lysated as in panel A, labelled with anti-cmyc. Panel C shows mouse brain homogenate labelled with anti-AQP4 antibody.

In figure 26 the same transfections as described above have been carried out in HeLa cells. The same patterns as in figure 25 A is visible when staining with anti Kir4.1 antibody. The

expression of Kir4.1 is weaker in HeLa cells than HEK 293 cells. Lane 4 shows unheated lysates and has three visible weak bands with size ~200 kDa, ~100 kDa and ~55 kDa. The heated lysate in lane 5 lacks signal in the ~200 kDa area. In HeLa cells a weak band has appeared in the 75 kDa area. This band could correspond to the unspesific labelling of Kir4.1 protein according to table 37. This band is not visible in the HEK 293 transfections. The corresponding membrane developed with anti-c myc is unfortunately not available due to failure with the scanner.

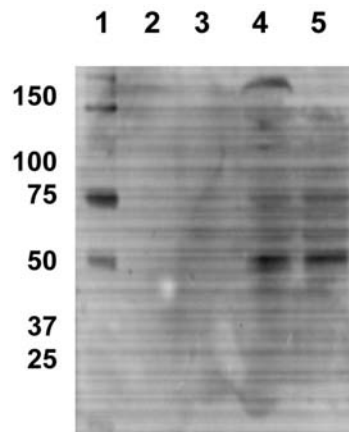


Figure 26. This figure shows HeLa cells transfected with Kir4.1/PatJ-myc in a SDS-PAGE assay stained with anti-Kir4.1 (Alomone). Lane 1 contains the weight marker. Lane 4 and 5 contains PatJ-myc alone and lane 4 and 5 contains cotransfection of Kir4.1/PatJ, unheated and heated respectively.

4.2.8.2 BN PAGE test of PatJ – Kir4.1 interaction

All the transfection lysates tested in the SDS-PAGE system were also run for the BN-PAGE assay to detect a possible interaction between the cytosolic protein PatJ and the membrane protein Kir4.1. Figure 27A and B shows lysates of PatJ-myc and Kir4.1 cotransfected in HEK293 cells and run in the BN-PAGE assay. In lack of a suitable protein weight marker, the Kir4.1 band is the guide towards protein size estimation. The Kir4.1 tetramer band in cell lysates is ~ 302 kDa.

Detection with the c-myc antibody in figure 27 A, reveals two PatJ-cmyc complexes with different size. Since there is no literature on how PatJ complexes will appear in a Blue Native Page system, it is difficult to estimate a protein size for the complexes. It was assumed that the protein size in BN-PAGE assay is overestimated by a factor of $1.8 \pm 10\%$ according to Sorbo and collaborators (Sorbo et al., 2008). The upper band in lane 1 corresponds to a protein complex with size approximately ~302 kDa (a Kir4.1 tetramer expressed in HEK293 cells), see Fig.27 B, lane 1. A hypothetical PatJ-dimer or tetramer can have different sizes

according to which isoform contributes to build the complex. A hypothetical protein complex of PatJ and Kir4.1 will also be difficult to estimate in this assay. Therefore, only the migrations patterns in the BN-PAGE assay will be evaluated. The two bands from PatJ-cmyc protein have the same localization in lane 1 and 2. If a complex of Kir4.1 and PatJ was present in lane 3, a band shift was expected, no shift was observed.

In figure 27 B, lane 1-2, no shifts in protein size was revealed between PatJ expressed with and without Kir4.1. One interesting observation is that there is only one band present in lane 5. This means that Kir4.1 do not follow the pattern of PatJ migrations in a co-transfection (panel A , lane 3) indicating possible interaction between these proteins. Another possibility is that the lowest band in Fig.27 A, lane 3 is not from PatJ protein.

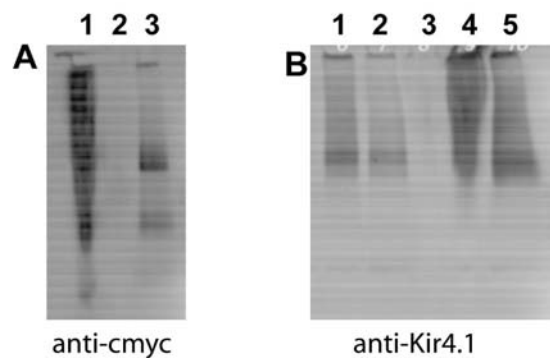


Figure 27. Panel A shows a BN:PAGE membrane probed with anti-cmyc antibody. In lane 1 a smear from PatJ expressed in HEK293 cells is seen. Three bands are slightly visible. In lane 2 Kir4.1 is loaded. Lane 3 contains the co-expression of Kir4.1 and PatJ-cmyc and only two bands are visible but located at the same size as in lane 1. Panel B is probed with anti-Kir4.1 and only one band is visible when Kir4.1 is expressed alone (lane 1-2). In lane 4-5 Kir4.1 is expressed together with PatJ-cmyc. Lane 3 is empty.

Fig. 27 C (see next side) shows the same as Fig. 27 A but with better transfer of protein. Lane 1-2 and 3 contains PatJc-myc, Kir4.1 and Kir4.1/PatJc-myc cotransfection, respectively. Four PatJ protein complexes are visible when this protein is expressed alone. When cotransfecting with Kir4.1-protein (lane 3), the two smallest PatJ-complexes disappear. One possibility is that a hypothetical protein complex of PatJ and Kir4.1 will always be bigger in size than a PatJ dimer or trimer, indicating that smaller complexes will not be formed. No evidence for this speculation is found in the literature. Another possibility is that the two smallest bands in lane 1 are unspecific staining of another protein.

The Kir4.1 bands in figure 27 D, lane 2 and 3 are wider than seen on other coexpression experiments. The bands indicate Kir4.1 (lane 2) and PatJ (panel C, lane 3) overlap in one

small area. If an interaction occurred, a smearier band would be expected for PatJ in panel C, lane 3.

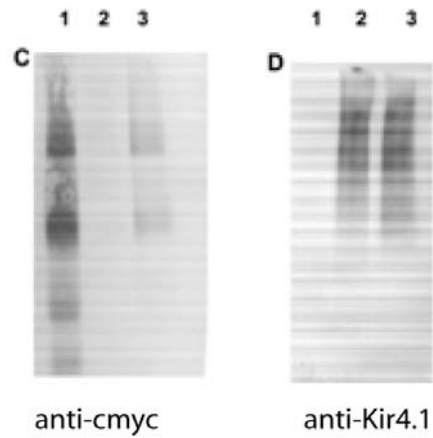


Figure 27. Panel C and D are the same BN-PAGE membranes developed with different antibodies. Lane 1,2 and 3 contains PatJ-cmyc, Kir4.1 and the coexpression of PatJ and Kir4.1, respectively.

In summary, no certain conclusions about protein-protein interactions can be drawn from the previous experiment on BN-PAGE assay. Difficulties about protein size estimation make the interpretation of the protein bands unclear, but one could argue that no clear shift in the signal distribution could be seen in the cotransfection compared to the single transfections.

PART III

4.3 Square arrays and protein-protein interactions in isoforms of AQP4

A part of the work of this thesis was to test the statement of Hiroaki and coworkers (2006), in which five specific interactions between adjacent AQP4 tetramer is the key to regulation of the orthogonal arrays, also called square arrays.

The hypothesis of Hiroaki and collaborators (2006) was tested by mutating critical amino acids in AQP4 and assaying the effects using BN-PAGE. Residues arginine (R)108, glycine (G)157, tryptophan (W)231, isoleucine (I)239 and tyrosine (Y)250 from the AQP4a, Hiroaki and group's (2006) crystal structure (see Fig. 5 for explanation) were mutated to alanine (A), and tested in the BN-PAGE system. Residue R108 from the Hiroaki and coworkers' (2006) crystal structure corresponds to residue R86 in the AQP4c amino acid sequence. Since the sequence of AQP4 (M1) and AQP4c (M23) differ by the length of 22 amino acids, the residues mutated in the AQP4c sequence are R86, G135, W209, I217 and Y228, which is the annotation that will be used in this thesis.

A part of the project was to test and optimize various experimental parameters of the BN-PAGE system. Much work on this issue was already done (Sorbo et al 2008), thus one main focus was to obtain easily reproducible transfer and visualization of the proteins. Specific conditions of the system were changed and tested. Amount of protein that were loaded, temperature of the buffers, different gel types, time and voltage of the protein transfer and antibody concentrations are some of the conditions that are of importance for the results.

The results obtained from the experiment described above were published by Strand and coworkers (2009), and parts of the results specific for this thesis work are presented here. All AQP4 mutations were expressed in HeLa cells as described in section 3.13. Some mutants were also tested in another cell line, HEK 293.

4.3.1 Single mutations in AQP4c

In order to investigate the presence of square arrays with AQP4c-single mutations, BN-PAGE analysis on AQP4c with an alanine substitution in one of the following amino acids,

Arginine (R)6, Glycine (G)135, Tryptophan (W)209 or Tyrosine (Y)228 and Isoleucine (I)239 was performed (Table 38).

Table 38. This table shows loading in figure 28A, and number of bindingsites affected by the different mutaions in AQP4c.

Lane	Sample	Number of binding sites affected
2	AQP4a (M1) control	-
3	AQP4c (M23) control	-
4	Single mut. R86A	1 binding site
5	Single mut. G135A	1 binding site
6	Single mut. W209A	1 binding site
7	Homogenat from thalamus	-
8	Single mut. _ Y228A	1 binding site

Lane 2 and 3 in fig 28, shows extracts and detection of AQP4a and AQP4c respectively, that were used as controls for formations of square arrays in this assay. AQP4a show no higher order bands above the 8 X band, as expected. AQP4c shows higher order band above the 8 X band. All the single mutations show higher order bands like AQP4c, indicating no effect by the mutations of the different tetramer-tetramer binding sites. The single mutation in I239 is not shown in this figure, due to problems with this spesific transfection. The pattern for the single mutation I239 is the same as for the other single mutations (Fig. 29, lane 10). I239 will give rise to two amino acid substitutions in one binding site (Table 39). The mutation does not influence the assembly of higher order band and the same pattern and results are as for the other single mutations.

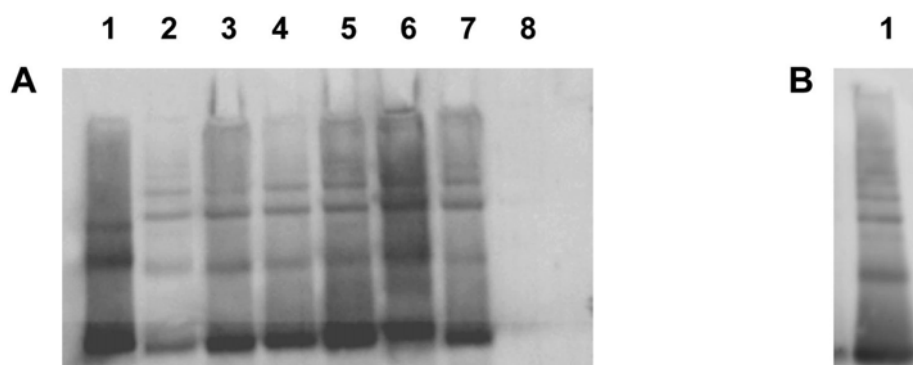


Figure 28. The figure show two BN-PAGE assays of AQP4c single mutations. Panel A, lane 1 and 2 shows AQP4a and AQP4c, respectively. Lane 1 and 2 functions as controls. Lane 3-6 shows the single mutations R86, G135, W209 and Y228 respectively. Lane 7 contains mouse homogenate from cortex and cerebellum. Lane 8 is empty. Panel B shows the single mutation I239 from another membrane. Antibody used in panel A and B is anti-AQP4 (Santa Cruz).

4.3.2 Double mutations in AQP4c

Since the single mutations in AQP4c had no effect on higher order band assembly, it was reasoned that perhaps the binding strength between the AQP4 tetramers was too high to be affected by just one mutation. The next step was then to test both double and triple mutations of AQP4c in the BN-PAGE assay.

Table 39: Loading in figure 29 and number of bindingsites affected by the different mutaions in AQP4c.

Well	Sample	Number of binding sites affected
1	Native Marker	-
2	M1 control	-
3	M23 control	-
4	Triple mutations :R86A+G+I	5 binding sites
5	Double mutation : R+G	4 binding sites
6	Double mutation R+I	3 binding sites
7	Double mutation: G+I	3 binding sites
8	Single mutation: R	1 binding site
9	Single mutation: G	1 binding site
10	Single mutation: I	1 binding site

In the figure 29, lane 5 to 7 shows the detection of the extracts were double mutations of AQP4c, R108/G157, R108/I228 and G157/I228 respectively were used. All the double mutations show higher order bands indicating no break down of square arrays, despite of three to four binding sites affected. Single mutations are also shown with the same pattern of higher order bands as double mutations. The signal in lane 6 is very weak, due to difficult loading and loss of material. Lane 4 and 10 shows a weaker signal than the other lanes. This can be because of difficulties with transfection (lane 4) or weaker transfer of protein, which were observed for lane 10 in many blots. This effect is most probably caused by the looser or tighter stacking on the membrane edge.

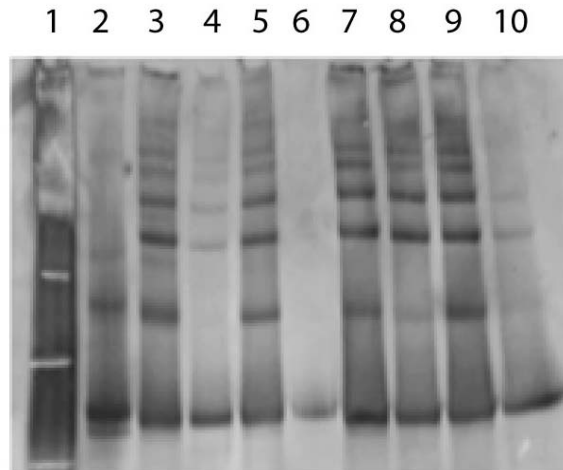


Figure 29. This figure shows a BN-PAGE assay with AQP4c single- and double mutations. Lane 1 contains the “Native Marker” (Invitrogen). Lane 2 and 3 show AQP4a and AQP4c, respectively. Lane 5-7 shows double mutations loaded according to table 39. Lane 8-10 contains single mutations. Lane 6 is almost empty. Lane 4 contains the RGI triple mutation. Antibody used in anti-AQP4 (Santa Cruz)

4.3.3 Triple mutations in AQP4c

According to the structure of AQP4 in the article by Hiroaki and coworkers (2006), five binding sites are responsible for the interaction between tetramers of AQP4 building up square arrays. Five mutations were made for the purpose of destroying the tetramer-tetramer interactions, and the assembly of square arrays.

Table 40. The triple mutations should influence all the interactions between two tetramers and should theoretically be seen as break down of higher order bands in the BN-PAGE system. Loading of figure 30.

Lane	Sample	Number of binding sites affected
1	M1 control	-
2	M23 control	-
3	R86A-W209A_I217A	5 binding sites
4	W209A_I217_Y228A	5 binding sites
5	R86A_G135_I217A	5 binding sites
6	G135A_I217A_Y228A	5 binding sites
7	I217A_Y228A	5 binding sites
8	Kir 4.1 transfected 30/1008	-

In figure 30, lane 3-6 contains triple mutations of AQP4c, R86A-W209A_I217A, W209A_I217_Y228A, R86A_G135_I217A and G135A_I217A_Y228A respectively. All the triple mutations show higher order bands indicating no break down of square arrays. It was expected that all interactions between tetramers should be affected by these mutations. Lane 7 contains a double mutation with higher order bands intact, as also seen in figure 29. In lane 8, Kir4.1 is added to test if binding with anti-AQP4 occurred. The weak band visible in lane 8 is

probably due to carry over from lane 7, and not cross reaction with anti. Kir4.1. The addition of Kir4.1, results in a different pattern than the AQP4c in the BN-PAGE system (Fig.22B).

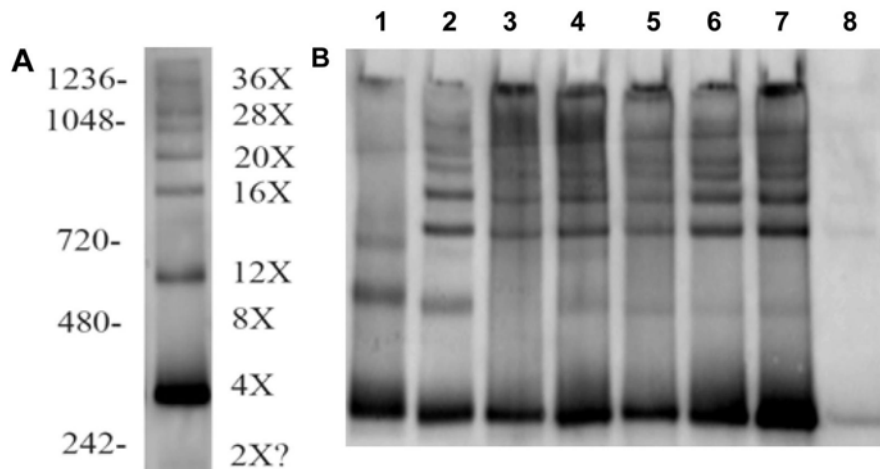


Figure30. This figure shows a BN-PAGE assay of AQP4c double and triples mutations. Panel A shows the “Native Marker” (Invitrogen). Panel B, lane 1 contains AQP4a and lane 2 contains AQP4c, respectively. Lane 3-6 contains triple mutations according to table 40. Lane 7 contains a double mutation. Lane 8 contains eluate from Kir4.1 transfected HeLa cells. Antibody used is anti-AQP4 (Santa Cruz)

4.3.4 AQP4c N-terminal mutations

Verkman and group (2009) proposed a theory that the N-terminal in AQP4c is a part necessary for square array assembly (Crane and Verkman, 2009). It was claimed that square arrays disappeared upon downstream deletions of AQP4 amino acids, from the amino acid methionin nr 23. To test this theory different amino acids in the N-terminal of AQP4c , Valine (V) nr 24, Alanine (A) nr 25, Phenylalanine (F) nr 26 , Lysine (K) nr 27 and Glycine (G) nr 28 were mutated. This is the amino acids Verkman and collaborators (2009) concluded were responsible for interactions in square array assembly and destabilization. As can be see in table 41, amino acids valine, alanine and phenylanlanine were mutated to glutamine (Q). Lysine (K) nr 27 was mutated to both alanine and phenylalanine (P) , and this was also the case for Glycine nr 28.

Table 41. Loading of samples in figure 31

Lane	Sample
1	AQP4c (M23)
2	V24Q
3	A25Q
4	F26Q
5	K27A
6	K27P
7	G28A
8	G28P

In figure 31 the N-terminal mutations in AQP4c are shown. The N-terminal mutations showed no effect on the disruption of the higher order bands. The higher order bands in the mutations V24Q, A25Q and G23P had weaker appearances. All lanes (including lane 2,3 and 8) are loaded with 5 μ g of protein each, so the lanes with weak signal should contain as much protein as the stronger lanes. These results are not quantified. The signal for the 8 X band is weaker in all the mutations compared to the AQP4 c control. All samples are from the same transfection, so difference in band strength can not be related to unequal properties in the transfection assay.

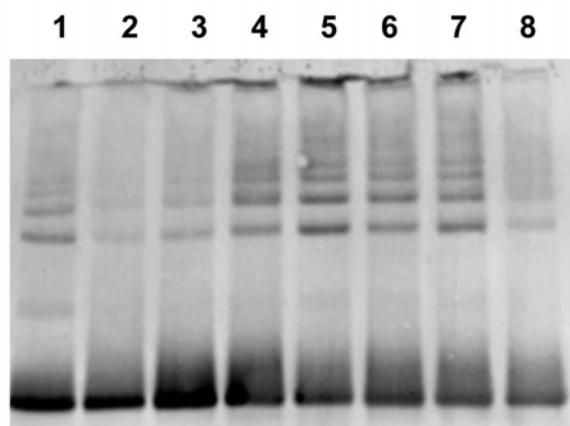


Figure 31. This figure shows a BN-PAGE assay of AQP4c N-terminal mutations. Lane 1 show AQP4a as control. Lane 2-8 contains different N-terminal mutations according to the loading in table 41. Antibody used is anti-AQP4 (Santa Cruz).

In conclusion, the N-terminal mutations of AQP4c showed no effect of destabilization of the assembly of the higher order bands.

5 GENERAL DISCUSSION AND CONCLUSION

The background for this thesis is to test several hypotheses proposing AQP4 as a molecular binding partner of another membrane protein (Kir4.1) and the cytosolic proteins (α -syntrophin and PatJ), as conclusive evidence for such interactions have not yet been published. AQP4 has been shown to be organized into big assemblies of square arrays, thus AQP4 protein-protein interactions must occur, at least with AQP4 isoforms themselves. Thus, investigation of protein interactions between AQP4 isoforms in square arrays is another main topic pursued in this thesis.

5.1 Specificity of antibodies against Kir4.1 protein

To investigate a hypothetical protein interaction of any protein, a possible cross reaction of antibodies has to be invalidated. Thus, an important starting point and theme of this thesis was to test the commercially available Kir4.1- antibodies.

In 2000, Kofuji and group generated a mouse line where they disrupted the Kir4.1 gene in order to prove the presence of Kir4.1 protein in retinal Müller cells (Kofuji et al., 2000). Kofuji and coworkers (2000) raised antibodies against the potassium channel Kir4.1, and demonstrated a lack of detection in the Kir4.1 knock out mice in contrast to the wild-type Kir4.1 mice, which was seen as a strong indication for the localization of Kir4.1 protein in the Müller cells. The Kir4.1 knockout mouse died at postnatal day 16-20.

The Kir4.1 antibody from Kofuji and coworkers (2000) was raised against a synthetic peptide corresponding to the amino acid sequence 8-30 in the C-terminus of the mouse-Kir4.1 protein. In a later study by the same group, this antibody was used to visualize interactions between Kir4.1 and proteins in the dystrophin-glycoprotein complex (Connors et al., 2004). Kofuji claimed to prove that Kir4.1 disappearing in AQP4-KO mice and α -syntrophin KO mice, suggesting an interaction between these proteins.

Another group of researchers (Djukic et al., 2007) generated in 2007 a conditional Kir4.1 knock-out mouse, in order to study the role of Kir4.1 channel according to spatial buffering of potassium in astrocytes. In this study the commercially available Alomone antibody (Jerusalem, Israel), which we also have depended upon, was used for detection of Kir4.1

protein in different tissues. By making a conditional KO-mouse (a tissue-specific inactivation of the Kir4.1 gene), they hoped to circumvent the premature lethality which was observed in the Kofuji KO-mouse. McCarthy and group (2007) observed a complete absence of Kir4.1 labeling in brain tissue of Kir4.1 KO mouse, where strong labeling was seen in kidney tissue from the same mouse (Djukic et al., 2007). In western blot, they show the presence of Kir4.1 (tetramer) as a ~200 kDa band, when using the Alomone antibody. No labeling of Kir4.1 monomer has been shown by this group when using Alomone antibody.

A research group in our department has several times tried to verify the Kir4.1 labeling results from McCarthy and coworkers, by the use of antibody from “Alomone Laboratories” as well as others (E.Nagelhus unpublished). By the use of KO-mouse brain tissue from McCarty’s lab, no endfoot labeling in astrocytes was shown. The antibody was also tested in Western blot and only the Kir4.1 tetramer (~200 kDa) was detected. No labeling of Kir4.1 monomer was seen. Another band with size ~75 kDa was detected in all brain tissues, also the KO tissue (personal communication). These results coincide with results of this thesis, when using the Alomone” antibody for visualization of Kir4.1 presence in SDS-PAGE assay.

Our laboratory had a couple of years ago the opportunity to test the Kir4.1 antibody made by Kofuji and coworkers in EM experiments. In this experiment labeling in Kir4.1 KO mouse was seen. This antibody also gave signal in AQP4 liposomes, and this could indicate a possible cross labeling of Kir4.1 and AQP4. Unfortunately this antibody is no longer available for the lab, thus there was a need to validate the Alomone Kir4.1 antibody by expressing the Kir4.1 protein in a cell line and evaluating the level of background labeling.

The Kir4.1 construct made in this thesis was verified, thus when expressing the Kir4.1 protein into HeLa cells, a slightly different pattern was found in SDS PAGE Kir4.1 labeling when compared with labeling of rat brain homogenate. The Alomone antibody revealed an additional band under the expected ~42 kDa Kir4.1 monomer band. According to Takumi (1995), Kir4.1 possesses an N-glycosylation motif in its extracellular domain (Takumi et al., 1995). A glycosylated Kir4.1 protein can alter its mobility in the gel, resulting in an additional, minor band.

Post-translational modifications (PTM) are processes which can change the properties of a protein by adding or cleaving amino acid residues after translation of protein. These

modifications can change localization, protein interactions and thus binding by antibodies. It is possible that HeLa cells glycosylate the Kir4.1 protein differently than in astrocytes in the brain. Also, in this study the construct used to verify labeling of Kir4.1 antibody is not made from full-length cDNA Kir4.1 (missing the 5' and 3' untranslated regions (UTR)). However, it is unclear, whether translation of the exogenous expressed cDNA in a cell system is dependent of untranslated regions, and thus could change post-translational modifications and give rise to other patterns in Western assays compared to endogenously expressed proteins.

All Kir4.1 antibodies used to study cross-reactivity in this study are polyclonal. Among these antibodies, only one of them have been verified in other assays than immuno-histochemistry (Connors and Kofuji, 2002). The specificity of an antibody can be changed in different assays, and it essential to test and characterize the antibody in the assay system which they are to be used. Most techniques involving electrophoresis will imply a certain degree of denaturation of the proteins, even in assays with native proteins. Only epitopes resistant to denaturations can therefore be detected. The antibodies against Kir4.1 used by Kofuji (2000) (Kofuji et al., 2000), McCarthy (2007) (Djukic et al., 2007) and Kurachi (2004) (Hibino et al., 2004) have been used on embedded tissues in LM and EM techniques. Insufficient data on embedding procedures make it very difficult to reason the ambiguous results of different labelling of Kir4.1 and a possible cross-reactivity. Western blot is a commonly used validation tool for confirming antibody specificity, thus there is often disagreement between results from Western and other assays. These results are seldom presented in the literature and non-agreeing data are rarely explained.

According to the results obtained in this study and unpublished results from other group members, there is a discrepancy between labelling results obtained in fixed tissue and in Western blot. The antibody from the Alomone laboratory used in Western blot analyses gives rise to an unspecific band of size 75 kDa. However, the staining of the ~200 kDa band is specific to a Kir4.1 tetramer. Another issue is the possible cross-reactivity of the Kir4.1 antibody labelling AQP4. In this study, it seems like the Alomone antibody is specific to Kir4.1 protein and no signals from AQP4 have been made from AQP4 construct transfected into cell systems. However, it is not known whether this conclusion can be applicable for detection of proteins in tissue samples, which can differ due to modified protein, isoforms and fixative used on the tissue.

The Abcam antibody (which is not available anymore) worked nicely in Western blots, but was not effective in LM and EM experiments. Antibody made by Kofuji (2000), worked nicely for some LM and EM experiment. This antibody show now batch-to-batch differences in labelling and a cross-reactivity of AQP4 in LM and EM experiment (Anna Thoren, personal communication).The Kurachi antibody against Kir4.1 is the best candidate for labelling Kir4.1 in both Western and fixed tissue. However, several attempts to receive a new batch with this antibody have failed.

In conclusion, the best antibody available to distinguish between AQP4- and Kir4.1 protein is the Kir4.1 antibody from Alomone (Jerusalem). However, this conclusion will only be valid for the Western assay. A thorough review of factors possibly influencing antibody specificity in different assays, are needed.

5.2 Possible protein-protein interaction between AQP4 and Kir4.1

Nagelhus and coworkers (1999) showed an precise co-localization between AQP4 and Kir4.1 in retinal Müller cells (Nagelhus et al., 1999). Postembedding immunogold labelling was used to investigate the distribution of these two proteins, and revealed almost identical patterns of AQP4 and Kir4.1 immunofluorescence on EM. The colocalization of these proteins suggested a physiological collaboration where waterflux (AQP4) and potassium siphoning (Kir4.1) were correlated.

The fact that AQP4 and Kir4.1 have close spatial relation (Nagelhus et al., 1999) and that they have a common consensus PDZ domain-motif (Hung and Sheng, 2002), and in addition are expressed in almost identical amounts in the endfeet membranes (Nagelhus et al., 1999; Kofuji et al., 2000), opened for speculations about a possible protein-protein interaction of AQP4 and Kir4.1.

Verkman and co-workers (2007) claimed to have evidence against a functional interaction between AQP4 and Kir4.1 (Ruiz-Ederra et al., 2007). They had investigated the Kir4.1 channel function in Müller cells from both wild type- and AQP4 KO-mice by using patch clamp techniques and immunocytochemistry. They found no differences on the Kir4.1 expression pattern or function between AQP4 KO- mice or wild type mice.

All data presented from the literature, shows only indirect evidence of an interaction between AQP4 and Kir4.1. No evidence for a direct protein-protein connection has been published. It was decided to test the hypothesis of a possible interaction by using the biochemical assay BN-PAGE, which was validated for protein interactions of AQP4 isoforms in Strand *et al* 2009. A Kir4.1 construct previously tested in co-expression studies, were used in the transfection assays together with AQP4. The hypothesis was that an interaction between AQP4c and Kir4.1 would be seen as Kir4.1 signals incorporated into the pattern of higher order complexes of AQP4c, in a similar manner to the myc-tagged isoforms AQP4a and AQP4e (Strand et al., 2009).

As discussed previously, only one suitable antibody-candidate for labelling Kir4.1 in BN PAGE and Western assays was available. The antibody from Alomone Lab (Jerusalem) is the one used in all BN-PAGE assays where presence of Kir4.1 protein should be detected. From the results obtained in section 4.2.1 it was concluded that Alomone antibody could be used for detection of native Kir4.1 complexes, since a specific labelling of Kir4.1 tetramer was shown. After disqualifying results from the cross-reactivity tests, another Kir4.1 antibody from Nordic Biosite was discarded.

Cotransfection of AQP4 and Kir4.1 was successful, since both AQP4 and Kir4.1 were present when using immunolabelling in both SDS-PAGE- and BN-PAGE assays. Higher order bands of AQP4c were seen in the co-expression with Kir4.1, even when AQP4 was myc-tagged. It is known from previous findings that presence of a myc tag does not influence the expression of protein or the assembly of higher order bands (Strand et al., 2009). When cotransfecting AQP4 and Kir4.1 there was no evidence of protein interactions by the use of the BN-PAGE assay. No signal from Kir4.1 was incorporated into the higher order bands of AQP4c, nor were coinciding signal from the Kir4.1 complex present in areas where signal from AQP4 was expected.

When cotransfecting AQP4 and Kir4.1, a weakening of higher order bands were seen. However, the 4X band of AQP4 showed the same intensity when expressed as one isoform and when coexpressed with another isoform. This is consistent with previous finding in Strand (2009), where they saw that a difference of expression ratios were influenced by the amount of AQP4 isoforms transfected into cells (Strand et al., 2009).

Since the weakening of the higher order bands arose when cotransfecting AQP4 and Kir4.1, a possible explanation can be retention of protein complexes intracellular. A hypothetical complex of AQP4 and Kir4.1 would be a large molecule. The size of the complex can influence expression in the cell system and result in intracellular retention, with subsequent lower expression of higher order bands. Another possibility is that the cell system doesn't support expression of complexes with this size.

BN-PAGE is a method especially useful for investigation of native protein complexes enabling a potential protein-protein interaction (Reisinger and Eichacker, 2008). To obtain a good resolution of complexes, the solubilization of membrane proteins are an important and difficult task. Solubilization conditions suitable for one protein cannot be generalized. A common artefact when working with membrane proteins in both SDS- and BN-PAGE, is the aggregation of protein, influencing both mobility and size estimation. Thus, differences in the solubilisation conditions could influence the hypothetical Kir4.1-AQP4 protein complex in such a way that a possible interaction could be concealed.

In addition, a Kir4.1 construct labelled with a myc tag where constructed, in order to avoid uncertainty of a possible cross labelling between AQP4 and Kir4.1 when using Kir4.1 antibody. Unfortunately, no results were obtained when the myc tagged version of Kir4.1 were used in co-expression studies.

In conclusion, no protein-protein interaction between AQP4 and Kir4.1 could be observed by the use of BN-PAGE assay. This could be interpreted as evidence against a direct interaction between Kir4.1 and AQP4. However, there are several factors that could influence the results in this section, such as detergent solubilisation choice mentioned above. Furthermore, only one cell line has been tested in the cotransfection study of AQP4 and Kir4.1. There is a possibility that another cell line can offer different conditions important for migration and assembly of complexes, affecting and contribute to another results. Cautions must be applied when interpreting the data achieved, and further analyses with other approaches would be required to obtain conclusive evidence against Kir4.1 and AQP4 interaction.

5.3 Possible protein-protein interaction between α -syntrophin and Kir4.1 and α -syntrophin and AQP4

As discussed previously, a precise co-localization between AQP4 and Kir4.1 has been shown in retinal Müller cells (Nagelhus et al., 1999). Kir4.1 helps to regulate the extracellular potassium concentration of glia cells by the process called spatial buffering (Kofuji, 2007). Kir4.1 harbors a PDZ binding-domain on its C terminal, and has been associated with proteins in the dystrophin-glycoprotein (DGC) complex which contains multiple PDZ domains. Possible candidates for a possible Kir4.1- interaction partner, which also possess a PDZ binding motif, are the syntrophins, which are found as part of the DGC complex (Adams et al., 1993).

Claudepierre and collaborates, (Claudepierre et al., 2000a; Claudepierre et al., 2000b), characterized the DGC complex in retinal Müller cells, and the localization patterns of AQP4 and Kir4.1 (Kofuji, 2007), indicating a possible dependence of the dystrophin Dp71 in the DGC complex. Astrocytes contain both α -dystrobrevin, β -dystroglycan, α -syntrophin and Dp 71 in the DGC complex (Neely et al., 2001).

In vivo tissue experiments of Kofuji and group has suggested, by the use of immunolabelling, that Kir4.1 is associated with the DGC. They also showed by *in vitro* immunoprecipitation assays, that Kir4.1 can bind directly to α -syntrophin, through the SSV sequence of the PDZ binding domain. It was concluded that the Kir4.1 was localized in glia cells via a link dependent of the syntrophins, since Kir4.1 failed to associate with the DGC complex in α -syntrophin KO mice (Connors et al., 2004). In a later experiment they showed that Kir4.1 failed to associate with the DGC complex, in the absence of α -syntrophin.

Another study by the same research group (Connors and Kofuji, 2006), claimed to prove that Kir4.1 could form a stable complex with dystrophin, syntrophin and dystrobrevin , which are all members of the DGC complex in mouse retina. In addition, a possible co-association with AQP4 and proteins in the DGC complex, links AQP4 and Kir4.1 together.

Since there have been suggestions of possible interactions between both Kir4.1 and α -syntrophin, and AQP4 and α -syntrophin, testing these hypotheses by a biochemical assay, could help describing these interactions. Cotransfections of Kir4.1 and α -syntrophin in HeLa

cells were tested in the BN-PAGE assay. The same procedure was performed for the cotransfection of AQP4 and α -syntrophin. In this testing, results were obtained for the Kir4.1 protein which was expressed and detected by the Alomone antibody (Jerusalem). No results were obtained from the transfection of α -syntrophin. The antibody used for detection of α -syntrophin worked nicely on rat-brain homogenate, and one specific band indicating presence of α -syntrophin was obtained. In theory this antibody should manage to detect α -syntrophin in a cell system, if expression of protein is satisfactory. Unfortunately, no detection of α -syntrophin was seen in any of the co-expression studies.

In this assay, there are several issues important for a satisfactory result. The reasons behind the observed results are therefore difficult to explain.

Fuentes-Mera and group, reported the identification of endogenous proteins of the DGC complex in the nucleus of HeLa cells (Fuentes-Mera et al., 2006). They found mRNA coding for both dystrophin Dp71 and syntrophins in the nucleus, and by the use of co-immunoprecipitation revealing complexes of DGC-proteins *in situ*. An existence of nuclear syntrophins in HeLa cells raise questions about the use of HeLa cells for expression of syntrophins. Small molecules under 45 kDa can freely move across the nuclear membrane (Akey and Goldfarb, 1989). A bigger molecule, as e.g. syntrophin, requires the presence of a localization signal assembled by a stretch of basic aminoacids. In Fuentes-Mera *et al* 2006, no such stretch of amino acids was found in α -syntrophin, maybe influencing the expression of the protein.

Other issues influencing the results can be the plasmid itself. Correct amplification of the cDNA was verified by sequencing and multiple alignments using BLAST. In one of the two transfections, cells were growing slowly, which may indicate problems with toxicity. No results were obtained in the co-expression study of AQP4 and α -syntrophin. This transfection was performed twice, but because of limitations of time, no further attempts of expression were performed.

No results were obtained in the co-expression study of AQP4 and α -syntrophin. This transfection was performed twice, but because of limitations of time, no further attempts of expression were performed.

In the BN-PAGE assay, a shift of band size occurred in the cotransfection of syntrophin and Kir4.1. This is a very interesting result, since this can indicate a possible interaction of Kir4.1 with another protein. A hypothetical complex of two proteins will show slowed migration in the gel according to the increased molecular size. A binding partner can also be retained intracellular. Unfortunately, a conclusion can not be made since the detection of α -syntrophin failed. It's tempting to speculate if the cell system used in this thesis, not possess all factors necessary for a satisfactory expression of α -syntrophin. Another issue is if endogenous proteins of the HeLa cells are able to mask or inhibit the translations or expression of exogenous α -syntrophin.

It would be useful to test other plasmids in attempt to express α -syntrophin in a cell system. Further testing of the observed band shift in figure 24B imposed to reveal the important result. Differences in the cellular metabolism, translation and modifications of proteins are properties which can influence protein-expression. HEK 293 cells and CRL2006 cells are good candidates for re-testing of this hypothesis.

5.4 Possible protein-protein interaction between Kir4.1 and PatJ

PatJ contains multiple PDZ domains and is localized to tight junctions and the apical membrane of epithelial cells. PDZ proteins have the ability to recognize sequences with a characteristic four-amino acid sequence found on the C-terminal of other proteins. In Sindic (2009), they claimed to prove an interaction between the protein MUPP-1, which is a paralog to PATJ, with an inwardly rectifying potassium channel, Kir4.2. In immunofluorescence studies on HEK293 cells, they saw a reduced expression of Kir4.2 on the membrane surface of the cells, when co-expressed with MUPP-1. They found MUPP-1 as a potential binding partner by using a yeast-two-hybrid screen with the COOH-terminal of Kir4.2 as bait. In addition, when testing coexpression of MUPP-1 with a Kir4.2 construct lacking the four COOH-terminal, no co-immunoprecipitations occurred. A selective interaction between Kir4.2 and the MUPP-1 protein was suggested.

Our hypothesis of a possible interaction between Kir4.1 and PatJ, was based on the results from Sindic (2009). (Sindic et al., 2009). In addition, it was tested whether the paralog PatJ was able to interact with another potassium channel (here: Kir4.1) in the same cell system.

MUPP1 and PatJ share several binding partners, and exhibit a similar subcellular distribution (Adachi et al., 2009).

In order to test for an interaction, a myc tagged version of the PatJ expression plasmid was used in the co-expression study with Kir4.1 and tested in both SDS-PAGE and BN-PAGE assay. There are no examples in the literature how the PatJ protein will behave in a native assay, and there are also several known isoforms found in different.

The predominant PatJ isoform expected in HeLa cells is ~200kDa in size according to Lemmers *et al* 2002. Known isoforms of PatJ in other tissues (HEK 293) have the approximate size of ~200 kDa, ~100 kDa and ~55 kDa. Since Sindic (2009), used HEK293 cells in their experiments, this cell line was used.

Inconsistent results were obtained from the SDS-PAGE and BN-PAGE analysis. Retained Kir4.1 protein was observed (Fig. 25 A), indicating a possible interaction with PatJ. Most proteins will not be able to sustain the dimer or multimers in presence of SDS. The presence of Kir4.1 tetramer band in SDS-PAGE assay has been reported from other researcher groups (Seifert et al., 2009). Sometimes, proteins with a hydrophobic “inside” will aggregate in the presence of SDS. The situations for these proteins are more aggregation when exposed to denaturizing conditions.

This could be the explanation for the unlike results seen in SDS-PAGE and BN-PAGE assay. However, the only difference between non-heated and heated protein seen in the SDS-PAGE assay, was when using HeLa transfected samples. The 200 kDa band of PatJ disappeared when boiling the sample. This should indicate that aggregation of protein is not the issue here. Since PatJ and Kir4.1 are hydrophobic proteins, a possible explanation for the big complexes observed in the SDS-PAGE can be unsatisfactory amount of SDS present. SDS helps to disrupt the hydrophobic interactions and unfold the secondary structure of the proteins. However, hydrophobic interactions tend to bind a bigger amount of SDS and a higher concentration is needed for the same denaturising effect even though reducing agents are used. One disadvantage in the SDS-PAGE assay is the absence of urea in the gel. Urea can be added for more efficient disruption of H-bond and decrease the hydrophobic interactions. For the case of Kir4.1, urea was tested in section 4.2 1 with no apparent change in the SDS-PAGE.

The preliminary data of SDS-PAGE and BN-PAGE are indicating different results for the two assays. Further testing on the denaturing conditions in the SDS-PAGE assay is necessary if these results should be compared. So far, the indicated complex of PatJ and Kir4.1 seen in SDS-PAGE is most probably due to incomplete denaturation of the proteins.

5.5 Triple mutations in AQP4c

AQP4 is found in high concentrations around blood vessels in the brain and is organized into complexes called square arrays. Recently, by the use of 2D BN-PAGE assay, three of six isoforms of AQP4, has been shown to contribute of the square array assembly (Sorbo et al., 2008). In Rash (2003) they found a difference of the two classical isoforms AQP4a and AQP4c, where only AQP4c was able to form square arrays in transfected cells (Furman et al., 2003).

In Hiroaki (2006) the crystal structure of AQP4 was demonstrated, where they claimed to prove which amino acids in the structure were responsible for the interactions between adjacent AQP4 tetramers (Hiroaki et al., 2006). The residues R108, G157, W231 and Y250 from the AQP4c sequence were pointed out as crucial for the tetramer-tetramer interactions.

The hypothesis from Hiroaki where tested in the BN-PAGE assay, by mutating the respective amino acid residues proposed to contribute to the interactions of tetramers. All residues mentioned were mutated to alanine. In the first attempt, only single mutations were introduced and tested in the BN-PAGE assay. We found that single mutations had no effect on the square array formation. The next step was to test if the introduction of double mutations would affect the assembly of the square arrays. The argument for testing double mutations was an assumption of high binding strength between the tetramers. Maybe a single mutation was not enough to overcome the binding strength between the tetramers, so we decided to test double mutations. No effect was seen on the assembly of the higher order bands. A weakening of the 8 x band were observed, and by testing triple mutations one hoped to see break down of the higher order bands. In a triple mutation, all binding sites in the Hiroaki crystal were mutated, affecting every interaction between the tetramers of AQP4. The higher order bands remained stable.

In the study using triple mutants of AQP4, the ability of AQP4c to assemble higher order bands was not diminished. An important question about the Hiroaki crystal structure arose from these results. These results showed a discrepancy between the arrays of tetramers from the *in vitro* 2D-crystal, and the organization of arrays formed *in vivo*. One has to assume that assembly of square arrays *in vivo* are organized differently than in a 2D crystal. Sorbo (2008) showed recently that another isoform of AQP4 (Mz) was contributing to the assembly of the square arrays *in vivo*, and can be the answer why the 2D crystal doesn't mirror the *in vivo* situation.

The difference between the Hiroaki crystal and the *in vivo* square array assembly were also supported in a later article (Crane et al., 2008). Alanine mutants of residue Arg108 and Tyr250 of AQP4 from the Hiroaki crystal were tested in a live-cell single-molecular tracking fluorescence image. These residues were claimed to affect and destroy formation of square arrays. If the Hiroaki crystal were correct there should be a difference of diffusion rate (which indicated formation of square arrays) between the mutants and the AQP4c. No difference was seen, and they concluded that the crystal structure had other contact-contact interactions between tetramers, than *in vivo* square arrays.

“Since higher order bands were present with all mutations tested in the BN-PAGE assay, it was concluded that the mutations results do not agree with the Hiroaki model of the proposed tetramer-tetramer interactions in the formation of square array assembly *in vivo*”. (Strand et al., 2009).

5.6 N-terminal mutations in AQP4c

Crane and Verkman used in 2009 the same assay of quantum dot single-molecular tracking and live cell images, to reveal the molecular determinants of square array formation in cell membranes. (Crane and Verkman, 2009). AQP4 was labelled with Qdot via a myc tag in its C-loop and the mutated AQP4 was tested in the system. By tracking the labelled native AQP4 and later AQP4 mutants, they tried to distinguish between AQP4a (which moves freely in the membrane) and AQP4c that are immobilized upon square array assembly. In order to test their hypothesis that distinct residues in the N-terminal of AQP4 were responsible for *preventing* formation of square arrays, they made AQP4 mutants where residues upstream of methionin

23, where changed. In their first attempt, many residues between methionin 1 and methionin 23 were mutated. No signs of square array formation were seen, except when cystein 17 was deleted. Large fractions of square arrays were formed, and these results supported the FFEM study of Suzuki (2008) where they used the same cystein mutation (Suzuki et al., 2008). However, when they mutated cystein 17 to alanine, no sign of square array formation was seen. Suzuki (2008), claimed that palmitylation of cystein 17 was required to obtain disruption of square arrays. However, alanine cannot undergo palmitylation. Crane and Verkman results did not support the results from Suzuki *et al*, and they concluded that palmitylation was not required for the disruption of square arrays.

From these results and other AQP4a mutants tested, it was claimed that residues just upstream of methionin 23 disrupted square arrays, by interfering with interactions where the downstream residues after methionin 23, where important. In their second attempt they tried to determine the *formation* of square array assembly. Seven residues downstream from methionin nr. 23 where mutated to alanine (V24A-F34A). Of these single mutations, F26A had a great effect on the lacking formation of square arrays. V24A had no effect on the disruption of square arrays, whereas a double mutation of V24A/F26A had some disruptive effect. K27A and G28A had also no effect on deletion of square arrays. Crane and Verkman (2008) suggested that “hydrophobic and aromatic residues downstream of methionin 23 are involved in square array formation”.

Since a small effect on square array destabilization had been seen with these mutants, we decided to test the same mutants in our BN-PAGE assay. Seven mutants of AQP4c were made, (V24Q, A25Q, F26Q, K27A, K27P, G28A and G28P), according to the Crane and Verkman article. Mutation A25Q and F26Q were made as a response to the suggestion about hydrophobic interactions responsible for the square array formation. Glutamines (Q) is a hydrophilic amino acid, and by introduce these mutations into the BN-PAGE assay, one hoped to see loss of higher order bands in the AQP4c mutants. Crane and Verkman had also tested the V24Q single mutation showing less disruptive effect than A25Q and F26Q. However, in our experiments none of these glutamine-mutations had any effect on the destabilization of higher order bands. Crane and Verkman claimed to see more effective destabilization if some of the mutations tested were substituted with more hydrophobic amino acids, like leucine. This was the case for A25 but not for e.g. F26. Leucine substitution of F26 showed no effect on the break down of square arrays, however an opposite effect was seen

when an additional hydroxyl group was added, suggesting an even more rigid structure of square arrays. This last suggestion has not been tested in the BN-PAGE assay.

Another theory of formation of square arrays was postulated by the same research group. They hypothesized that those interactions producing square arrays required a definite spatial positioning of the hydrophobic residues downstream from methionin 23, to fit into a hypothetical binding pocket in the adjacent tetramer. In response to these suggestions we tested the residues K27 and G28 mutated to proline in the BN-PAGE assay. Proline has a cyclic structure, which give the amino acid a rigid conformational structure. In addition proline has a nick name as “helix breaker”, since it has an ability to disrupt a helical backbone conformations.

Neither this time were any disruptions of the higher order bands seen when proline-mutations were tested in the BN-PAGE assay, even though Crane and Verkman showed completely loss of square arrays with their proline-substitutions. They concluded that by changing secondary structure downstream of methionin 23, more effective square array destabilization where seen in contrast to reduced hydrophathy in the same area.

In conclusion, none of the mutants tested in the BN-PAGE assay where able to show any effect on disrupted square array formation. These results are in disagreement to the results obtained by Crane and Verkman (2008), and further testing must be accomplice in order to reveal the specific nature and site of intermolecular interactions responsible for the formation of square arrays.

5.7 Some possible methodological limitations of BN-PAGE

Rash and co-workers demonstrated that the morphological appearance of square arrays differed in size when isoforms of AQP4 (M1 and M23) were expressed alone and together (Furman et al., 2003). They also found that the average square arrays contained 17 intramembrane particles (IMP). M23- transfected cells contained large rafts (>100 IMP's), ten times larger than observed in normal astrocyte endfeet. In contrast, mostly single IMP's were observed when M1 where transfected into cells. An AQP4 monomer is approximately 32 kDa in size. If an IMP corresponds to an AQP4 tetramer, the average size of a square array will have a total size of >2000 kDa. According to the BN-PAGE protocol, this method covers

a mass range of native complexes from <100 kDa to ~10 MDa (Wittig et al., 2006) .Since there has been discrepancy of the results from interaction-study of AQP4a and AQP4c obtained *in vivo* and by the use of BN-PAGE, one have to consider the possibility that the smaller complexes shown in BN-PAGE do not mirror the *in vivo* situations of square array assembly. However, the method is capable to handle an approximately sized square array of 17 IMP.

Another disadvantage in the BN-PAGE assay is problems with size estimations of native proteins. In this study, the native protein marker was difficult to use, since smeary results were seen when secondary antibody from goat where used for visualization. Since the approximately size of AQP4a was known and tested in this assay, the results were often compared with the AQP4 monomer band. In the BN-PAGE assay, the migrating complex during electrophoresis consists of the protein itself and G250 bound to it. In Heuberger (2002), they demonstrated that membrane proteins bound approximately 1.8 times more G250 than commonly used molecular weight markers soluble in water (Heuberger et al., 2002). Thus, this can implicate that protein size in BN-PAGE must be divided by 1.8 to arrive at an estimate of the absolute molecular weight. This approach has been used in Sorbo (2008), and also in this thesis.

Another approach for estimating molecular size in the BN-PAGE assay where used Shukolyukov and group (Shukolyukov, 2009). A calibration curve where made after the relative mobility of known proteins, e.g. BSA monomer and trimer. The logarithmic function of the relative mobility where used as an estimate for the molecular mass and this method will in a better way, considers the secondary and tertiary structure of the proteins and how they influence the mobility.

Solubility of membrane proteins is difficult in both SDS-PAGE and BN-PAGE assay. Unsolubilized protein in the SDS-PAGE assay can give rise to a false low monomer signal. For AQP4, self made gel with urea was necessary for a good resolution of the different isoforms. If the protein was heated prior to loading, aggregation of AQP4 was seen, leading to false molecular weight estimations. However, in BN-PAGE assay, the anionic dye G250 is used for native solubilisation step. It can bind to hydrophobic areas in membrane proteins, making the membrane protein water soluble. This lowers the risk for aggregation of membrane proteins. Thus, for very hydrophobic proteins, a large number of dye molecules are

required to solubilise the target protein. This can influence the relative molecular size, leading to false interpretations of size.

In summary, the conditions discussed above are able to influence the observed appearance and migration patterns of both native and denatured protein. Therefore the results and conclusions reached with the BN-PAGE methodology should be treated with caution when they disagree with the FFEM and single-molecule tracking square array data.

REFERENCE LIST

- Adachi M, Hamazaki Y, Kobayashi Y, Itoh M, Tsukita S, Furuse M, Tsukita S (Similar and distinct properties of MUPP1 and Patj, two homologous PDZ domain-containing tight-junction proteins. *Mol Cell Biol* 29:2372-2389.2009).
- Adams ME, Butler MH, Dwyer TM, Peters MF, Murnane AA, Froehner SC (Two forms of mouse syntrophin, a 58 kd dystrophin-associated protein, differ in primary structure and tissue distribution. *Neuron* 11:531-540.1993).
- Agre P, Saboori AM, Asimos A, Smith BL (Purification and partial characterization of the Mr 30,000 integral membrane protein associated with the erythrocyte Rh(D) antigen. *J Biol Chem* 262:17497-17503.1987).
- Akey CW, Goldfarb DS (Protein import through the nuclear pore complex is a multistep process. *J Cell Biol* 109:971-982.1989).
- Amiry-Moghaddam M, Ottersen OP (The molecular basis of water transport in the brain. *Nature Reviews Neuroscience* 4:991-1001.2003).
- Amiry-Moghaddam M, Xue R, Haug FM, Neely JD, Bhardwaj A, Agre P, Adams ME, Froehner SC, Mori S, Ottersen OP (Alpha-syntrophin deletion removes the perivascular but not endothelial pool of aquaporin-4 at the blood-brain barrier and delays the development of brain edema in an experimental model of acute hyponatremia. *FASEB J* 18:542-544.2004).
- Borgnia MJ, Agre P (Reconstitution and functional comparison of purified GlpF and AqpZ, the glycerol and water channels from *Escherichia coli*. *Proc Natl Acad Sci U S A* 98:2888-2893.2001).
- Butt AM, Kalsi A (Inwardly rectifying potassium channels (Kir) in central nervous system glia: a special role for Kir4.1 in glial functions. *J Cell Mol Med* 10:33-44.2006).
- Casamassima M, D'Adamo MC, Pessia M, Tucker SJ (Identification of a heteromeric interaction that influences the rectification, gating, and pH sensitivity of Kir4.1/Kir5.1 potassium channels. *J Biol Chem* 278:43533-43540.2003).
- Claudepierre T, Dalloz C, Mornet D, Matsumura K, Sahel J, Rendon A (Characterization of the intermolecular associations of the dystrophin-associated glycoprotein complex in retinal Muller glial cells. *J Cell Sci* 113 Pt 19:3409-3417.2000a).
- Claudepierre T, Mornet D, Pannicke T, Forster V, Dalloz C, Bolanos F, Sahel J, Reichenbach A, Rendon A (Expression of Dp71 in Muller glial cells: a comparison with utrophin- and dystrophin-associated proteins. *Invest Ophthalmol Vis Sci* 41:294-304.2000b).
- Connors NC, Adams ME, Froehner SC, Kofuji P (The potassium channel Kir4.1 associates with the dystrophin-glycoprotein complex via alpha-syntrophin in glia. *J Biol Chem* 279:28387-28392.2004).

Connors NC, Kofuji P (Dystrophin Dp71 is critical for the clustered localization of potassium channels in retinal glial cells. *J Neurosci* 22:4321-4327.2002).

Connors NC, Kofuji P (Potassium channel Kir4.1 macromolecular complex in retinal glial cells. *Glia* 53:124-131.2006).

Crane JM, Van Hoek AN, Skach WR, Verkman AS (Aquaporin-4 dynamics in orthogonal arrays in live cells visualized by quantum dot single particle tracking. *Mol Biol Cell* 19:3369-3378.2008).

Crane JM, Verkman AS (Determinants of aquaporin-4 assembly in orthogonal arrays revealed by live-cell single-molecule fluorescence imaging. *J Cell Sci* 122:813-821.2009).

Dietzel I, Heinemann U, Hofmeier G, Lux HD (Transient Changes in the Size of the Extracellular-Space in the Sensorimotor Cortex of Cats in Relation to Stimulus-Induced Changes in Potassium Concentration. *Exp Brain Res* 40:432-439.1980).

Djukic B, Casper KB, Philpot BD, Chin LS, McCarthy KD (Conditional knock-out of Kir4.1 leads to glial membrane depolarization, inhibition of potassium and glutamate uptake, and enhanced short-term synaptic potentiation. *J Neurosci* 27:11354-11365.2007).

Felgner PL, Gadek TR, Holm M, Roman R, Chan HW, Wenz M, Northrop JP, Ringold GM, Danielsen M (Lipofection: a highly efficient, lipid-mediated DNA-transfection procedure. *Proc Natl Acad Sci U S A* 84:7413-7417.1987).

Fraysse LC, Wells B, McCann MC, Kjellbom P (Specific plasma membrane aquaporins of the PIP1 subfamily are expressed in sieve elements and guard cells. *Biol Cell* 97:519-534.2005).

Fu D, Libson A, Miercke LJ, Weitzman C, Nollert P, Krucinski J, Stroud RM (Structure of a glycerol-conducting channel and the basis for its selectivity. *Science* 290:481-486.2000).

Fuentes-Mera L, Rodriguez-Munoz R, Gonzalez-Ramirez R, Garcia-Sierra F, Gonzalez E, Mornet D, Cisneros B (Characterization of a novel Dp71 dystrophin-associated protein complex (DAPC) present in the nucleus of HeLa cells: members of the nuclear DAPC associate with the nuclear matrix. *Exp Cell Res* 312:3023-3035.2006).

Furman CS, Gorelick-Feldman DA, Davidson KG, Yasumura T, Neely JD, Agre P, Rash JE (Aquaporin-4 square array assembly: opposing actions of M1 and M23 isoforms. *Proc Natl Acad Sci U S A* 100:13609-13614.2003).

Gonen T, Walz T (The structure of aquaporins. *Q Rev Biophys* 39:361-396.2006).

Gonzalez-Mariscal L, Nava P (Tight junctions, from tight intercellular seals to sophisticated protein complexes involved in drug delivery, pathogens interaction and cell proliferation. *Adv Drug Deliv Rev* 57:811-814.2005).

Grootjans JJ, Zimmermann P, Reekmans G, Smets A, Degeest G, Durr J, David G (Syntenin, a PDZ protein that binds syndecan cytoplasmic domains. *Proc Natl Acad Sci U S A* 94:13683-13688.1997).

Guan XG, Su WH, Yi F, Zhang D, Hao F, Zhang HG, Liu YJ, Feng XC, Ma TH (NPA motifs play a key role in plasma membrane targeting of aquaporin-4. *IUBMB Life* 62:222-226.2010).

Hasegawa H, Ma T, Skach W, Matthay MA, Verkman AS (Molecular cloning of a mercurial-insensitive water channel expressed in selected water-transporting tissues. *J Biol Chem* 269:5497-5500.1994).

Heuberger EH, Veenhoff LM, Duurkens RH, Friesen RH, Poolman B (Oligomeric state of membrane transport proteins analyzed with blue native electrophoresis and analytical ultracentrifugation. *J Mol Biol* 317:591-600.2002).

Hibino H, Fujita A, Iwai K, Yamada M, Kurachi Y (Differential assembly of inwardly rectifying K⁺ channel subunits, Kir4.1 and Kir5.1, in brain astrocytes. *J Biol Chem* 279:44065-44073.2004).

Hibino H, Inanobe A, Furutani K, Murakami S, Findlay I, Kurachi Y (Inwardly rectifying potassium channels: their structure, function, and physiological roles. *Physiol Rev* 90:291-366.2010).

Higashi K, Fujita A, Inanobe A, Tanemoto M, Doi K, Kubo T, Kurachi Y (An inwardly rectifying K⁽⁺⁾ channel, Kir4.1, expressed in astrocytes surrounds synapses and blood vessels in brain. *Am J Physiol Cell Physiol* 281:C922-C931.2001).

Hiroaki Y, Tani K, Kamegawa A, Gyobu N, Nishikawa K, Suzuki H, Walz T, Sasaki S, Mitsuoka K, Kimura K, Mizoguchi A, Fujiyoshi Y (Implications of the aquaporin-4 structure on array formation and cell adhesion. *J Mol Biol* 355:628-639.2006).

Hung AY, Sheng M (PDZ domains: structural modules for protein complex assembly. *J Biol Chem* 277:5699-5702.2002).

Ishibashi K, Sasaki S, Fushimi K, Uchida S, Kuwahara M, Saito H, Furukawa T, Nakajima K, Yamaguchi Y, Gojobori T, . (Molecular cloning and expression of a member of the aquaporin family with permeability to glycerol and urea in addition to water expressed at the basolateral membrane of kidney collecting duct cells. *Proc Natl Acad Sci U S A* 91:6269-6273.1994).

Jung JS, Bhat RV, Preston GM, Guggino WB, Baraban JM, Agre P (Molecular characterization of an aquaporin cDNA from brain: candidate osmoreceptor and regulator of water balance. *Proc Natl Acad Sci U S A* 91:13052-13056.1994).

Kang S, Xu H, Duan X, Liu JJ, He Z, Yu F, Zhou S, Meng XQ, Cao M, Kennedy GC (PCD1, a novel gene containing PDZ and LIM domains, is overexpressed in several human cancers. *Cancer Res* 60:5296-5302.2000).

Kofuji PaCNC (Molecular substrates of potassium spatial buffering in glial cells. *Molecular Neurobiology*:195-208.2007).

Kofuji P, Ceelen P, Zahs KR, Surbeck LW, Lester HA, Newman EA (Genetic inactivation of an inwardly rectifying potassium channel (Kir4.1 subunit) in mice: phenotypic impact in retina. *J Neurosci* 20:5733-5740.2000).

Landis DM, Reese TS (Membrane structure in mammalian astrocytes: a review of freeze-fracture studies on adult, developing, reactive and cultured astrocytes. *J Exp Biol* 95:35-48.1981).

Lemmers C, Medina E, Delgrossi MH, Michel D, Arsanto JP, Le BA (hINADI/PATJ, a homolog of discs lost, interacts with crumbs and localizes to tight junctions in human epithelial cells. *J Biol Chem* 277:25408-25415.2002).

Leonoudakis D, Conti LR, Anderson S, Radeke CM, McGuire LM, Adams ME, Froehner SC, Yates JR, III, Vandenberg CA (Protein trafficking and anchoring complexes revealed by proteomic analysis of inward rectifier potassium channel (Kir2.x)-associated proteins. *J Biol Chem* 279:22331-22346.2004).

Linderstrøm-Lang KU (1952) "Proteins and Enzymes", *Lane Medical Lectures.*, vol. 6: Stanford University Press.

Lu M, Lee MD, Smith BL, Jung JS, Agre P, Verdijk MA, Merckx G, Rijss JP, Deen PM (The human AQP4 gene: definition of the locus encoding two water channel polypeptides in brain. *Proc Natl Acad Sci U S A* 93:10908-10912.1996).

Ma T, Yang B, Gillespie A, Carlson EJ, Epstein CJ, Verkman AS (Generation and phenotype of a transgenic knockout mouse lacking the mercurial-insensitive water channel aquaporin-4. *J Clin Invest* 100:957-962.1997).

Moe SE, Sorbo JG, Sogaard R, Zeuthen T, Petter OO, Holen T (New isoforms of rat Aquaporin-4. *Genomics* 91:367-377.2008).

Murata K, Mitsuoka K, Hirai T, Walz T, Agre P, Heymann JB, Engel A, Fujiyoshi Y (Structural determinants of water permeation through aquaporin-1. *Nature* 407:599-605.2000).

Nagelhus EA, Horio Y, Inanobe A, Fujita A, Haug FM, Nielsen S, Kurachi Y, Ottersen OP (Immunogold evidence suggests that coupling of K⁺ siphoning and water transport in rat retinal Muller cells is mediated by a coenrichment of Kir4.1 and AQP4 in specific membrane domains. *Glia* 26:47-54.1999).

Neely JD, Christensen BM, Nielsen S, Agre P (Heterotetrameric composition of aquaporin-4 water channels. *Biochemistry* 38:11156-11163.1999).

Neely JD, miry-Moghaddam M, Ottersen OP, Froehner SC, Agre P, Adams ME (Syntrophin-dependent expression and localization of Aquaporin-4 water channel protein. *Proc Natl Acad Sci U S A* 98:14108-14113.2001).

Nielsen S, Nagelhus EA, miry-Moghaddam M, Bourque C, Agre P, Ottersen OP (Specialized membrane domains for water transport in glial cells: high-resolution immunogold cytochemistry of aquaporin-4 in rat brain. *J Neurosci* 17:171-180.1997).

Orci L, Perrelet A, Malaisse-Lagae F, Vassalli P (Pore-like structures in biological membranes. *J Cell Sci* 25:157-161.1977).

- Pao GM, Wu LF, Johnson KD, Hofte H, Chrispeels MJ, Sweet G, Sandal NN, Saier MH, Jr. (Evolution of the MIP family of integral membrane transport proteins. *Mol Microbiol* 5:33-37.1991).
- Petersen JD, Chen X, Vinade L, Dosemeci A, Lisman JE, Reese TS (Distribution of postsynaptic density (PSD)-95 and Ca²⁺/calmodulin-dependent protein kinase II at the PSD. *J Neurosci* 23:11270-11278.2003).
- Ranganathan R, Ross EM (PDZ domain proteins: scaffolds for signaling complexes. *Curr Biol* 7:R770-R773.1997).
- Reisinger V, Eichacker LA (Solubilization of membrane protein complexes for blue native PAGE. *J Proteomics* 71:277-283.2008).
- Ruiz-Ederra J, Zhang H, Verkman AS (Evidence against functional interaction between aquaporin-4 water channels and Kir4.1 potassium channels in retinal Muller cells. *J Biol Chem* 282:21866-21872.2007).
- Sambrook J, Russel DW (2001) *Molecular Cloning*, vol. 1-7: Cold Spring Harbor Laboratory Press, New York 2001.
- Schagger H, von JG (Blue native electrophoresis for isolation of membrane protein complexes in enzymatically active form. *Anal Biochem* 199:223-231.1991).
- Seifert G, Huttmann K, Binder DK, Hartmann C, Wyczynski A, Neusch C, Steinhauser C (Analysis of Astroglial K⁺ Channel Expression in the Developing Hippocampus Reveals a Predominant Role of the Kir4.1 Subunit. *J Neurosci* 29:7474-7488.2009).
- Shin K, Straight S, Margolis B (PATJ regulates tight junction formation and polarity in mammalian epithelial cells. *J Cell Biol* 168:705-711.2005).
- Shin K, Wang Q, Margolis B (PATJ regulates directional migration of mammalian epithelial cells. *EMBO Rep* 8:158-164.2007).
- Shukolyukov SA (Aggregation of frog rhodopsin to oligomers and their dissociation to monomer: application of BN- and SDS-PAGE. *Biochemistry (Mosc)* 74:599-604.2009).
- Silberstein C, Bouley R, Huang Y, Fang P, Pastor-Soler N, Brown D, Van Hoek AN (Membrane organization and function of M1 and M23 isoforms of aquaporin-4 in epithelial cells. *Am J Physiol Renal Physiol* 287:F501-F511.2004).
- Sindic A, Huang C, Chen AP, Ding Y, Miller-Little WA, Che D, Romero MF, Miller RT (MUPP1 complexes renal K⁺ channels to alter cell surface expression and whole cell currents. *Am J Physiol Renal Physiol* 297:F36-F45.2009).
- Sorbo JG, Moe SE, Ottersen OP, Holen T (The molecular composition of square arrays. *Biochemistry* 47:2631-2637.2008).
- Storrs CH, Silverstein SJ (PATJ, a tight junction-associated PDZ protein, is a novel degradation target of high-risk human papillomavirus E6 and the alternatively spliced isoform 18 E6. *J Virol* 81:4080-4090.2007).

Strand L, Moe SE, Solbu TT, Vaadal M, Holen T (The roles of AQP4 isoforms and amino acids in square array assembly. *Biochemistry*.2009).

Suzuki H, Nishikawa K, Hiroaki Y, Fujiyoshi Y (Formation of aquaporin-4 arrays is inhibited by palmitoylation of N-terminal cysteine residues. *Biochim Biophys Acta* 1778:1181-1189.2008).

Sykova E (Ionic and volume changes in neuronal microenvironment. *Physiol Res* 40:213-222.1991).

Takumi T, Ishii T, Horio Y, Morishige K, Takahashi N, Yamada M, Yamashita T, Kiyama H, Sohmiya K, Nakanishi S, . (A novel ATP-dependent inward rectifier potassium channel expressed predominantly in glial cells. *J Biol Chem* 270:16339-16346.1995).

Takumi Y, Nagelhus EA, Eidet J, Matsubara A, Usami S, Shinkawa H, Nielsen S, Ottersen OP (Select types of supporting cell in the inner ear express aquaporin-4 water channel protein. *Eur J Neurosci* 10:3584-3595.1998).

Tanghe A, Van DP, Thevelein JM (Why do microorganisms have aquaporins? *Trends Microbiol* 14:78-85.2006).

Tani K, Mitsuma T, Hiroaki Y, Kamegawa A, Nishikawa K, Tanimura Y, Fujiyoshi Y (Mechanism of aquaporin-4's fast and highly selective water conduction and proton exclusion. *J Mol Biol* 389:694-706.2009).

Van Valen LVCM (HeLa a new microbial species. *Evolutionary Theory*.1991).

Wittig I, Braun HP, Schagger H (Blue native PAGE. *Nat Protoc* 1:418-428.2006).

Wolburg H (Orthogonal arrays of intramembranous particles: a review with special reference to astrocytes. *J Hirnforsch* 36:239-258.1995).

Wu H, Feng W, Chen J, Chan LN, Huang S, Zhang M (PDZ domains of Par-3 as potential phosphoinositide signaling integrators. *Mol Cell* 28:886-898.2007a).

Wu J, Yang Y, Zhang J, Ji P, Du W, Jiang P, Xie D, Huang H, Wu M, Zhang G, Wu J, Shi Y (Domain-swapped dimerization of the second PDZ domain of ZO2 may provide a structural basis for the polymerization of claudins. *J Biol Chem* 282:35988-35999.2007b).

Yang B, van Hoek AN, Verkman AS (Very high single channel water permeability of aquaporin-4 in baculovirus-infected insect cells and liposomes reconstituted with purified aquaporin-4. *Biochemistry* 36:7625-7632.1997).

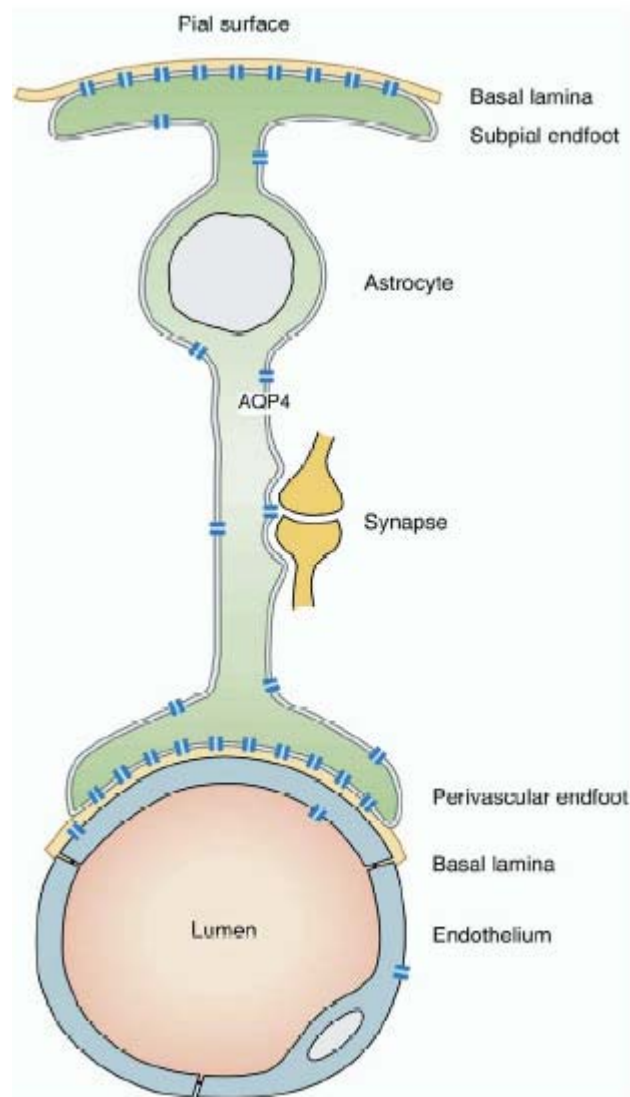
Yasui M, Kwon TH, Knepper MA, Nielsen S, Agre P (Aquaporin-6: An intracellular vesicle water channel protein in renal epithelia. *Proc Natl Acad Sci U S A* 96:5808-5813.1999).

Yong J.and TongHui M. (Importance of NPA motifs in the expression and function of water channel aquaporin-1 . *Chin Sci Bull* Volume 52, Number 6 / March, 2007.2007).

APPENDIX

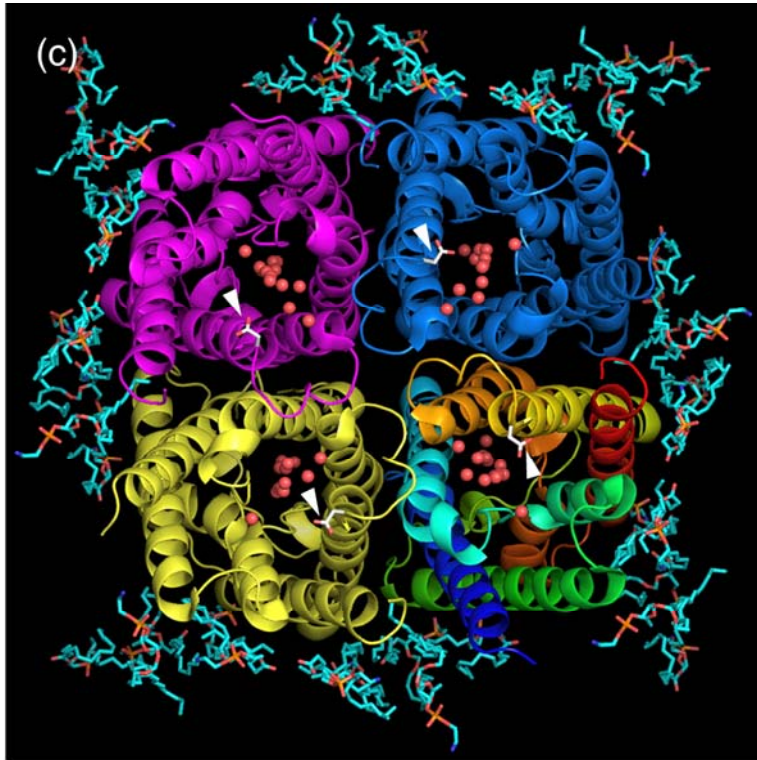
Appendix 1

The perivascular endfoot of an astrocyte (bottom). (Reprinted from M.Amiry-Moghaddam *et al.* (2008)).



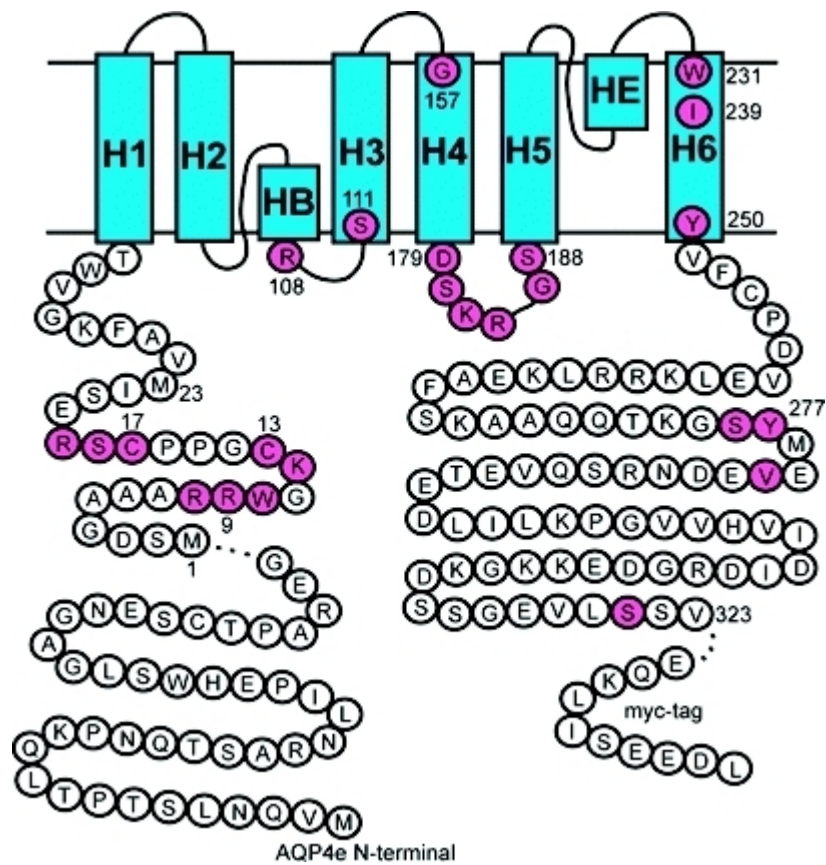
Appendix 2

Four AQP4 monomers together forming a tetramer. Water molecules inside the pore are indicated as red spheres. (Reprinted from Tani *et al.* (2009)).



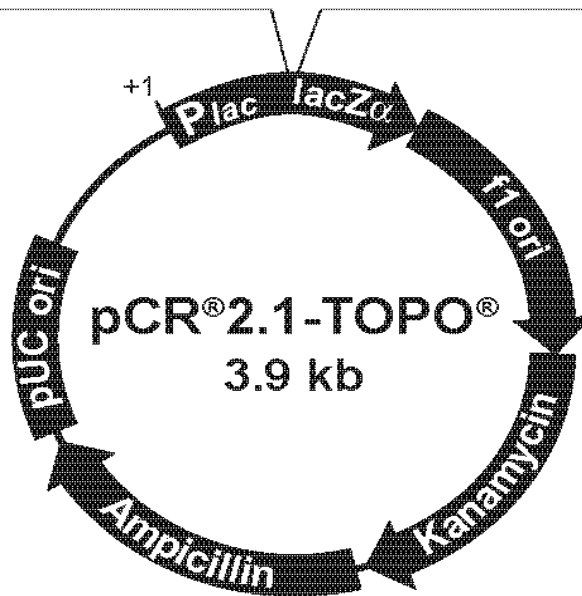
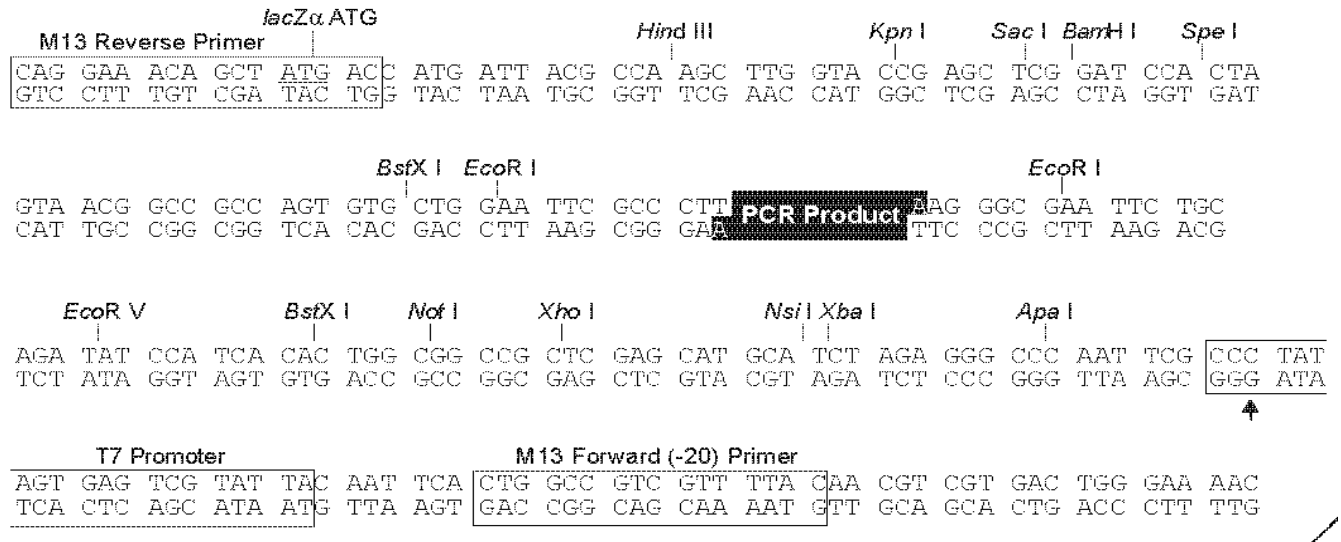
Appendix 3

The AQP4a transmembrane protein. Major and minor transmembrane helices are colored blue. Numbering and red coloring indicate mutated amino acid residues. The first amino acid of AQP4c is numbered M23. (Reprinted from Strand *et al.* (2008)).



Appendix 4

Diagram indicating a chart of pCR2.1-TOPO plasmid. (Reprinted from www.invitrogen.com).



Appendix 5

Example of a multiple alignment of Kir4.1 (NM_0010394) and endo-maxiprep eluat from ligation of Kir4.1 into pcDNA3.1/Zeo(+). Mx 8 eluate sequenced with T7 primer.

Start codon: ATG, Kozak: GCCACC, HindIII: AAGCTT, EcoRI: GAATTC

QTWRMGKTWWMYTTAAGCTTGGWMCAGACTCGGATCCACTAGTCCAGKGGTGGAAATTCGCCCYMYKYTTGCC
ACC

Alignment:

```
Query 78 ATGACGTCGGTCGCTAAGGTCTATTACAGYCAGACGACTCAGACAGAGAGCCGCCCTA 137
|||||
Sbjct 243 ATGACGTCGGTCGCTAAGGTCTATTACAGT CAGACGACTCAGACAGAGAGCCGCCCTA 302

Query 138 GTGGCCCCAGGAATACGCCGAGGAGGGTCTCACGAAAGACGGCCGAGCAATGTGAGA 197
|||||
Sbjct 303 GTGGCCCCAGGAATACGCCGAGGAGGGTCTCACGAAAGACGGCCGAGCAATGTGAGA 362

Query 198 ATGGAGCACATTGCTGACAAGCGTTTCCTCTACCTCAAGGATCTATGGACGACCTTCATT 257
|||||
Sbjct 363 ATGGAGCACATTGCTGACAACGTTTCCTCTACCTCAAGGATCTATGGACGACCTTCATT 422

Query 258 GACATGCAATGGCGCTACAAGCTTCTGCTCTTCTCTGCAACCTTTGCAGGCACGTGGTTC 317
|||||
Sbjct 423 GACATGCAATGGCGCTACAAGCTTCTGCTCTTCTCTGCAACCTTTGCAGGCACGTGGTTC 482

Query 318 CTCTTTGGTGTGGTGTGGTATCTGGTAGCTGTGGCCATGGGGACCTGTTGGAGCTGGGA 377
|||||
Sbjct 483 CTCTTTGGTGTGGTGTGGTATCTGGTAGCTGTGGCCATGGGGACCTGTTGGAGCTGGGA 542

Query 378 CCTCTGCCAACCACACGCCTTGTGTGGTGCAGGTGCACACGCTCACCGGAGCCTTCCTC 437
|||||
Sbjct 543 CCTCTGCCAACCACACGCCTTGTGTGGTGCAGGTGCACACGCTCACCGGAGCCTTCCTC 602

Query 438 TTCTCCCTGGAATCCAGACACCACATCGGCTATGGCTTCCGCTACATCAGTGAGGAATGC 497
|||||
Sbjct 603 TTCTCCCTGGAATCCAGACACCACATCGGCTATGGCTTCCGCTACATCAGTGAGGAATGC 662

Query 498 CCACTGGCCATCGTGCTCCTTATTGCGCAGCTGGTGCTCACCACCATTCTGGAAATCTTC 557
|||||
Sbjct 663 CCACTGGCCATCGTGCTCCTTATTGCGCAGCTGGTGCTCACCACCATTCTGGAAATCTTC 722

Query 558 ATCACAGGTACCTTCCTTGCAAAGATTGCCCGGCCTAAGAAGAGGGCCGAGACGATCCGC 617
|||||
Sbjct 723 ATCACAGGTACCTTCCTTGCAAAGATTGCCCGGCCTAAGAAGAGGGCCGAGACGATCCGC 782

Query 618 TTCAGCCAGCATGCCGTTGTGGCTTCCCACAACGGGAAGCCTTGCCTTATGATCCGGGTT 677
|||||
Sbjct 783 TTCAGCCAGCATGCCGTTGTGGCTTCCCATAACGGGAAGCCTTGCCTTATGATCCGGGTT 842

Query 678 GCCAATATGCGGAAGAGTCTCCTCATTGGATGCCAGGTGACAGGCAAACCTGCTTCAAACG 737
|||||
Sbjct 843 GCCAATATGCGGAAGAGTCTCCTCATTGGATGCCAGGTGACAGGCAAACCTGCTTCAAACG 902

Query 738 CACCAGACAAAGGAGGGTGAGAATATTCGGCTCAACCAGGTCAACGTGACTTTCCAAGTA 797
|||||
Sbjct 903 CACCAGACAAAGGAGGGTGAGAATATTCGGCTCAACCAGGTCAACGTGACTTTCCAAGTA 962

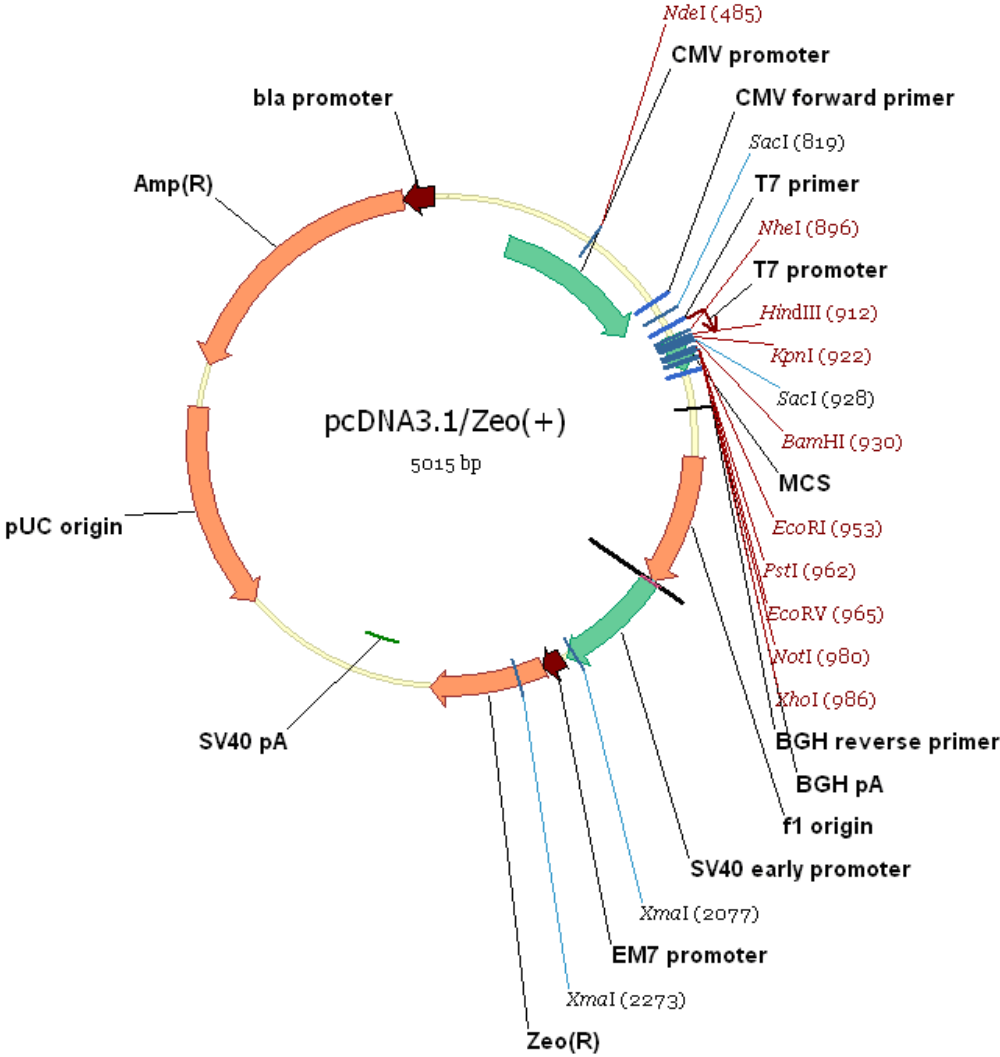
Query 798 GACACAGCCTCAGACAG-CCCTTCTCATCTACCCCTGACTTTCTA-CATGT-GTAGAT 854
|||||
Sbjct 963 GACACAGCCTCAGACAGCCCTTCTCATCTACCCCTGACTTTCTAACCACGTGGTAGAT 1022

Query 855 GAGAGCAGCCC--TTAAAGATCTCCSCTCCGCAGKGGGGA-GGGGACTTTGAGCTGGTG 911
|||||
Sbjct 1023 GAGACCAGCCCTTAAAGATCTCCGCTCCGCAGTGGGAGGGGACTTTGAGCTGGTG 1082

Query 912 CTGATCCTGA 921
|||||
Sbjct 1083 CTGATCCTGA 1092
```

Appendix 6

Diagram showing the chart of pcDNA3.1/ Zeo(+) plasmid. (Printed with permission from Torgeir Holen (unpublished)).



Appendix 7

Diagram showing the chart of pCR2.1-TOPO-mKir4.1 plasmid.(Printed with permission from Torgeir Holen (unpublished)).

